

# Ward identities and local potential approximation for large time quantum $(2+p)$ -spin glass dynamics

Bêm-Biéri Barthélémy Natta<sup>\*2</sup>, Vincent Lahoche<sup>†1</sup>, Dine Ousmane Samary<sup>‡1,2</sup>, and Parham Radpay<sup>§1</sup>

<sup>1</sup>Université Paris-Saclay, CEA, Palaiseau, F-91120, France

<sup>2</sup>Faculté des Sciences et Techniques (ICMPA-UNESCO Chair)

Université d'Abomey-Calavi, 072 BP 50, Benin

19th November 2024

---

## Abstract

This paper aims to study the functional renormalization group for quantum  $(2+p)$ -spin dynamics of a  $N$ -vector  $\boldsymbol{x} \in \mathbb{R}^N$ . By fixing the gauge symmetry in the construction of the FRG, that breaks the  $O(N)$ -symmetry and deriving the corresponding non-trivial Ward identity we can: In the first time coarse grain and focus on this study using a more attractive method such as the effective vertex expansion, and in the second time explore this model beyond the symmetry phase. We show finite scale singularities due to the disorder, interpreted as the signal in the perturbation theory. The unconventional renormalization group approach is based on coarse-graining over the eigenvalues of matrix-like disorder, viewed as an effective kinetic term, with an eigenvalue distribution following a deterministic law in the large  $N$  limit. As an illustration, the case where  $p = 3$  is scrutinized.

---

**keywords:** Functional renormalization group, Stochastic field theory, random matrix theory, non-local field theory.

---

\*[nattabarth@gmail.com](mailto:nattabarth@gmail.com)

†[vincent.lahoche@cea.fr](mailto:vincent.lahoche@cea.fr)

‡[dine.ousmanesamary@cipma.uac.bj](mailto:dine.ousmanesamary@cipma.uac.bj)

§[parham.radpay@cea.fr](mailto:parham.radpay@cea.fr)

---

# Contents

<b>1</b>	<b>Introduction</b>	<b>3</b>
<b>2</b>	<b>Technical preliminaries</b>	<b>4</b>
2.1	Definition of the model . . . . .	4
2.2	Large $N$ limit field theory . . . . .	6
2.3	Effective replicated non-local field theory . . . . .	9
2.4	Functional renormalization group . . . . .	11
2.5	Perturbation theory and large $N$ closed equations . . . . .	15
2.6	Scaling and dimensions . . . . .	18
<b>3</b>	<b>Ward identities and anomalous dimension</b>	<b>19</b>
3.1	Ward identities for internal symmetries . . . . .	20
3.2	Time reversal symmetric relations between observables . . . . .	23
<b>4</b>	<b>Effective vertex expansion</b>	<b>25</b>
<b>5</b>	<b>Venturing beyond symmetric phase</b>	<b>29</b>
5.1	Expansion around non-zero uniform local vacuum . . . . .	30
5.2	Flow equations . . . . .	38
5.3	Numerical investigations . . . . .	44
<b>6</b>	<b>Enhanced vertex expansion – a first look</b>	<b>49</b>
6.1	Truncation including multi-replica . . . . .	49
6.2	Deep IR numerical analysis . . . . .	51
<b>7</b>	<b>Conclusion and open issues</b>	<b>54</b>
<b>A</b>	<b>Classical solution for <math>p = 0</math></b>	<b>57</b>

---

# 1 Introduction

Over the last two decades, many approaches to quantum spin glasses have been explored in the literature. The most popular approach is the so-called quantum ferromagnet model, which can be viewed as a quantum analogue of the Heisenberg model, with classical three-dimensional spin vectors replaced by quantum spins represented by Pauli matrices [1, 2]. Another prominent example is the fermionic Sachdev-Ye-Kitaev (SYK) model, known for its maximal chaos and widely studied as an effective quantum model for black holes, with applications in condensed matter physics and quantum gravity [3–7]. This paper investigates a third, less common model, sometimes called the quantum spherical  $p$ -spin-glass model, which describes the behavior of a quantum particle moving in a  $N$ -dimensional random energy landscape [8, 9].

Specifically, we consider a "2+p" random energy landscape, where the coupling constants are entries from both a random Gaussian matrix and a random tensor of rank  $p$ . The corresponding classical problem of spherically constrained soft spins with "2+p" interactions can be solved "exactly" using replica symmetry breaking theory [10]. In this work, we extend our previous investigations [11] using functional renormalization group (RG) formalism [12, 13]. Our approach employs an unconventional RG scheme based on coarse-graining over the empirical spectrum of matrix-like disorder, which converges to the deterministic Wigner spectrum in the large  $N$  limit. A distinctive feature of this RG approach is that the canonical dimensions depend on the RG scale and on other two-point observables, such as the mass. In our previous work, we established the mathematical framework and focused on simpler cases, examining situations where these dependencies of the canonical dimension were minimal. Specifically, we addressed: Perturbation theory around the Gaussian fixed point. Vertex expansion is the leading order of the derivative expansion in the deep infrared (IR) regime. Vertex expansion in the critical regime.

In the first and third regimes, the canonical dimension primarily depends on the scale, but not on the mass. In the deep IR, power counting shows that the Gaussian theory behaves like an ordinary Euclidean field theory in four dimensions. In the second case, while the power counting resembles that of an ordinary field theory, the theory exhibits non-local interactions. Our investigation revealed notable features related to the impact of tensorial disorder, including Finite-scale singularities, appearing as "cusps" or sharp analytical singularities depending on the regime. The existence of attractors in phase space for trajectories emerging from critical conditions in the IR, accompanied by rapid oscillations around these attractors. Some of these phenomena have been observed in other glassy systems [14, 15] and beyond [16]. In our previous work, we found evidence suggesting that these singularities are linked to the emergence of correlations between replicas, based on a two-particle irreducible (2PI) formalism. We showed that the effective potential associated with these correlations develops a non-zero minimum (without replica symmetry breaking) as singularities are approached, compatible with a first-order transition. In this paper, we will not return to the 2PI formalism, as we plan to address it comprehensively in future work. Instead, we aim to develop a more complete framework to investigate the phase space beyond the symmetric phase. The formalism presented here should help distinguish the singularities related to replica correlations from those associated with second-order phase transitions to an ordered phase, thus focusing solely

on correlations between replicas. This forms the core of the second and main part of the paper.

The first part is dedicated to constructing next-to-leading-order solutions using Ward identities that arise due to the gauge fixing required by the RG construction. Additionally, we improve the symmetric-phase RG equations beyond the standard vertex expansion approach used in our previous paper [11], by utilizing the effective vertex expansion developed in [17]. While this section diverges slightly from our primary focus, readers interested solely in RG aspects beyond the symmetric phase in the large  $N$  limit may skip it. Finally, we note that this work is accompanied by a forthcoming paper [11], which examines the quantum  $p$ -spin model via RG with coarse-graining over frequencies.

To conclude this introduction, let us emphasize one additional point. Although canonical dimensions suggest that all local couplings are relevant in the UV, this does not imply that the renormalization group is ineffective. For instance, in some discrete quantum gravity models, such as random matrix models [18–21], all couplings are technically irrelevant, yet the flow admits a non-trivial fixed point with a relevant direction, where the critical exponent corresponds to the double scaling limit [22].

The paper is organized as follows: In Section 2, we present the model, conventions, and basics of the Wetterich-Morris formalism,  $1/N$  expansion, and perturbation theory. In Section 3, we use Ward identities to construct next-to-leading-order corrections from the leading order, while Section 4 applies effective vertex expansion to improve the standard vertex expansion. Section 5 develops and studies a formalism based on an expansion around the vacuum of the local potential, examining an artificially simplified case to illustrate key mechanisms. Section 6 extends the vertex expansion to include non-local couplings and replica interactions. Finally, Section 7 outlines open issues for future research.

## 2 Technical preliminaries

In this section, we define the model, conventions, and tools that we will use throughout the rest of this paper. Specifically, we introduce the basics of the functional renormalization group and the formal large  $N$  solutions of the underlying field theory, as considered in our previous work [11].

### 2.1 Definition of the model

Let us begin with the definition of the model. We consider a Euclidean (non-relativistic) quantum particle in a space of dimension  $N$ , moving through a rough landscape characterized by the combination of two types of disorder: one represented by a random Gaussian matrix  $K$ , and the other by a Gaussian random tensor  $J$  of size  $q > 2$ . A version of this quantum mechanical model, without matrix disorder, was considered in [8] and references therein. The particle wave function  $\psi(\mathbf{x}, t) \in \mathbb{C}$ ,  $\mathbf{x} \equiv (x_1, \dots, x_N) \in \mathbb{R}^N$  evolves accordingly with the Schrödinger equation:

$$\boxed{\hbar \frac{\partial}{\partial t} \psi(\mathbf{x}, t) = -\hat{\mathcal{H}} \psi(\mathbf{x}, t),} \quad (2.1)$$

where the Hamiltonian  $\hat{\mathcal{H}}$  reads in the generalized position space basis:

$$\hat{\mathcal{H}} = -\frac{\hbar^2}{2m_0} \frac{\partial^2}{\partial \mathbf{x}^2} + U_{J,K}(\mathbf{x}) + V(\mathbf{x}^2). \quad (2.2)$$

The *deterministic* potential  $V(\mathbf{x}^2)$  is some polynomial function involving powers of the  $O(N)$  length square variable  $\mathbf{x}^2 := \sum_{i=1}^N x_i^2$ :

$$V(\mathbf{x}^2) := N \sum_{n=1}^{n_0} \frac{h_n}{(2n)!} \left( \frac{\mathbf{x}^2}{N} \right)^n, \quad (2.3)$$

where coupling constants  $h_n$  must be positive or negative real number, excepts for  $h_{n_0} > 0$  because of the stability condition and the powers of  $N$  ensure the existence of the  $1/N$  expansion – see [23] and subsection 2.5. The *random* potential  $U_{J,K}(\mathbf{x})$  contain the disorder effects:

$$U_{J,K}(\mathbf{x}) := \frac{1}{2} \sum_{i,j=1}^N K_{ij} x_i x_j + \frac{1}{q!} \sum_{i_1, \dots, i_p} J_{i_1 \dots i_p} x_{i_1} \cdots x_{i_p}, \quad (2.4)$$

where:

- $K_{ij}$  are the entries of a  $N \times N$  symmetric random matrix, distributed accordingly with a Gaussian orthogonal law with finite variance  $\sigma$  and zero means.
- $J_{i_1 \dots i_p}$  are the component of some symmetric Gaussian random tensor with rank  $p$  and size  $N^p$ , such that:

$$\overline{J_{i_1 \dots i_p}} = 0, \quad \overline{J_{i_1 \dots i_p} J_{j_1 \dots j_p}} = \frac{\lambda}{N^{p-1}} \sum_{\pi \in \mathfrak{P}_p} \prod_{m=1}^p \delta_{i_m j_{\pi(m)}}. \quad (2.5)$$

The coupling  $\lambda$  characterizes the intensity of the disorder,  $\mathfrak{P}_p$  is the set of permutations for  $p$  elements and the overline means averaging with respect to the probability distribution for  $J$ . The potential  $V(\mathbf{x}^2)$  suppresses large  $\mathbf{x}$  configurations in the classical equation of motion:

$$m_0 \frac{d^2 x_i}{dt^2} = -\frac{\partial}{\partial x_i} (U_{J,K}(\mathbf{x}) + V(\mathbf{x}^2)). \quad (2.6)$$

This equation is analytically investigated for  $p = 0$  in the quenched regime for late time in Appendix A.

Operational quantum mechanical formalism is not the most suitable for considering the renormalization group (RG), and we move to the path of integral formalism. The Hermitian operator evolution:

$$U(t, t_0) := e^{-\frac{t-t_0}{\hbar} \hat{\mathcal{H}}}, \quad (2.7)$$

can be ‘‘Trotterized’’ accordingly with the standard procedure [24] to construct path integral, and the Euclidean propagator looks as the partition function of a real-time system in contact with a thermal bath at inverse temperature  $\beta = t - t_0$  [25]:

$$\mathcal{Z}_\beta[K, J, \mathbf{L}] = \int [\mathcal{D}x(t)] e^{-\frac{1}{\hbar} S_{\text{cl}}[\mathbf{x}(t)] + \frac{1}{\hbar} \int_{-\beta/2}^{\beta/2} dt \sum_{k=1}^N L_k(t) x_k(t)}, \quad (2.8)$$

where  $\mathbf{L} = (L_1, \dots, L_N)$  and where the *classical action*  $S_{\text{cl}}[\mathbf{x}(t)]$  is:

$$S_{\text{cl}}[\mathbf{x}(t), J, K] := \int_{-\beta/2}^{\beta/2} dt \left( \frac{1}{2} \dot{\mathbf{x}}^2 + U_{J,K}(\mathbf{x}) + V(\mathbf{x}^2) \right), \quad (2.9)$$

provided with periodic boundary conditions  $\mathbf{x}(t) = \mathbf{x}(t + \beta)$ , and in this paper we essentially focus on the limit  $\beta \rightarrow \infty$  i.e. for vanishing temperature. Note that we use the notation  $[\mathcal{D}x(t)]$  for the path integral “measure”, to distinguish it from the standard Lebesgue integration measure  $d\mathbf{x}$ . Furthermore, because the mass  $m_0$  does not renormalize in the large  $N$  limit in the symmetric phase (it corresponds to the field strength renormalization, see below), we set  $m_0 = 1$ .

As is usual in quantum field theory (QFT), the path integral (2.8) allows computing vacuum-vacuum expectation value of field correlations at different times<sup>1</sup> [26]:

$$\langle 0|T \hat{x}_{i_1}(t_1)\hat{x}_{i_2}(t_2)\cdots\hat{x}_{i_n}(t_n)|0\rangle = \frac{1}{\mathcal{Z}[K, J, 0]} \frac{\partial^n \mathcal{Z}[K, J, \mathbf{L}]}{\partial L_{i_1}(t_1)\partial L_{i_2}(t_2)\cdots\partial L_{i_n}(t_n)} \Bigg|_{J=0}. \quad (2.10)$$

These correlations can be computed using perturbation theory, and the perturbative expansion is structured as a power series in  $\hbar$ . The limit  $\hbar \rightarrow 0$  corresponds to the so-called *classical limit*. Finally, as  $\beta$  remains fixed, paths can be decomposed into modes,

$$\mathbf{x}(t) = \frac{1}{\sqrt{\beta}} \sum_{k=0}^{\infty} \tilde{\mathbf{x}}(\omega_k) e^{i\omega_k t}, \quad (2.11)$$

where frequencies are :

$$\omega_k := \frac{2\pi k}{\beta}. \quad (2.12)$$

## 2.2 Large $N$ limit field theory

The physical content of the partition function (2.8) can be investigated using perturbation theory. Note that despite the fact that the model has no divergence, the perturbation theory does not adequate to define the partition function, because summation of the perturbation series is usually a non-trivial issue requiring advanced constructive tools – see [27] and references therein. Nevertheless, we can leave this problem aside and focus only on the perturbative definition of observables, as is the case in QFT.

Consider the  $2n$ -point 1PI vertex function  $\Gamma^{(2n)}$ . In the standard perturbation theory, the different terms in the expansion are Feynman amplitudes, indexed by 1PI Feynman graphs:

$$\Gamma^{(2n)} = \sum_{\mathcal{G} \in \mathbb{G}_{2n}} \frac{1}{s(\mathcal{G})} \mathcal{A}(\mathcal{G}). \quad (2.13)$$

where  $\mathbb{G}_{2n}$  is the set of 1PI Feynman diagrams with  $2n$  external points, and the additional factor,  $s(\mathcal{G})$  called *symmetry factor*, depends on the dimension of the automorphism group

---

<sup>1</sup>The hat means quantum operator.

of the graph [28]. Feynman diagrams are sets of vertices materializing interactions and edges materializing Wick contractions. These Wick contractions can be easily understood by exploiting the global  $O(N)$  global symmetry of the theory. Indeed, because the probability distributions for  $K$  and  $J$  are both  $O(N)$  invariant<sup>2</sup> one can always fix the gauge, and to choose a coordinate system such that  $K$  is diagonal. Namely, let  $\{u^{(\mu)}\}$  the set of  $N$  orthonormal eigenvectors, such that:

$$\sum_{j=1}^N K_{ij} u_j^{(\mu)} = \xi_\mu u_i^{(\mu)}, \quad (2.14)$$

where eigenvalues  $\{\xi_\mu\}$  are reals. We then introduce the orthogonal transformation:

$$x_\mu(t) := \sum_{i=1}^N x_i u_i^{(\mu)}. \quad (2.15)$$

In this basis, the bare propagator is diagonal, and its components read, in the Fourier basis:

$$C(\omega_k, \xi_\mu) := \frac{1}{\omega^2 + \xi_\mu + h_1}. \quad (2.16)$$

A typical Feynman graph  $\mathcal{G}$  involves the subgraphs  $g_n \subset \mathcal{G}$  made of cycles (called faces, see below) involving a summed product of propagator, of the form:

$$I_n(\Omega_1, \dots, \Omega_n) := \sum_{\mu} \prod_{i=1}^n C(\Omega_i, \xi_\mu), \quad (2.17)$$

where the  $\Omega_i$  are external frequencies of the subgraph. In the large  $N$  limit, such a sum can be converted to an integral using the well-known Wigner theorem [29, 30]:

**Theorem 1** *Let  $M := \{M_{ij}\}$  be a symmetric  $N \times N$  random matrix whose  $N(N+1)/2$  independent entries on the upper triangle are identically and independently distributed (i.i.d). More precisely, we assume that distributions have zero means and expectation values:  $\mathbb{E}(M_{ii}^2) < \infty$  and  $\mathbb{E}(M_{ij}^2) = \sigma^2/N < \infty$ , for  $i \neq j$ . This set defines the Wigner ensemble, and in the large  $N$  limit, the empirical eigenvalue distribution:*

$$\mu_{em}(x) := \frac{1}{N} \sum_{\mu=1}^N \delta(x - \xi_\mu), \quad (2.18)$$

converges weakly toward the Wigner semicircle law:

$$\mu_{em}(x) \xrightarrow{N \rightarrow \infty} \mu_W(x) \quad (2.19)$$

where:

$$\mu_W(x) := \begin{cases} \frac{\sqrt{4\sigma^2 - x^2}}{2\pi\sigma^2} & \text{if: } -2\sigma \leq x \leq 2\sigma \\ 0 & \text{if: } |x| > 2\sigma, \end{cases}$$

is normalized such that  $\int \mu_W(x) dx = 1$ .

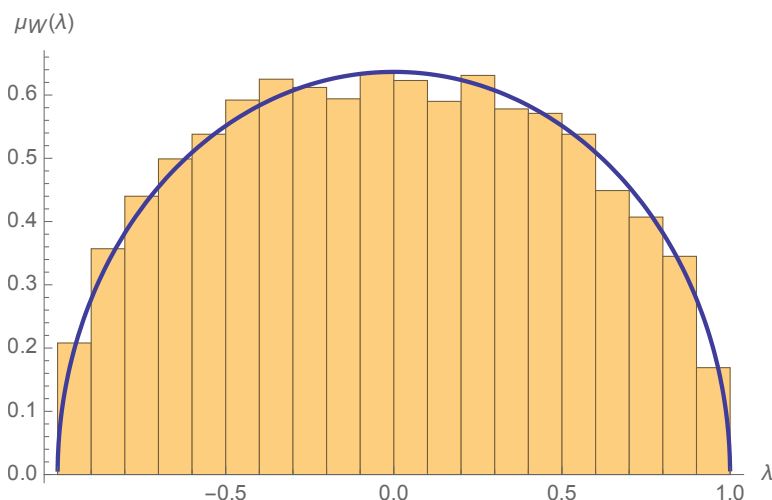


Figure 1: Illustration of the convergence toward Wigner distribution. Histogram shows the eigenvalues distribution a  $10^4 \times 10^4$  i.i.d sample random matrix.

Figure 1 illustrates this theorem. The Gaussian orthogonal ensemble is an example of Wigner matrices for which  $\mathbb{E}(M_{ii}^2) = 2\sigma^2/N$ , and the  $n$  external points Feynman amplitude  $I_n$  for the subgraph  $g_n$  becomes:

$$\frac{1}{N} I_n(\Omega_1, \dots, \Omega_n) \xrightarrow{N \rightarrow \infty} I_n^{(\infty)}(\Omega_1, \dots, \Omega_n) \equiv \int_{-2\sigma}^{+2\sigma} \mu_W(x) dx \prod_{i=1}^n C(\Omega_i, x). \quad (2.20)$$

It is suitable for large  $N$  calculations to introduce the *generalized momentum*  $p^2$ , looking as a positive variable in the limit  $N \rightarrow \infty$ :

$$p^2 := x + 2\sigma. \quad (2.21)$$

Then, provided that we define the *physical bare mass*  $m^2$  as<sup>3</sup>

$$m^2 := h_1 - 2\sigma, \quad (2.22)$$

the Feynman amplitude for the subgraph  $g_n$  becomes:

$$I_n^{(\infty)}(\Omega_1, \dots, \Omega_n) = \int_0^{+4\sigma} \rho(p^2) dp^2 \prod_{i=1}^n \tilde{C}(\Omega_i, p^2), \quad (2.23)$$

where the propagator  $\tilde{C}$ , involving the generalized momentum  $p^2$  is:

$$\tilde{C}(\omega, p^2) := \frac{1}{\omega^2 + p^2 + m^2}, \quad (2.24)$$

<sup>2</sup>This means that for instance  $J \equiv \{J_{i_1 \dots i_q}\}$  and  $O \triangleright J \equiv \{\sum_{j_1 \dots j_q} O_{i_1 j_1} \dots O_{i_q j_q} J_{j_1 \dots j_q}\}$  cannot be distinguished from the probability law, for some orthogonal matrix  $O$ .

<sup>3</sup>Note that the effective mass, as  $p^2$  is defined for arbitrary  $N$ , but  $p^2$  is positive definite only in this limit. A clever way to define  $p^2$  for any finite  $N$  sample of  $K$  could be to translate from the smallest eigenvalue; an irrelevant subtlety for our purpose.



and where in (2.23), the distribution  $\rho(p^2)$  is induced from  $\mu_W(x)$  from the definition of  $p^2$  i.e.  $\rho(p^2)$  vanishes outside the interval  $p^2 \in [0, 4\sigma]$ , where it takes the value:

$$\rho(p^2) = \frac{\sqrt{p^2(4\sigma - p^2)}}{2\pi\sigma^2}. \quad (2.25)$$

Formally the amplitude (2.23) looks as the Feynman amplitude for an ordinary but non-local field theory's subgraph, where  $p^2$  plays the role of a square-length momentum. Remark that for such a field theory in space dimension  $D$ , the momentum distribution is  $\rho_{\mathbb{R}^D}(\vec{p}^2) \sim (\vec{p}^2)^{\frac{D-2}{2}}$ . In particular, for  $p^2$  small enough,  $\rho(p^2) \simeq (p^2)^{\frac{1}{2}}$ , and the theory looks as a 3D Euclidean field theory. The analogy does not need to be pushed too far, however, and we can simply note that an ordinary field theory, such as the one we are considering here, can be characterized by a generalized moment distribution and a definition of locality [31, 32]. This point of view allows considering a more abstract point of view concerning the notion of dimension, which we will consider in subsection 2.4.

### 2.3 Effective replicated non-local field theory

In the point of view of the previous section, the two disorders  $K$  and  $J$  are viewed in two different ways. Indeed, because of the properties of the large  $N$  limit spectra of Wigner random matrices, the random spectrum for the matrix-like disorder converges toward a deterministic distribution and looks like an effective kinetics. No such equivalent property exists for the tensorial counterpart, despite efforts to construct it [33–36] (and reference therein). We will therefore make use of the self-averaging assumption two times. A first time to replace the effect of the disorder  $K$  by the asymptotic expression of its eigenvalue density; A second time to construct an average with respect to the disorder  $J$  from its explicit Gaussian probability density. This last point opens the question of the type of average we are aiming to consider. *Annealed average* takes the averaging of the partition function (2.8) resulting in a non-local field theory with respect to generalized momenta and time. Physically, this kind of averaging corresponds to a situation where the typical timescale for disorder and quantum particles are the same. In the opposite *quenched average*, suppose that the typical timescale for the quantum particle is very small compared to the typical timescale for  $J$ , and that  $J$  averaging can be performed on the free energy  $\mathcal{F}_\beta[K, J, \mathbf{L}] := \ln \mathcal{Z}_\beta[K, J, \mathbf{L}]$  rather than on the partition function. This issue is generally solved by introducing replica [37–41] throughout the elementary formula:

$$\overline{\mathcal{F}_\beta[K, J, \mathbf{L}]} = \lim_{n \rightarrow 0} \frac{\overline{\mathcal{Z}_\beta^n[K, J, \mathbf{L}]} - 1}{n}. \quad (2.26)$$

Besides it is formally valid, this formula poses the delicate issue of the limit, the averaging over the  $n$ th copies of the disorder assuming implicitly that  $n$  is an integer. This in particular opens the possibility of a *replica symmetry breaking* which is one of the strong indicators to recognize glassy phases. Another way, less mathematically debated and more appropriate for functional renormalization group application is to construct averaging from *cumulants* of the random quantity  $W[K, J, \mathbf{L}]$  [14, 15]. This requires breaking explicitly the replica symmetry, providing a different source for different replicas, assuming

$n \in \mathbb{N}^*$ . Hence, the strategy we will adopt looks like a *multi-local* expansion, depending on the order of the cumulant as  $W[K, J, \mathbf{L}]$  we will consider. These cumulants are defined as usual:

$$\begin{aligned}\mathcal{W}^{(1)}[\mathbf{L}_\alpha] &= \lim_{N \rightarrow \infty} \overline{W[K, J, \mathbf{L}_\alpha]} \\ \mathcal{W}^{(2)}[\mathbf{L}_\alpha, \mathbf{L}_\beta] &= \lim_{N \rightarrow \infty} \overline{W[K, J, \mathbf{L}_\alpha]W[K, J, \mathbf{L}_\beta]} - \mathcal{W}^{(1)}[\mathbf{L}_\alpha]\mathcal{W}^{(1)}[\mathbf{L}_\beta] \\ \mathcal{W}^{(3)}[\mathbf{L}_\alpha, \mathbf{L}_\beta, \mathbf{L}_\gamma] &= \lim_{N \rightarrow \infty} \overline{W[K, J, \mathbf{L}_\alpha]W[K, J, \mathbf{L}_\beta]W[K, J, \mathbf{L}_\gamma]} - \dots\end{aligned}$$

where Greek indices  $\alpha, \beta, \gamma \dots$  running from 1 to  $n$  labels different sources, namely different replicas of the system and the  $\dots$  in the last line means we subtract the complete list of disconnected contributions. These cumulants are furthermore generated by the functional:

$$\begin{aligned}\lim_{N \rightarrow \infty} \ln \overline{\mathcal{Z}_\beta^n[K, J, \{\mathbf{L}_\alpha\}]} &= \sum_\alpha \mathcal{W}^{(1)}[\mathbf{L}_\alpha] + \frac{1}{2!} \sum_{\alpha, \beta} \mathcal{W}^{(2)}[\mathbf{L}_\alpha, \mathbf{L}_\beta] \\ &+ \frac{1}{3!} \sum_{\alpha, \beta, \gamma} \mathcal{W}^{(3)}[\mathbf{L}_\alpha, \mathbf{L}_\beta, \mathbf{L}_\gamma] + \dots, \quad (2.27)\end{aligned}$$

where the generating functional  $\mathcal{Z}_\beta^n[K, J, \{\mathbf{L}_\alpha\}]$  is now defined as:

$$\begin{aligned}\mathcal{Z}_\beta^n[K, J, \{\mathbf{L}_\alpha\}] &:= \exp \sum_{\alpha=1}^n W[K, J, \mathbf{L}_\alpha] \\ &\equiv \int \prod_{\alpha=1}^n [\mathcal{D}x_\alpha(t)] \exp \left( -\frac{1}{\hbar} \sum_{\alpha=1}^n S_{\text{cl}}[\mathbf{x}_\alpha] + \int_{-\beta/2}^{+\beta/2} dt \sum_{k=1, \alpha=1}^{N, n} L_{k, \alpha}(t) x_{k, \alpha}(t) \right). \quad (2.28)\end{aligned}$$

Note that as usual, each replica corresponds to the same sample of the disorder, and performing the averaging from the Gaussian distribution for  $J$ , we get:

$$\overline{\mathcal{Z}_\beta^n[K, J, \{\mathbf{L}_\alpha\}]} := \int \prod_{\alpha=1}^n [\mathcal{D}x_\alpha(t)] e^{-\frac{1}{\hbar} \overline{S_{\text{cl}}[\{\mathbf{x}\}] + \mathcal{J}}} \equiv \exp \left( \mathcal{W}_\beta^{(n)}[K, J, \{\mathbf{L}_\alpha\}] \right), \quad (2.29)$$

where the source term is:

$$\mathcal{J} := \int_{-\beta/2}^{+\beta/2} dt \sum_{k=1, \alpha=1}^{N, n} L_{k, \alpha}(t) x_{k, \alpha}(t), \quad (2.30)$$

and the *classical averaged action* reads, in the thermodynamic limit:

$$\boxed{\overline{S_{\text{cl}}[\{\mathbf{x}_\alpha\}]} := \sum_\alpha S_{\text{cl}}[\mathbf{x}_\alpha(t), J = 0, K] - \frac{\lambda N}{2\hbar} \int_{-\beta/2}^{+\beta/2} dt dt' \sum_{\alpha, \beta} \left( \frac{\mathbf{x}_\alpha(t) \cdot \mathbf{x}_\beta(t')}{N} \right)^p}, \quad (2.31)$$

**Remark 1** *Let us notice that the path integral does not converge for any  $p$ , except if the higher interaction in the confining potential  $V(\mathbf{x}^2)$  has a positive coupling and in at least of order  $2(p+1)$ . In particular, for  $p=3$ , the path integral convergences safely if the confining potential involves a positive octic interaction. Note furthermore that the coupling corresponding to the non-local contribution has to be negative to remain associated with something like a tensorial Gaussian disorder.*

## 2.4 Functional renormalization group

Since the pioneering work of Wilson and Kadanoff [42, 43], various forms of the RG have been developed for different contexts, intersecting with probability and information theories [44–48]. RG appears to be a general concept in physics rather than a topic confined to QFT or condensed matter theory. Notably, RG enables the exploration of effective infrared (IR) physics by progressively integrating out short-wavelength fluctuations. In field theory, this process is well-defined as long as the theory includes a canonical notion of scale. In QFT, this scale is often derived from the background space or space-time, which provides canonical definitions of *microscopic* and *macroscopic* physics, allowing wavelength modes to be uniquely ordered by these boundaries [28]. The RG flow can also be defined in a more abstract framework that does not depend on background structures like space-time, as long as quantum fluctuations can be sized. Here, this size is determined by the spectrum of the Gaussian kernel, with fluctuations, in the corresponding eigenbasis, ordered by the size of their eigenvalues [17, 31, 49, 50]. From an information-theoretic perspective, the Gaussian kernel functions as the Fisher information metric [51], so that intrinsic scaling acquires a geometric interpretation via the eigenvalues of this metric [46, 52]. For other unconventional recent applications of RG, see [53–57] and references therein.

In the field theory we consider in this paper, there exists a one-dimensional background manifold, time, that provides a canonical notion of scale. Consequently, a renormalization group can, in principle, be constructed through coarse-graining over frequencies. Such coarse-graining has recently been studied in contexts like classical spin glass kinetics [55, 58], out-of-equilibrium field theories, such as model A and the Kardar-Parisi-Zhang (KPZ) equation [59, 60], and quantum mechanical systems [61–63]. However, in this paper, we consider a more abstract RG approach, based on coarse-graining over the spectrum of the kinetic disorder  $K$ , specifically over the generalized momentum—see Figure 2. Unlike frequencies, this spectrum does not relate to any background scaling and serves as an example of the abstract scaling mentioned earlier. Moreover, it provides a canonical notion of “what is ultraviolet” (UV) and “what is infrared” (IR), corresponding respectively to the regions  $p^2 \approx 4\sigma$  and  $p^2 \approx 0$ . We can then construct a coarse-grained description of the underlying IR effective physics by partially integrating out UV fluctuations associated with large generalized momenta.

One could also consider a “mixed” coarse-graining approach, incorporating both frequency and momentum. In similar cases, this mixed approximation has been shown to offer significant qualitative benefits [59]. However, our objective in this paper is to develop the formalism, so we simplify the process by focusing solely on coarse-graining over the generalized momentum, reserving a more detailed examination of the mixed approach for a forthcoming paper [64]. This approach has been explored in our previous work [11] and in other studies across various contexts [65–69]. Essentially, this amounts to examining the system’s behavior *in the long-time limit*, which is the limit our approach will take in this article.

In the literature, there exist several popular “exact” equations that describe how the physical representation of a field theory changes as degrees of freedom within specific

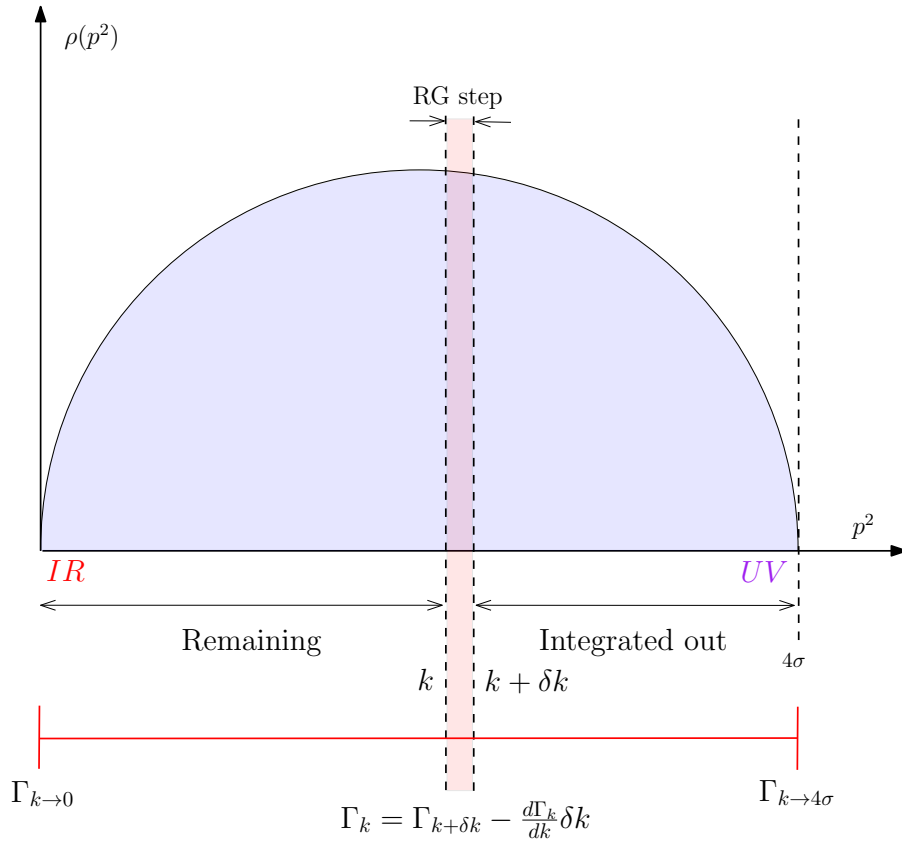


Figure 2: A summary of the coarse-graining definition of the Wigner RG flow. Modes are partially integrated from UV to IR, and the effective average action changes from each step.

momentum windows are integrated out. The Polchinski equation [28, 70] is an exact equation that describes how the classical (bare) action changes during each infinitesimal RG step. It serves as a formally exact equation and a deep mathematical realization of Wilson's RG. However, there is another, less widely known approach developed by Wetterich and Morris [12, 13, 19, 71]. This approach, known as the *effective average action* (EAA) method, differs from Wilson's perspective in the choice of mathematical object. Instead of focusing on the classical action, the Wetterich approach centers on the "effective action of integrated-out modes."

Furthermore, the EAA approach differs from Wilson's in how the fundamental cut-off is applied. In the Wilson-Polchinski framework, the bare action is varied, and the fundamental cut-off around which fluctuations are integrated is rescaled at each RG step. In contrast, within the EAA formalism, the fundamental cut-off and the bare action remain fixed, with contributions from IR fluctuations to the full effective action being gradually suppressed until reaching an IR cut-off. The EAA formalism offers several advantages over the Wilson-Polchinski formalism, particularly for nonperturbative analysis and studies of phases with broken symmetries. Notably, this approach helps regularize the infrared divergences that typically arise in the broken symmetry region when the mass becomes negative.

Let us proceed with the explicit construction of the formalism. Following [12], we add to the classical averaged action  $\bar{S}$  a scale-dependent mass term, referred to as the *regulator*:

$$\Delta S_k[\mathbf{x}_\alpha] := \frac{1}{2} \int dt \sum_{\alpha=1}^n \sum_{\mu=1}^N x_{\mu\alpha}(t) R_k^{(N)}(p_\mu^2) x_{\mu\alpha}(t), \quad (2.32)$$

and denote the modified averaged partition function by  $\overline{\mathcal{Z}_{\beta,k}^n}$ . Note that the regulator is assumed to be diagonal in both time and replica space. This choice is expected to be sufficiently general; however, other options have been explored in the literature, especially in the context of the random field Ising model [14, 15]. We nevertheless believe this regulator is suitable for studying the system at long times [11].

The regulator function  $R_k^{(N)}$  depends on the *infrared scale*  $k$ , and we have added an index  $N$  since we view  $R_k^{(N)}$  as a random quantity, depending on the specific sample of the kinetic matrix  $K$ . In the limit as  $N \rightarrow \infty$ ,  $R_k^{(N)}$  converges to a deterministic function  $R_k$ .

The *effective average action*  $\Gamma_k$ , which represents the effective action for UV modes integrated out up to the scale  $k$ , is defined by the following relation:

$$\Gamma_k[\mathcal{M}] + \Delta S_k[\mathcal{M}] = W_k^{(n)}[\mathcal{L}] - \sum_{\alpha=1}^n \int_{-\beta/2}^{+\beta/2} dt \mathbf{L}_\alpha(t) \cdot \mathbf{M}_\alpha(t), \quad (2.33)$$

where  $W_k^{(n)}[\mathcal{L}]$  is the free energy of the modified partition function:

$$\mathcal{W}_{\beta,k}^{(n)}[K, J, \mathcal{L}] := \ln \overline{\mathcal{Z}_{\beta,k}^n}[K, J, \{\mathbf{L}_\alpha\}], \quad (2.34)$$

$\mathcal{L} := \{\mathbf{L}_\alpha\}$  and  $\mathcal{M} := \{\mathbf{M}_\alpha\}$  are the sets of sources and classical fields (each an  $N$ -dimensional vector per replica). The components of the classical field are given by:

$$\frac{\delta}{\delta L_{i\alpha}} \mathcal{W}_{\beta,k}^{(n)}[K, J, \mathcal{L}] = M_{i\alpha}, \quad (2.35)$$

Formally, the regulator function ensures that  $\Gamma_k[\mathcal{M}]$  provides a smooth transition between the bare action  $\overline{S_{\text{cl}}}$  as  $k \rightarrow 4\sigma$  (when no fluctuations are integrated out) and the full effective action  $\Gamma$  at  $k = 0$ , which corresponds to the full Legendre transform of the free energy (2.29) (when all fluctuations are integrated out). Specifically, the regulator becomes large for  $p_\mu \lesssim k$ , effectively freezing large-scale degrees of freedom by giving them a large effective mass. In contrast, microscopic degrees of freedom with  $p_\mu \gtrsim k$  are minimally affected by the regulator and are thus integrated out. These conditions require in particular:

1.  $\lim_{k \rightarrow 0} R_k(p_\mu^2) = 0$ , meaning that all the degrees of freedom are integrated out as  $k \rightarrow 0$  (infrared (IR) limit).
2.  $\lim_{k \rightarrow 4\sigma} R_k(p_\mu^2) \rightarrow \infty$ , meaning that no fluctuations are integrated out in the deep ultraviolet (UV) limit  $k \rightarrow 4\sigma$ .

The equation that describes how the effective function  $\Gamma_k$  changes with  $k$  is the Wetterich equation [13]:

$$\dot{\Gamma}_k = \frac{1}{2\beta} \sum_{\omega} \sum_{p_\mu, p_\nu, \alpha} \dot{R}_k(p_\mu^2) G_k(\omega, p_\mu, p_\nu, \alpha), \quad (2.36)$$

where the dot denotes differentiation with respect to  $s := \ln(k/4\sigma)$ , and  $G_k$  is the *effective 2-point function* (diagonal with respect to the replica and generalized momentum indices), such that:

$$[G_k^{-1}(\omega, p_\mu, p_\nu, \alpha) + R_k(p_\mu^2)\delta_{\mu\nu}]\delta_{\omega, -\omega'}\delta_{\alpha\beta} := \frac{\delta^2 \Gamma_k}{\delta M_{\mu\alpha} \delta M_{\nu\beta}}, \quad (2.37)$$

As we focus on the large  $N$  limit to compute the flow equations, only the limit function  $R_k := \lim_{N \rightarrow \infty} R_k^{(N)}$  is relevant and needs to be defined in practice. In this paper, we adopt a slightly modified version of the standard Litim regulator [72]:

$$R_k(p_\mu^2) := \frac{4\sigma}{4\sigma - k^2} (k^2 - p_\mu^2) \theta(k^2 - p_\mu^2), \quad (2.38)$$

where  $\theta(x)$  is the Heaviside step function. The prefactor in this expression ensures that the boundary conditions for  $k = 0$  and  $k = 2\sqrt{\sigma}$  are satisfied. This type of regulator has been used in our previous work [11] and in recent studies [55, 56, 73, 74]. Other regulator choices, such as the exponential regulator, are also widely used in the literature [12]. Additionally, the dependency of results on the regulator choice could be investigated, as the approximations used to solve the equation may introduce spurious dependency on the chosen regulator [59, 75, 76]; we leave these considerations for future work.

The equation (2.36) is exact but impossible to solve exactly, and this paper aims to construct approximate solutions exploiting symmetries. Even to close this section, we will recall some results about perturbation theory and formal large  $N$  results in the symmetric phase which will be relevant for the rest of this paper. Figure 2 summarizes the construction. At this stage, it should be necessary to remark:

**Remark 2** As explained in [56] for instance, the construction of the RG assumes that the number of degrees of freedom remains fixed by  $N$ , and the standard deviation  $\sigma$  for the matrix-like disorder is recalled after each RG transformation. More precisely, as we integrated out the momenta in the windows  $[\Lambda, s\Lambda]$ , we rescale  $\sigma$  by a factor  $s^{-1}$ , and we define the dimensionless standard deviation  $\bar{\sigma} := k\sigma$ . In this paper, we rescale the couplings by a suitable power of  $\bar{\sigma}$ , such that this parameter disappears from our flow equations. This is done explicitly in the reference [56] and this is also assumed in the reference [77] and reference therein. This is equivalent to describing the flow with respect to the referential that follows the flow of  $\bar{\sigma}$ . Note that the elimination of degrees of freedom is not strictly necessary for the RG construction, and as firstly pointed out by Wegner, a suitable change of variables could effectively accomplish the same thing – see [78–80] and reference therein. Note that one can easily construct the relation between the point of view of this paper and the point of view where the number of effective degrees of freedom changes. Considering, for instance, the quartic theory, and as  $N_{\text{eff}}(k)$  and  $g_4(k)$  the effective degrees of freedom at the scale  $k$  and the corresponding effective quartic coupling, we find that has to be related with the effective quartic coupling  $u_4(k)$  for our point of view in this paper as (see also (3.25)):

$$\frac{1}{N_{\text{eff}}(k)}g_4(k) = \frac{1}{N} \underbrace{\left( \frac{N}{N_{\text{eff}}(k)}g_4(k) \right)}_{:=u_4(k)}, \quad (2.39)$$

where explicitly:

$$\frac{N_{\text{eff}}(k)}{N} = \int_0^{k^2} \rho(p^2)dp^2. \quad (2.40)$$

Because there is no real benefit for one or the other formulation (in particular, the canonical dimensions depend on the scale in both cases), we assume their equivalents.

## 2.5 Perturbation theory and large $N$ closed equations

Perturbation theory for the averaged replicated theory can be constructed accordingly with the standard Feynman rules, and Feynman diagrams look again as a set of vertices materializing interactions involved in the classical averaged action (2.31) and edges materializing Wick contractions. However, the theory we consider distinguishes from ordinary QFT by the specific non-localities of interactions regarding the underlying  $O(N)$  symmetry, from the time non-locality, and from replica indices structure. Then we have to construct graphical rules to represent Feynman graphs accommodating these three specificities. We will adopt the same convention as in our previous paper [11], itself inspiring from [58]. Vertices are realized by sets of black nodes, corresponding to the fields  $x_\alpha$ , linked together by solid edges representing Euclidean scalar products of vectors, explicitly:

$$\bullet \text{---} \bullet \equiv \sum_{i=1}^N x_{i\alpha}(t)x_{i\alpha}(t). \quad (2.41)$$





cycle is nothing but a sum over a path involving the product of propagators, which are diagonal in the basis  $u^{(\mu)}$ . Hence, a given face  $f$  with length  $n$  involves the contribution:

$$\sum_{\mu=1}^N \prod_{i=1}^n \tilde{C}(\omega_i, p_\mu^2) \rightarrow N \left( \int_0^{+4\sigma} \rho(p^2) dp^2 \prod_{i=1}^n \tilde{C}(\omega_i, p^2) \right), \quad (2.43)$$

and then shares a global factor  $N$ . Then, considering some Feynman graph  $\mathcal{G}$ , denoting as  $V_{2s}$  the number of vertices of valence  $2s$  and  $F$  the number of faces, the corresponding Feynman amplitude scale as:

$$\mathcal{A}(\mathcal{G}) \sim N^{-\sum_s (s-1)V_{2s} + F}. \quad (2.44)$$

The leading order (LO) graphs, in the large  $N$  limit, are then those that maximize the number of faces, keeping fixed the number of vertex, and taking into account all the constraints imposed by the external dashed edges. For the quartic theory, the structure of these LO graphs is more transparent using the *loop vertex representation* (LVR) [17, 55, 81–83]. In those representations, vertices look like edges and vertices as closed loops; and LO diagrams are trees.

To conclude, let us recall the main results obtained in our previous work for  $p = 3$  [11]. The self-energy is diagonal in the basis  $\{u^{(\mu)}\}$ , and in the large  $N$  limit, the diagonal elements  $\gamma(\omega)$  depend only on the external frequency  $\omega$ . Hence, focusing on a deterministic quartic potential, we get:

$$\begin{aligned} \gamma(\Omega) = & - \int \frac{d\omega}{2\pi} \rho(p^2) dp^2 \left( \frac{\hbar^2}{6} G_k(\omega, p_\mu, p_\mu, \alpha) \right. \\ & \left. - 6\lambda \int \rho(q^2) dq^2 G_k(\omega, p, p, \alpha) G_k(-\omega - \Omega, q, q, \alpha) \right), \end{aligned} \quad (2.45)$$

which can be generalized for higher order local potential [23]. Here,  $G_k(\omega, p_\mu, p_\mu, \alpha)$  is the effective propagator (including regulator):

$$G_k(\omega, p_\mu, p_\nu, \alpha) = \frac{\delta_{\mu\nu}}{\omega^2 + p_\mu^2 + m^2 - \gamma(\omega) - R_k(p_\mu^2) + i\epsilon}. \quad (2.46)$$

Another relevant quantity is the 1PI 2-point correlation between replica:

$$q_{\mu,\nu,\alpha\beta}(t, t') := \langle x_{\mu,\alpha}(t) x_{\nu,\beta}(t') \rangle_{\text{1PI}}, \quad (2.47)$$

which is a  $\mathcal{O}(N^{-1})$  quantity, satisfying the equation at the leading order of the  $1/N$  expansion (in Fourier space):

$$q_{\alpha\beta}(\Omega, \Omega') = \frac{12\lambda}{N} \int \rho(p^2) dp^2 \left( \int d\omega G_k(\omega, p, p, \alpha) \right)^2 \delta(\Omega) \delta(\Omega'). \quad (2.48)$$

## 2.6 Scaling and dimensions

To conclude these preliminary, let us discuss the notion of dimension. Usually, the dimension is fixed by extra-structures like background space-time. Here this structure is of dimension 1, and the dimensions for couplings are fixed by the requirement that the classical action (divided by  $\hbar$ ) is dimensionless, and in units with  $\hbar = 1$  we get:

$$[m^2] = 2, \quad [\lambda] = 4, \quad [h_2] = 3. \quad (2.49)$$

Usually for standard QFT, the dimensions of the couplings are related to the properties of the flow near the Gaussian fixed point. This relation between the dimension (fixed by the background space) and the behavior of the flow arises because coarse-graining is performed along the spectrum of the Laplacian (for Euclidean theories), which is itself an operator defined on the manifold. Here the situation is different. The spectrum along which we perform the coarse-graining description is for the matrix  $K$ , which is not related to the extra temporal dimension. Furthermore, the shape of the momenta distribution does not behave accordingly with a power law, as is usually the case. For such a kind of theory, for which the coarse-graining is not related to some background space, a dimension can be defined also, from the behavior of the flow near the Gaussian fixed point [17, 56, 84], up to a global rescaling of couplings in order to cancel the global  $k$ -dependency of the effective loop integrals. Because the shape of the momentum distribution does not follow a power law, the dimension defined in this way depends on the energy scale, which has been also encountered in other theories – see for instance [85] in the context of tensorial field theories.

First of all, note that vertex expansion of the Wetterich equation (2.36) involve the sum of diagrams made of a single loop, of the form (setting to zero external frequencies):

$$L_n(k) := \int d\omega \int_0^{4\sigma} dp^2 \rho(p^2) \dot{R}_k(p^2) \prod_{i=1}^n G(\omega, p, p, \alpha), \quad (2.50)$$

where we assumed the limit  $\beta \rightarrow \infty$ . As  $k \ll 1$ , because the selected windows of momenta is around  $k$  (and precisely between 0 and  $k$  we the Litim regulator), we can approximate  $\rho(p^2)$  by  $(p^2)^{\frac{1}{2}}/(2\pi\sigma^2)$ . In this limit, the dependency of the integral  $L_n(k)$  follows a power law, corresponding exactly to what we obtain for a 4-dimensional field theory, as expected, and the asymptotic dimensionless couplings as to be:

$$\bar{\mu}_{2n} = k^{-\omega_{2n}} \mu_{2n}, \quad \bar{\lambda} = k^{-\nu} \lambda, \quad (2.51)$$

with, dot  $p = 3$ :

$$\omega_{2n} = 4 - 2n, \quad \nu = -1, \quad (2.52)$$

which are respectively the *IR canonical dimensions* for  $\mu_{2n}$  and  $\lambda$  respectively.

The canonical dimension for arbitrary  $k$  is non-trivial, and we return on this issue in section 5. We can however define it easily for the critical theory, or in the perturbative regime, assuming the influence of the mass irrelevant on the denominator of effective propagators  $G(\omega, p, p, \alpha)$ . In this way, each loops involve the integral:

$$\Omega'(k) := k^3 \int dp^2 \frac{\rho(p^2) \dot{R}_k(p^2)}{(p^2 + R_k(p^2))^{3/2}} = \frac{8k^5}{3\pi\sqrt{4 - k^2}}, \quad (2.53)$$

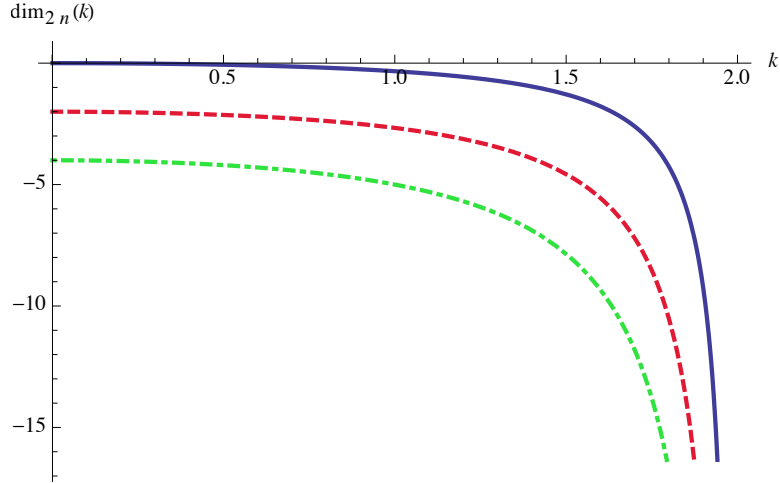


Figure 4: Dependency on critical canonical dimensions ( $\sigma = 1$ ) for  $n = 2$  (solid blue curve),  $n = 3$  (dashed red curve) and  $n = 4$  (dashed-dotted green curve).

and to cancel the explicit dependency on  $k$  on the loops, it is suitable to define the dimensionless couplings such that:

$$\bar{\mu}_{2n} = \mu_{2n} \frac{1}{k^2} \left( \frac{\Omega'(k)}{k^3} \right)^{n-1}. \quad (2.54)$$

Within this definition, the linear part of flow equations reads:

$$\dot{\bar{u}}_{2n} = -\text{dim}_{2n}(k) \bar{u}_{2n} + \dots, \quad (2.55)$$

and a straightforward calculation leads to:

$$\boxed{\text{dim}_{2n}(k) := (n-1)\text{dim}_4(k) + 2(2-n)}, \quad (2.56)$$

and:

$$\boxed{\text{dim}_4(k) := \frac{d}{dt} \ln (k^5(\Omega')^{-1}(k)) = \frac{k^2}{k^2-4}}. \quad (2.57)$$

Let us notice that as  $k \rightarrow 0$ , we recover the previous result:

$$\text{dim}_{2n}(k) = \omega_{2n} + \frac{k^2}{4} (1-n) + \mathcal{O}(k^3), \quad (2.58)$$

as expected. It differs significantly from the ordinary  $4D$  power counting when we go back up the flow towards the UV, as Figure 4 shows.

### 3 Ward identities and anomalous dimension

In the first part of this section, we discuss the constraints on the RG flow arising because of the Ward identities. In particular, because of the Gauge fixing (2.15), the  $O(N)$

symmetry is explicitly broken by the kinetic action, and Ward identities corresponding to the underlying  $O(N)$  symmetry of the original model become non-trivial. This first part follows the discussions of [56, 73], themselves inspiring from [17]. In the second part, we discuss an improvement of the standard vertex expansion considered in [11] and called *effective vertex expansion*, which exploit the large  $N$  relations between observables to close the hierarchy of the flow equations – see [17, 55].

### 3.1 Ward identities for internal symmetries

The Ward identities related to some classical transformations can be classified into two categories:

- Type 1 transformations, which left the path integral measure invariant but not the classical action.
- Type 2 transformations, which left both the path integral measure and the classical action invariant.

Usually, these two kinds of transformation provide different kinds of Ward identities. For transformations of the second kind, the variation of the path integral reads:

$$\begin{aligned} \langle \delta \mathcal{J} \rangle &= \int_{-\infty}^{\infty} dt \sum_{k=1, \alpha=1}^{N, n} L_{k, \alpha}(t) \delta \langle x_{k, \alpha}(t) \rangle \\ &= \int_{-\infty}^{\infty} dt \sum_{k=1, \alpha=1}^{N, n} \frac{\delta \Gamma}{\delta \langle x_{k, \alpha}(t) \rangle} \delta \langle x_{k, \alpha}(t) \rangle = \delta \Gamma = 0, \end{aligned} \quad (3.1)$$

but we are mainly interested in transformations arising from transformations of the first kind in this paper (see remark 3.1 at the end of the subsection).

The original model – before averaging and gauge fixing – is invariant under  $O(N)$  transformations because of the formal translation invariance of the path integral measure and the  $O(N)$  invariance of the probability densities for  $J$  and  $K$ . As we stated before, the Gauge fixing breaks explicitly the  $O(N)$  symmetry of the classical action. Note that the averaging over  $J$  introduce an additional subtlety. The interaction part of the classical action, that we denote  $\overline{S_{\text{cl, int}}[\{\mathbf{x}_\alpha\}]}$  (i.e. the terms involving power of the field higher than 2) is again invariant under *global rotations* acting independently on the different replica:

$$x_{\mu, \alpha} \rightarrow x'_{\mu, \alpha} = \sum_{\nu=1}^N O_{\mu\nu} x_{\nu, \alpha}, \quad \forall \alpha. \quad (3.2)$$

In addition one can consider rotations acting differently on the replica, what we call *local rotations*, namely:

$$x_{\mu, \alpha} \rightarrow x'_{\mu, \alpha} = \sum_{\nu=1}^N O_{\mu\nu}^{(\alpha)} x_{\nu, \alpha}. \quad (3.3)$$

The interaction part of the classical action  $\overline{S_{\text{cl,int}}}[\{\mathbf{x}_\alpha\}]$  is invariant under global rotations but not under the local ones. The partition function however is still invariant in both cases because of the formal translation invariance of the measure [86, 87]. Let us formalize these observations.

To begin, let us consider the global transformation (3.2). We will compute the infinitesimal transformation of the partition function corresponding to some infinitesimal rotation:

$$O_{\mu\nu} = \delta_{\mu\nu} + \varepsilon_{\mu\nu} + \mathcal{O}(\varepsilon^2), \quad (3.4)$$

where  $\varepsilon_{\mu\nu}$  are the entries of a skew-symmetric matrix,  $\varepsilon_{\mu\nu} = -\varepsilon_{\nu\mu}$ . Denoting as  $\overline{S_{\text{cl,int}}}[\{\mathbf{x}_\alpha\}]$  and  $\overline{S_{\text{cl,kin}}}[\{\mathbf{x}_\alpha\}]$  respectively the interacting and the kinetic parts of the classical action  $\overline{S_{\text{cl,int}}}[\{\mathbf{x}_\alpha\}]$ , the variation (at order  $\varepsilon$ ) of the partition function  $\overline{\mathcal{Z}_{\beta,k}^n[K, J, \{\mathbf{L}_\alpha\}]}$  reads (let us recall that  $\hbar = 1$ ):

$$\delta \overline{\mathcal{Z}_{\beta,k}^n[K, J, \{\mathbf{L}_\alpha\}]} = \int \prod_{\alpha=1}^n [\mathcal{D}x_\alpha(t)] [-\delta \overline{S_{\text{cl,kin}}}[\{\mathbf{x}_\alpha\}] + \delta \mathcal{J}] e^{-(\overline{S_{\text{cl}}}[\{\mathbf{x}\}] + \Delta S_k[\{\mathbf{x}_\alpha\}] + \mathcal{J})} \equiv 0, \quad (3.5)$$

the last equality arises because of the formal invariance of the path integral measure from global translation. Furthermore,  $\delta \overline{S_{\text{cl,int}}}[\{\mathbf{x}_\alpha\}] = 0$  because interactions are explicitly invariants. We then have to compute each variation explicitly. For the source term  $\mathcal{J}$ , we get:

$$\begin{aligned} \delta \mathcal{J} &= \int_{-\beta/2}^{+\beta/2} dt \sum_{\mu,\nu,\alpha=1}^{N,n} L_{\mu,\alpha}(t) x_{\nu,\alpha}(t) \varepsilon_{\mu\nu} \\ &= \frac{1}{2} \int_{-\beta/2}^{+\beta/2} dt \sum_{\mu,\nu,\alpha=1}^{N,n} (L_{\mu,\alpha}(t) x_{\nu,\alpha}(t) - L_{\nu,\alpha}(t) x_{\mu,\alpha}(t)) \varepsilon_{\mu\nu}, \end{aligned} \quad (3.6)$$

where for the second line we exploited the symmetries of the matrix  $\varepsilon$ . Now, let us compute the variation of the kinetic action. Because the contribution  $\dot{\mathbf{x}}^2$  is  $O(N)$  invariant, as well as the mass term, the relevant contribution comes from the regulator  $\Delta S_k$  and from the effective kinetics arising because matrix  $K$ . We get:

$$\begin{aligned} \delta \overline{S_{\text{cl,kin}}}[\{\mathbf{x}_\alpha\}] &= \int_{-\beta/2}^{+\beta/2} dt \sum_{\mu,\alpha} (p_\mu^2 + R_k^{(N)}(p_\mu^2)) x_\nu(t) x_\mu(t) \varepsilon_{\mu\nu} \\ &= \frac{1}{2} \int_{-\beta/2}^{+\beta/2} dt \sum_{\mu,\nu,\alpha} (p_\mu^2 + R_k^{(N)}(p_\mu^2) - p_\nu^2 - R_k^{(N)}(p_\nu^2)) x_\nu(t) x_\mu(t) \varepsilon_{\mu\nu}, \end{aligned} \quad (3.7)$$

and the total variation of the partition function reads finally:

$$\begin{aligned} &\int_{-\beta/2}^{+\beta/2} dt \sum_{\mu,\nu,\alpha} \varepsilon_{\mu\nu} \left[ (p_\mu^2 + R_k^{(N)}(p_\mu^2) - p_\nu^2 - R_k^{(N)}(p_\nu^2)) \frac{\delta^2}{\delta L_{\mu,\alpha}(t) \delta L_{\nu,\alpha}(t)} - \right. \\ &\quad \left. - L_{\mu,\alpha}(t) \frac{\partial}{\partial L_{\nu,\alpha}(t)} + L_{\nu,\alpha}(t) \frac{\partial}{\partial L_{\mu,\alpha}(t)} \right] \exp \left( \mathcal{W}_{\beta,k}^{(n)}[K, J, \mathcal{L}] \right) = 0. \end{aligned} \quad (3.8)$$

This result should be true for any infinitesimal element of the Lie algebra  $\varepsilon \in \mathfrak{so}(N)$ , and because the variation in front has been suitably skew-symmetrized, we have the following statement:

**Theorem 2** *The observable of the gauged and averaged theory satisfies the identity:*

$$\int_{-\beta/2}^{+\beta/2} dt \sum_{\alpha} \left[ \left( p_{\mu}^2 + R_k^{(N)}(p_{\mu}^2) - p_{\nu}^2 - R_k^{(N)}(p_{\nu}^2) \right) \frac{\delta^2}{\delta L_{\mu,\alpha}(t) \delta L_{\nu,\alpha}(t)} - L_{\mu,\alpha}(t) \frac{\partial}{\partial L_{\nu,\alpha}(t)} + L_{\nu,\alpha}(t) \frac{\partial}{\partial L_{\mu,\alpha}(t)} \right] \exp \left( \mathcal{W}_{\beta,k}^{(n)}[K, J, \mathcal{L}] \right) = 0. \quad (3.9)$$

Now let us consider local rotations. The group of local rotations is  $(O(N))^n$  i.e.  $n$  copies of the rotation group, and a local rotation is a set  $\mathcal{R}_O^{(n)} := (O_1, O_2, \dots, O_n)$  of  $n$  independent rotations. We then consider an infinitesimal rotation along the component  $\alpha$  only:

$$\mathcal{R}_O^{(n)} = (\mathbf{I}, \dots, \mathbf{I} + \varepsilon_{\alpha}, \dots, \mathbf{I}) + \mathcal{O}(\varepsilon^2), \quad (3.10)$$

where  $\mathbf{I}$  denotes the  $N \times N$  identity matrix. The deterministic potential is invariant again, but the non-local one is not. The variation of the interacting action then reads at the first order in  $\varepsilon_{\alpha}$ :

$$\overline{S_{\text{cl,int}}[\{\mathbf{x}_{\alpha}\}]} = q\lambda \times \int dt dt' \sum_{\beta, \mu, \nu} (X_{\alpha\beta})^{q-1} (x_{\mu',\alpha}(t) x_{\mu,\beta}(t') - x_{\mu,\alpha}(t) x_{\mu',\beta}(t')) \varepsilon_{\alpha,\mu\nu}, \quad (3.11)$$

where:

$$X_{\alpha\beta}(t, t') := \frac{1}{N} \sum_{\mu=1}^N x_{\mu,\alpha}(t) x_{\mu,\beta}(t'). \quad (3.12)$$

Then, this term adds to the global variation, and because we skew-symmetrized the contracted tensor with  $\varepsilon_{\alpha,\mu\nu}$ , we have the following statement:

**Theorem 3** *Because of the breaking of the local Gauge invariance due to the averaging over disorder, the gauged and averaged theory satisfy furthermore the identity:*

$$\int_{-\beta/2}^{+\beta/2} dt \left[ \left( p_{\mu}^2 + R_k^{(N)}(p_{\mu}^2) - p_{\nu}^2 - R_k^{(N)}(p_{\nu}^2) \right) \frac{\delta^2}{\delta L_{\mu,\alpha}(t) \delta L_{\nu,\alpha}(t)} - L_{\mu,\alpha}(t) \frac{\partial}{\partial L_{\nu,\alpha}(t)} + L_{\nu,\alpha}(t) \frac{\partial}{\partial L_{\mu,\alpha}(t)} \right] \exp \left( \mathcal{W}_{\beta,k}^{(n)}[K, J, \mathcal{L}] \right) - q\lambda \times \int dt dt' \sum_{\gamma} \langle (X_{\alpha\gamma})^{q-1} (x_{\mu',\alpha}(t) x_{\mu,\gamma}(t') - x_{\mu,\alpha}(t) x_{\mu',\gamma}(t')) \rangle = 0. \quad (3.13)$$

**Remark 3** *In addition to internal  $O(N)$  global and local symmetries, there are external symmetries, arising because of the existence of extra-structure like space-time manifold. In our case, because space-time has dimension 1, transformations reduce to translations,*

dilatation, or general time re-parametrization. Note that classically the choice of the time parameter is closely related to the existence of a preferred equilibrium thermodynamic state, and must be viewed in the non-relativistic quantum mechanics as a property of Von-Neumann algebra [88, 89]. The theory can be also formulated in a purely covariant manner (i.e. including time in the set of coordinates). The parametrization invariance then imposes a constraint on the Hilbert space, and solving it is exactly equivalent to imposing Schrödinger equation; this leads essentially to translation or dilatation transformations:

$$t \rightarrow t' = t + t_0, \quad t \rightarrow t' = K_0 \times t. \quad (3.14)$$

To these transformations we have to add also Galilean transformations, mixing both time and the coordinates field  $\mathbf{x}$ :

$$x_\mu \rightarrow x'_\mu = x_\mu - (\mathbf{V} \cdot \mathbf{e}_\mu)t, \quad (3.15)$$

where  $\mathbf{e}_\mu$  is the unit vector along direction  $\mu$  and  $\mathbf{V}$  the velocity of the relative frame.

### 3.2 Time reversal symmetric relations between observables

The global Ward identity given by theorem 2 can be rewritten as, using Fourier variables:

$$\sum_\omega \sum_\alpha \left[ \delta E_k(p_\mu^2, p_\nu^2) (G_k(\omega, p_\mu, p_\nu) + M_{\mu,\alpha}(\omega) M_{\nu,\alpha}(-\omega)) - \right. \\ \left. - L_{\mu,\alpha}(\omega) M_{\nu,\alpha}(-\omega) + L_{\nu,\alpha}(\omega) M_{\mu,\alpha}(-\omega) \right] = 0, \quad (3.16)$$

where:

$$\delta E_k(p_\mu^2, p_\nu^2) := p_\mu^2 + R_k^{(N)}(p_\mu^2) - p_\nu^2 - R_k^{(N)}(p_\nu^2), \quad (3.17)$$

and:

$$M_{\mu,\alpha}(\omega) := \frac{\delta \mathcal{W}_{\beta,k}^{(n)}}{\delta L_{\mu,\alpha}(-\omega)}, \quad G_k(\omega, p_\mu, p_\nu) \delta_{\omega,-\omega'} := \frac{\delta^2 \mathcal{W}_{\beta,k}^{(n)}}{\delta L_{\mu,\alpha}(-\omega') \delta L_{\nu,\alpha}(\omega)}. \quad (3.18)$$

Note that we omitted the index  $\alpha$  with respect to the definition (2.37) to simplify the notations. Using this definition, and taking derivatives with respect to  $M_{\mu_1,\alpha}(\omega_1)$  and  $M_{\mu_2,\alpha}(\omega_2)$ , we have<sup>4</sup>:

$$\sum_\omega \sum_{p_\sigma, p_{\sigma'}} \left[ \delta E_k(p_\mu^2, p_\nu^2) \left( - G_k(\omega, p_\mu, p_\sigma) \Gamma_{k,p_\sigma, p_{\sigma'}, p_{\mu_1}, p_{\mu_2}}^{(4)}(\omega, -\omega, \omega_1, \omega_2) G_k(\omega, p_{\sigma'}, p_\sigma) \right. \right. \\ \left. \left. + (\delta_{\mu_1} \delta_{\nu_2} \delta_{\omega, \omega_1} \delta_{-\omega, \omega_2} + \delta_{\mu_2} \delta_{\nu_1} \delta_{-\omega, \omega_1} \delta_{\omega, \omega_2}) \right) - \frac{\delta L_{\mu,\alpha}(\omega)}{\delta M_{\mu_1,\alpha}(\omega_1)} \delta_{\nu_2} \delta_{\omega_2, -\omega} \right. \\ \left. - \frac{\delta L_{\mu,\alpha}(\omega)}{\delta M_{\mu_2,\alpha}(\omega_2)} \delta_{\nu_1} \delta_{\omega_1, -\omega} + \frac{\delta L_{\nu,\alpha}(-\omega)}{\delta M_{\mu_1,\alpha}(\omega_1)} \delta_{\mu_2} \delta_{\omega_2, \omega} + \frac{\delta L_{\nu,\alpha}(-\omega)}{\delta M_{\mu_2,\alpha}(\omega_2)} \delta_{\mu_1} \delta_{\omega_1, \omega} \right] = 0. \quad (3.19)$$

<sup>4</sup>We assume that  $G_k(\omega, p_\mu, p_\nu)$  is an even function with respect to its variables, and depends on  $\omega^2$ ,  $p_\mu^2$  and  $p_\nu^2$ . In the same way we assume that  $\Gamma_k^{(2)}(p^2, \omega)$  depends only on  $\omega^2$  (time-reversal symmetry).

The functional derivatives of the source field (at the fixed classical field), can be computed from the Legendre transform properties [90] and we get, for instance, imposing the external field vanishes on the right-hand side:

$$\frac{\delta L_{\mu,\alpha}(\omega)}{\delta M_{\mu_2,\alpha}(\omega_2)} = \delta_{\mu,\mu_2} \delta_{\omega,\omega_2} \left( \Gamma_k^{(2)}(p_\mu^2, \omega) + R_k^{(N)}(p_\mu^2) \right), \quad (3.20)$$

and imposing that source field vanishes on the left-hand side of equation (3.19), we get:

$$\begin{aligned} & \sum_{\omega} \sum_{p_\sigma, p_{\sigma'}} \left[ \delta E_k(p_\mu^2, p_\nu^2) \left( -G_k(\omega, p_\mu, p_\sigma) \Gamma_{k,p_\sigma,p_{\sigma'},p_{\mu_1},p_{\mu_2}}^{(4)}(\omega_1, \omega_2, \omega, -\omega, ) G_k(\omega, p_{\sigma'}, p_\sigma) \right. \right. \\ & \left. \left. + (\delta_{\mu\mu_1} \delta_{\nu\mu_2} \delta_{\omega,\omega_1} \delta_{-\omega,\omega_2} + \delta_{\mu\mu_2} \delta_{\nu\mu_1} \delta_{-\omega,\omega_1} \delta_{\omega,\omega_2}) \right) \right. \\ & \left. + \delta_{\mu\mu_1} \delta_{\nu\mu_2} \delta_{\omega,\omega_1} \delta_{-\omega,\omega_2} \left( \Gamma_k^{(2)}(p_\nu^2, \omega) + R_k^{(N)}(p_\nu^2) - \Gamma_k^{(2)}(p_\mu^2, \omega) - R_k^{(N)}(p_\mu^2) \right) \right. \\ & \left. + \delta_{\mu\mu_2} \delta_{\nu\mu_1} \delta_{-\omega,\omega_1} \delta_{\omega,\omega_2} \left( \Gamma_k^{(2)}(p_\nu^2, \omega) + R_k^{(N)}(p_\nu^2) - \Gamma_k^{(2)}(p_\mu^2, \omega) - R_k^{(N)}(p_\mu^2) \right) \right]. \quad (3.21) \end{aligned}$$

In the symmetric phase, the propagator is diagonal with respect to generalized momenta,

$$G_k(\omega, p_\mu, p_\nu) =: \tilde{G}(p_\mu^2, \omega^2) \delta_{\mu\nu}; \quad (3.22)$$

then, sending  $p_\mu^2 - p_\nu^2 = \delta p^2 \rightarrow 0$  we get, assuming  $\omega_1 = -\omega_2$ :

$$\begin{aligned} & (\delta_{\mu\mu_1} \delta_{\nu\mu_2} + \delta_{\mu\mu_2} \delta_{\nu\mu_1}) \left[ \left( 1 + \frac{R_k^{(N)}(p_\mu^2) - R_k^{(N)}(p_\nu^2)}{\delta p^2} \right) \tilde{G}_k(p_\mu^2, \omega_1^2) \right. \\ & \left. \times A_{k,p_\mu,p_\nu,p_{\mu_1},p_{\mu_2}}(\omega_1, \omega_2, \omega) \tilde{G}_k(p_\nu^2, \omega_2^2) - \frac{\Sigma_k(p_\mu^2, \omega_1^2) - \Sigma_k(p_\nu^2, \omega_1^2)}{\delta p^2} = 0 \right], \quad (3.23) \end{aligned}$$

where we used the standard definition for self-energy:

$$\Gamma_k^{(2)}(p_\mu^2, \omega^2) = \omega^2 + p_\mu^2 + \mu_1 - \Sigma(p_\mu^2, \omega^2). \quad (3.24)$$

Furthermore, we assumed the frequency conservation for  $\Gamma_k^{(4)}$ :

$$\Gamma_{k,p_{\mu_1},p_{\mu_2},p_{\mu_3},p_{\mu_4}}^{(4)}(\omega_1, \omega_2, \omega_3, \omega_4) := \delta(\omega_1 + \omega_2 + \omega_3 + \omega_4) A_{k,p_{\mu_1},p_{\mu_2},p_{\mu_3},p_{\mu_4}}(\omega_1, \omega_2, \omega_3).$$

In the local potential approximation,

$$A_{k,p_{\mu_1},p_{\mu_2},p_{\mu_3},p_{\mu_4}}(\omega_1, \omega_2, \omega_3) =: \frac{8u_4(k)}{N} (\delta_{\mu_1\mu_2} \delta_{\mu_3\mu_4} + \delta_{\mu_1\mu_3} \delta_{\mu_2\mu_4} + \delta_{\mu_1\mu_4} \delta_{\mu_2\mu_3}). \quad (3.25)$$

This approximation may seem questionable since it ignores the dependence of the vertices on external frequencies. However, since the theory is just renormalizable, one can expect these contributions to be irrelevant, so that in the vicinity of the Gaussian point, and asymptotically in the IR, this approximation is justified [71]. Note that in the large



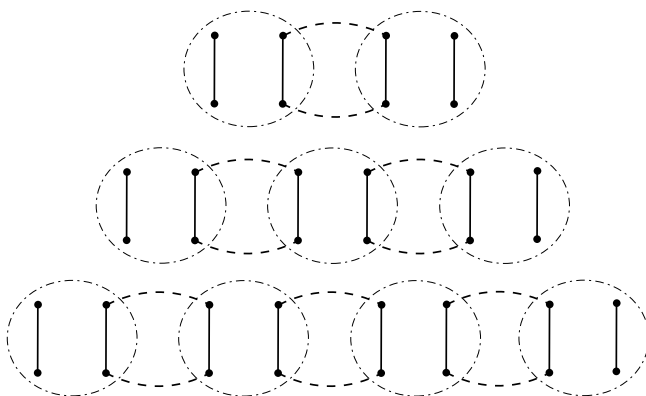


Figure 5: Leading order contribution to the quartic effective vertex.

$N$  limit, no dependency with respect to the external generalized momenta is expected, because of the leading order diagrams structure (see Figure 5 and [77]). Setting  $\mu_1 = \mu$ ,  $\mu_2 = \nu$  ( $\mu \neq \nu$ ) local approximation leads to, at the leading order with respect to  $\delta p^2$ :

$$\boxed{\frac{8u_4(k)}{N} \left( 1 + \frac{R_k(p_\mu^2) - R_k(p_\nu^2)}{\delta p^2} \right) \tilde{G}_k^2(p_\mu^2, \omega_1^2) - \frac{\Sigma_k(p_\mu^2, \omega_1^2) - \Sigma_k(p_\nu^2, \omega_1^2)}{\delta p^2} = \mathcal{O}(\delta p^2)}. \quad (3.26)$$

This equation shows that the variation of the self-energy with respect to the generalized moment is next to the leading order ( $\mathcal{O}(1/N)$ ), which is indeed expected. Because of the  $1/N$  factor in front of the left-hand side, the propagator can be computed in the leading order,

$$\tilde{G}_k(p_\mu^2, \omega_1^2) = \frac{1}{\omega_1^2 + p_{\mu_1}^2 + u_2(k)}, \quad (3.27)$$

where  $u_2(k)$  is the large  $N$  effective mass, which is fixed by a closed equation recalled in [11]. Taking the limit  $\delta p^2 \rightarrow 0$ , and defining the wave function renormalization  $Z(k)$  as:

$$Z(k, \omega^2) := \frac{d}{dp_\mu^2} \tilde{G}^{-1}(p_\mu^2, \omega^2) \Big|_{p_\mu=0} = 1 - \frac{d}{dp_\mu^2} \Sigma(p_\mu^2, \omega^2) \Big|_{p_\mu=0}. \quad (3.28)$$

Finally, setting to zero the external momenta:

$$\boxed{\frac{8u_4(k)}{N} \frac{1 + R'_k(0)}{(\omega^2 + \mu_2(k))^2} + Z(k, \omega^2) - 1 = 0}. \quad (3.29)$$

## 4 Effective vertex expansion

The vertex expansion we constructed in our previous work is assumed good enough for such a kind of theory, for which in the deep IR the local quartic interactions are just-renormalizable. For a similar context, we for instance show a good agreement between

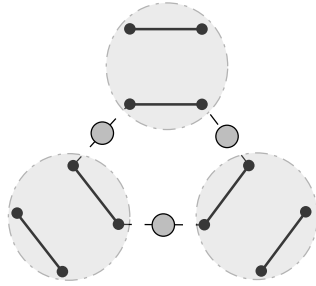


Figure 6: Structure of the effective 6-point function in the large  $N$  limit for the local quartic theory (in the symmetric phase). Dashed edges with grey discs are the effective 2-point function  $G_k$  and the grey bubble with valence 4 materialize the 4-point function  $\Gamma_k^{(4)}$ .

the leading order vertex expansion and advanced method in [56, 73]. We expect this good agreement because, close enough to the Gaussian fixed point and far enough from the deep UV scale, the irrelevant couplings become invaluable. In the large  $N$  limit and in the symmetric phase, it is however suitable to make use of the non-trivial Schwinger-Dyson relation arising between local observables. This method was first introduced in the context of tensorial field theories [17], whose non-localities recall the one we encounter here, and also applied in [55] in the spin glass context.

The kind of relation we expect is pictured in Figure 6, for a local quartic theory, and the figure shows the large  $N$  exact 6-point function. In this section, we mainly focus on the sextic theory with rank 3 disorder tensor. The relevant effective diagrams and numerical factors have been computed in the companion paper [64], and we are just going to use the results from this paper. Accordingly, with the notations of this reference, we denote as  $\Gamma_{k,L}^{(6)}$  and  $\Gamma_{k,NL}^{(6)}$  respectively the local and non-local sextic effective vertices, and we have, graphically:

$$\begin{aligned}
 \Gamma_{k,L}^{(6)} = & \text{Diagram 1} + \text{Diagram 2} + \text{Diagram 3} + \text{Diagram 4} + \text{Diagram 5} \\
 & + \text{Diagram 6} + \text{Diagram 7} + \text{Diagram 8}, \tag{4.1}
 \end{aligned}$$

and

$$\Gamma_{k,\text{NL}}^{(6)} = \text{Diagram} \quad (4.2)$$

Note that the last relation means nothing but the non-local vertex does not renormalize. Diagrams can be computed using the leading order of the derivative expansion and the local approximation for vertices. We then obtain a relation between the UV local and non-local couplings  $u_6(0)$ ,  $\tilde{u}_6(0)$  and the effective local coupling  $u_6(k)$  in the deep IR<sup>5</sup>:

$$u_6(0) = k^{-2} \frac{\tilde{u}_6(k) - 24L_3(\tilde{u}_2)\tilde{u}_4^3 + \tilde{u}_6(0) (12\tilde{u}_4^3\tilde{L}_4(\tilde{u}_2) - 8\tilde{u}_4^2\tilde{L}_3(\tilde{u}_2) + 3\tilde{u}_4\tilde{L}_2(\tilde{u}_2))}{1 - 12\tilde{u}_4^3L_2^3(\tilde{u}_2) + 8\tilde{u}_4^2L_2^2(\tilde{u}_2) - 3\tilde{u}_4L_2(\tilde{u}_2)}, \quad (4.3)$$

where:

$$\tilde{L}_2 := \frac{1}{6\pi^3(1 + \tilde{u}_2)^2}, \quad (4.4)$$

$$\tilde{L}_3 := \int \prod_{i=1}^2 \rho(p_{\mu_i}^2) dp_{\mu_i}^2 \int \frac{d\omega}{2\pi} G_k^2(p_{\mu_1}^2, \omega^2) G_k^2(p_{\mu_2}^2, \omega^2), \quad (4.5)$$

$$\tilde{L}_4 := \int \prod_{i=1}^3 \rho(p_{\mu_i}^2) dp_{\mu_i}^2 \int \frac{\prod_{i=1}^2 d\omega_i}{(2\pi)^2} G_k^2(p_{\mu_1}^2, \omega_1^2) G_k^2(p_{\mu_2}^2, \omega_2^2) G_k^2(p_{\mu_3}^2, (\omega_1 + \omega_2)^2), \quad (4.6)$$

$$L_2(\tilde{u}_2) := \frac{\frac{6}{\sqrt{\tilde{u}_2+1}} + \frac{2}{(\tilde{u}_2+1)^{3/2}} - 3 \left( \log \left( \frac{2\sqrt{\tilde{u}_2+1} + \tilde{u}_2 + 2}{64} \right) + 4 \right) - 6 \log(k)}{12\pi}, \quad (4.7)$$

$$L_3(\tilde{u}_2) := \frac{1 - \frac{1}{(1+\tilde{u}_2)^{5/2}}}{8\pi\tilde{u}_2}. \quad (4.8)$$

We furthermore recall the definition of effective couplings in the local sector:

$$\Gamma_k^{(2n)}(\{p_i, \omega_i\}) := \frac{u_{2n}}{(2n)!N^{n-1}} \delta \left( \sum_{i=1}^{2n} \omega_i \right) \sum_{\pi} \delta_{p_{\pi(1)}p_{\pi(2)}} \cdots \delta_{p_{\pi(2n-1)}p_{\pi(2n)}}, \quad (4.9)$$

where  $\pi$  denotes some permutation of the  $2n$  external indices. Note the presence of the logarithm, which dominates the flow in the deep IR. The flow equation for  $\tilde{u}_6$  can be derived from the observation that  $u_6(0)$  does not depend on  $k$ . Taking the derivative of (4.3) with respect to  $s := \ln k$ , we get:

$$\dot{\tilde{u}}_6 = (u_6 + a) \left( \frac{\dot{\tilde{u}}_2 \partial_{\tilde{u}_2} b + \dot{\tilde{u}}_4 \partial_{\tilde{u}_4} b}{b} + 2 \right) - (\dot{\tilde{u}}_2 \partial_{\tilde{u}_2} a + \dot{\tilde{u}}_4 \partial_{\tilde{u}_4} a) + 5a, \quad (4.10)$$

where we defined:

$$a(\tilde{u}_2, \tilde{u}_4) := -24L_3(\tilde{u}_2)\tilde{u}_4^3 + \tilde{u}_6(0) (12\tilde{u}_4^3\tilde{L}_4(\tilde{u}_2) - 8\tilde{u}_4^2\tilde{L}_3(\tilde{u}_2) + 3\tilde{u}_4\tilde{L}_2(\tilde{u}_2)), \quad (4.11)$$

$$b(\tilde{u}_2, \tilde{u}_4) := 1 - 12\tilde{u}_4^3L_2^3(\tilde{u}_2) + 8\tilde{u}_4^2L_2^2(\tilde{u}_2) - 3\tilde{u}_4L_2(\tilde{u}_2). \quad (4.12)$$

<sup>5</sup>We use the same notations as in [64], and  $u_6(0)$ ,  $\tilde{u}_6(0)$  here are the bare couplings i.e. the couplings in the deep UV, not in the deep IR. The context avoids ambiguities.

The first thing we can study is the presence of asymptotic fixed points. Indeed, if there cannot exist a global fixed point (including the coupling of disorder), there can exist “fixed trajectories” cancelling all the other  $\beta$  functions. We are mainly interested in fixed trajectories admitting a limit in the deep IR, and we will consider separately the sextic and quartic cases, admitting or not local sextic interactions at the level of the classical action. Let  $\text{Sol}(\bar{u}_2)$  the function obtained by substituting the solutions for  $\dot{\bar{u}}_2 = \dot{\bar{u}}_4 = 0$  into the  $\beta$  function for the sextic coupling. The two  $\beta$ -functions for  $\bar{u}_2$  and  $\bar{u}_4$  having been established in our previous work [11]:

$$\dot{\bar{u}}_2 = -2\bar{u}_2 - \frac{\bar{u}_4}{36\pi} \frac{1}{(1 + \bar{u}_2)^{\frac{3}{2}}}, \quad (4.13)$$

$$\dot{\bar{u}}_4 = -\frac{\bar{u}_6}{30\pi^2} \frac{1}{(1 + \bar{u}_2)^2} - \frac{\bar{u}_6}{60\pi} \frac{1}{(1 + \bar{u}_2)^{\frac{3}{2}}} + \frac{\bar{u}_4^2}{12\pi} \frac{1}{(1 + \bar{u}_2)^{\frac{5}{2}}}. \quad (4.14)$$

Figure 7 shows the behavior of the function  $\text{Sol}(\bar{u}_2)$  for the sextic and the quartic theory. Interestingly, no asymptotic fixed point is expected for the sextic theory, and the positive mass fixed point which appears in the IR regime disappears asymptotically as  $-\ln(k) \rightarrow \infty$ . In contrast, two fixed point solutions are found for the quartic theory, for the values:

$$\text{FP1} := \{\bar{u}_{2,\infty} \approx 0.003, \quad \bar{u}_{4,\infty} \approx -0.69, \quad \bar{u}_{6,\infty} \approx 2.37, \} \quad (4.15)$$

$$\text{FP1} := \{\bar{u}_{2,\infty} \approx -0.003, \quad \bar{u}_{4,\infty} \approx 0.68, \quad \bar{u}_{6,\infty} \approx 2.35, \} \quad (4.16)$$

the subscript  $\infty$  meaning  $-\ln(k) \rightarrow \infty$ . Their respective critical exponents (in the  $(\bar{u}_2, \bar{u}_4)$  plane) are moreover:

$$\Theta_{1,\infty} = \{\theta_1 \approx 2.87, \theta_2 \approx 0.04\}, \quad (4.17)$$

$$\Theta_{2,\infty} = \{\theta_1 \approx 1.17, \theta_2 \approx -0.03\}. \quad (4.18)$$

We have, however, some reasons to doubt the validity of the fixed point FP2. Indeed, the estimate of the local sextic coupling in the classical action remains quite large (about 0.002, against  $\approx 10^{-14}$  for the first fixed point). The characteristics of the first fixed point also correspond essentially to those that we had obtained by the truncation method in our previous work [11].

Finally, it is still easy to see that the finite-time singularity phenomenon also appears with the EVE, as shown in Figure 8, although the appearance of this singularity seems less abrupt than with the vertex expansion. In the Figure, we see that singular points, cusps, form as the disorder becomes significant, and for a disorder of the order of  $\bar{u}_6 \sim 10^5$  (the precise value depending on the initial conditions), the flow ends up developing a finite-time singularity. Our interpretation of these singularities follows the one we gave in our previous work and that we recalled in the introduction i.e. the consequence of the instability of the potential for some observable quantifying correlations between replicas, signalling that some interactions are missing from the perturbation theory.

In the rest of this article, we will explicitly highlight the relationship between these instabilities and the appearance of divergences, by considering a flow “improved” by observables correlating the replicas. For this, we will consider two different approximation

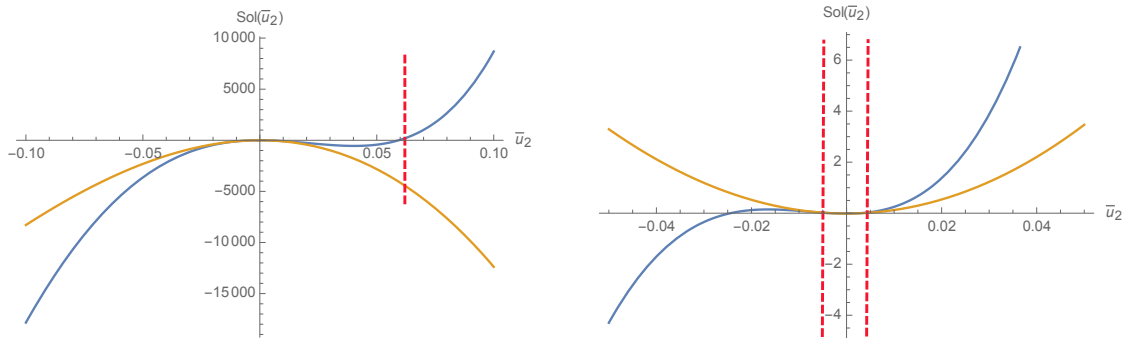


Figure 7: The function  $\text{Sol}(\bar{u}_2)$  for the sextic theory (on left) and the quartic theory (on right). We set  $\bar{\tilde{u}}_6 = -10$  for the blue and  $\bar{\tilde{u}}_6 = 0$  for yellow curves, respectively for  $k = 10^{-2}$  and  $k = 10^{-4}$ .

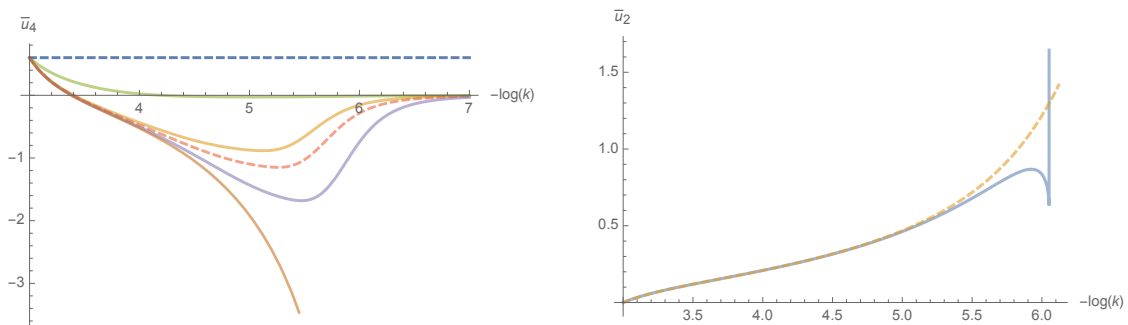


Figure 8: On the left: RG trajectories for initial conditions  $\bar{u}_2(k_0) = -10^{-5}$ ,  $\bar{u}_4(k_0) = 0.6$  and  $k_0 = 0.05$ . Respectively:  $\bar{\tilde{u}}_6(k_0) = 0$  (dashed blue curve),  $\bar{\tilde{u}}_6 = -498$  (yellow curve),  $\bar{\tilde{u}}_6(k_0) = -300$  (green curve),  $\bar{\tilde{u}}_6(k_0) = -508$  (dashed red curve) and  $\bar{\tilde{u}}_6(k_0) = -515$  (purple curve). The remaining curve is for the critical value  $\bar{\tilde{u}}_6(k_0) = -519.8$  and is singular for  $k_c \approx 0.002$ . On the right: Behavior of  $u_2(k)$  for  $\bar{\tilde{u}}_6(k_0) = -519.8$  (blue curve) and for  $\bar{\tilde{u}}_6(k_0) = -519.7$  just above the critical value (in dashed yellow).

schemes, the first will be a development around the vacuum of the local potential for uniform fields in the IR, and the second approximation will be a vertex expansion, similar to the one we built in our previous work [11]. In both cases, we will focus on the leading order of the derivative expansion, and neglect the flow of the anomalous dimension. This choice can be explained by the fact that the critical dimension is only asymptotically reached by the flow, and because of the  $N \rightarrow \infty$  limit.

## 5 Venturing beyond symmetric phase

In our previous work [11], as well as in the companion paper [64], we found that the presence of disorder leads to the appearance of “finite-scale” singularities. As we have pointed out, these singularities are probably a sign that interactions forbidden by perturbation theory (and notably correlations between replicas) become important. However, we have

chosen in our previous investigations to focus on the vertex expansion, and these singularities could also be related to the choice of an unstable vacuum. In this section, we propose to construct a different approximation, by expanding the non-local interactions around the vacuum of the local potential, in the limit  $N \rightarrow \infty$ .

## 5.1 Expansion around non-zero uniform local vacuum

The classical action looks at a multi-local expansion including local and bi-local interactions. If we put aside the derivative interactions, we can hope to construct a satisfactory approximation by keeping only the local and bi-local components of the effective action  $\Gamma_k$ . Note that correlations between replicas are not the only ones that we have “forgotten” in this treatment. Derivative interactions, for local potentials could also have an influence, and be as relevant as some effects at play in our study. However, since the local quartic sector is marginal in the deep IR, these effects are not necessarily expected to play a major role, although they may well be as large as some of the effects we seek to highlight. We will ignore derivative interactions completely in this paper, reserving their study for later work.

We will consider the construction of the flow in the deep IR ( $k \ll 1$ ). Instead of projecting the flow equations around the vacuum  $M_{\mu\alpha}(\omega) = 0$ , we could like to construct a projection around a non-zero field that is both uniform in time, and whose only macroscopic component  $\mu = 0$  (corresponding to the zero momentum  $p_\mu = 0$ ) is different from zero:

$$M_{\mu\alpha}^{(0)}(t) = \epsilon_\alpha \sqrt{2N\rho_\alpha} \delta_{\mu 0}, \quad (5.1)$$

where  $\epsilon_\alpha = \pm 1$ . Generally, the local potential formalism requires a projection onto a homogeneous field [13], corresponding to the macroscopic component  $\vec{p} = 0$  of the Fourier modes. Here, it is the generalized moment that plays this role, since it is on its spectrum that we construct the coarse-graining of the theory. Note moreover that the number of “sites” in the underlying network does not change, because:

$$2\rho_\alpha = \frac{1}{N} \sum_{\mu} (M_{\mu\alpha}^{(0)}(t))^2 = \frac{1}{N} \sum_{i=1}^N M_{i\alpha}^2(t). \quad (5.2)$$

**Remark 4** *Note that one could question the relevance of this approximation since one does not construct a coarse-graining on the frequencies. Considering a uniform field amounts to linking the time scales to the abstract scales linked to the eigenvalues of the matrix disorder. An approximation that is not exotic in the literature, see for instance [59, 91].*

Let us move on to the construction of the theory space. We keep for the kinetic action (power 2 of the field) the form given in (2.46) for the vertex expansion, disregarding the flows of the anomalous dimensions. However, we must include non-local and multi-replica

contributions:

$$\begin{aligned}
\Gamma_{k,\text{kin}} &= \frac{1}{2} \int dt \sum_{\mu=1}^N \sum_{\alpha=1}^n M_{\mu\alpha}(t) \left( -Y(k) \frac{d^2}{dt^2} + Z(k) p_\mu^2 \right) M_{\mu\alpha}(t) \\
&+ \frac{1}{2} \int dt \int dt' \sum_{\mu=1}^N \sum_{\alpha,\beta} q_{\alpha\beta}(k) M_{\mu\alpha}(t) M_{\mu\beta}(t') \\
&+ \frac{1}{2} \int dt \sum_{\mu=1}^N \sum_{\alpha,\beta} q'_{\alpha\beta}(k) M_{\mu\alpha}(t) M_{\mu\beta}(t). \tag{5.3}
\end{aligned}$$

The coupling  $q_{\alpha\beta}(k)$  is between different replicas at different times, and  $q'_{\alpha\beta}(k)$  is a coupling between different replicas at the same time. For simplicity in the rest of this section, we assume replica symmetry  $q'_{\alpha\beta}(k) =: q'(k)$ . Mathematically, these couplings describe the flow of the disorder effects, and as pointed out in our previous work [11], the flow of these couplings is closely related to the appearance of finite-scale singularities – see also Figure 9 and discussion before. It should be noted that the operator  $q$  which can also be interpreted as random magnetic field, breaks the time translation invariance in the symmetric phase, but only asymptotically, since these contributions are invisible at frequencies  $\omega \neq 0$ . If we limit ourselves to not having a random magnetic field, the presence of this  $q$  coupling may seem somewhat artificial, and we will see below that it introduces some difficulties. Physically, one could think of a more realistic operator also breaking the time translation invariance, analogous to the choice we made in [55]:

$$V_k^{(2)} \propto \frac{1}{2} \int d\omega d\omega' \sum_{\mu=1}^N \sum_{\alpha} \Delta(k) M_{\mu\alpha}(\omega) M_{\mu\alpha}(\omega'). \tag{5.4}$$

Although the breaking of time-translation invariance is also a characteristic of glassy phases, we will ignore these effects for the moment, focusing on the correlations between replicas.

Now consider the interaction part of the effective average action. Keeping only the bi-local contributions [64], the interaction part of the action moreover reads (see also [92]):

$$\Gamma_{k,\text{int}} = \int dt \left( \sum_{\alpha} \underbrace{U_k[\mathbf{M}_{\alpha}^2(t)]}_{\text{Local}} + \frac{1}{2} \sum_{\alpha,\beta} \underbrace{V_k(\|\mathbf{M}_{\alpha}(t)\|, \|\mathbf{M}_{\beta}(t)\|, u_{\alpha\beta}(t, t))}_{\text{Coupling replica}} \right) \tag{5.5}$$

$$+ \frac{1}{2} \int dt' \sum_{\alpha,\beta} \underbrace{W_k(\|\mathbf{M}_{\alpha}(t)\|, \|\mathbf{M}_{\beta}(t')\|, u_{\alpha\beta}(t, t'))}_{\text{Non-local}}, \tag{5.6}$$

where  $\mathbf{M}_{\alpha} = (M_{1\alpha}, \dots, M_{N\alpha})$ ,  $\mathbf{M}_{\alpha}^2 := \sum_i M_{i\alpha}^2$ , and

$$u_{\alpha\beta}(t, t') := \frac{\mathbf{M}_{\alpha}(t)}{\|\mathbf{M}_{\alpha}(t)\|} \cdot \frac{\mathbf{M}_{\beta}(t')}{\|\mathbf{M}_{\beta}(t')\|}. \tag{5.7}$$

The local potential  $U_k$  depends on fields at the same time and the same replica index, and for the rest of this paper we will assume that  $U_k$  expands around the global minimum

$\kappa(k)$  as:

$$\frac{U_k[\mathbf{M}_\alpha^2(t)]}{N} = \frac{u_4(k)}{2} \left( \frac{\mathbf{M}_\alpha^2(t)}{2N} - \kappa(k) \right)^2 + \frac{u_6(k)}{3} \left( \frac{\mathbf{M}_\alpha^2(t)}{2N} - \kappa(k) \right)^3 + \dots \quad (5.8)$$

The non-local potential  $V_k$  in contrast is assumed to expand in power of field until order 4, and we assume to keep only contributions up to the sextic order. Graphically:

$$V_k = \underbrace{\text{diagram}}_{v_{4,1}} + \underbrace{\text{diagram}}_{v_{4,2}} + \underbrace{\text{diagram}}_{v_{6,1}} + \underbrace{\text{diagram}}_{v_{6,2}} + \underbrace{\text{diagram}}_{v_{6,3}}, \quad (5.9)$$

$$W_k = \underbrace{\text{diagram}}_{w_{4,1}} + \underbrace{\text{diagram}}_{w_{4,2}} + \underbrace{\text{diagram}}_{w_{6,1}} + \underbrace{\text{diagram}}_{w_{6,2}} + \underbrace{\text{diagram}}_{w_{6,3}} + \underbrace{\text{diagram}}_{w_{6,4}}. \quad (5.10)$$

Note that nodes with different colors (red or blue) along a given bubble have different replica indices. Explicitly for instance:

$$\underbrace{\text{diagram}}_{v_{4,1}} := \int dt \sum_{\alpha, \beta} (\mathbf{M}_\alpha(t) \cdot \mathbf{M}_\beta(t))^2. \quad (5.11)$$

Before projection along the vacuum (5.1), all the replicated fields are along the same axis, and  $u_{\alpha\beta} \rightarrow \epsilon_{\alpha\beta}$ ,  $\forall \alpha, \beta$ . Then:

$$V_k|_{M_\alpha=M_\alpha^{(0)}} = N \left( v_{4,1} \rho_\alpha \rho_\beta + v_{4,2} \epsilon_{\alpha\beta} \rho_\alpha \sqrt{\rho_\alpha \rho_\beta} + \epsilon_{\alpha\beta} v_{6,1} \sqrt{\rho_\alpha^3 \rho_\beta^3} + v_{6,2} \rho_\alpha^2 \rho_\beta + \epsilon_{\alpha\beta} v_{6,3} \rho_\alpha^2 \sqrt{\rho_\alpha \rho_\beta} \right), \quad (5.12)$$

and:

$$W_k|_{M_\alpha=M_\alpha^{(0)}} = N \left( w_{4,1} \rho_\alpha \rho_\beta + \epsilon_{\alpha\beta} w_{4,2} \rho_\alpha \sqrt{\rho_\alpha \rho_\beta} + \epsilon_{\alpha\beta} w_{6,1} \sqrt{\rho_\alpha^3 \rho_\beta^3} + w_{6,2} \rho_\alpha^2 \rho_\beta + \epsilon_{\alpha\beta} w_{6,3} \rho_\alpha^2 \sqrt{\rho_\alpha \rho_\beta} + \epsilon_{\alpha\beta} w_{6,4} \rho_\alpha \rho_\beta \sqrt{\rho_\alpha \rho_\beta} \right), \quad (5.13)$$

relations, which defines also the normalization of the different couplings  $v_{2n,p}$  and  $w_{2n,p}$ . Note that couplings  $v$ 's are introduced for the same reason as  $q'$ . This truncation is the large one, including bi-local sextic cumulants. However, it includes a very large number of couplings which makes the flow equations quite complicated to study. Note that, regarding the non-local couplings, only  $w_{4,1}$  and  $w_{6,1}$  are interpretable in terms of a disorder of rank 2 and 3 respectively, provided that they are negative, in the same way that  $q < 0$  is interpretable as a disorder of rank 1. The presence of a disorder of



rank 2 in this formalism simply corrects the variance of the original matrix, the sum of two Wigner matrices of variances  $\sigma^2$  and  $\tau^2$  respectively, being a Wigner matrix [30] of variance  $\sigma^2 + \tau^2$ . However, in the approximation we consider here, where the field has only a macroscopic component independent of time, these non-local correlations do not provide additional information compared to the local interactions correlating different responses; despite that these non-local interactions will retro-act on the latter.

However, the underlying logic of our approach allows us to consider some simplifications (provided that they give consistent results – this will be verified later). In our previous work [11], as well as in the companion paper [64], we have been able to see that finite-scale singularities are linked to an instability of the effective potential 2PI for  $q'$  (the so-called *Ward-Luttinger functional*). More precisely, we observed that the potential develops a second stable minimum for a value  $q'_0 \neq 0$ , and that this minimum tends to become deeper than the minimum at  $q' = 0$ . In Figure 9, we reproduced the behavior of the *Ward-Luttinger functional* for  $q'$  computed from vertex expansion in our previous paper (in the symmetric phase), for some RG trajectory having a finite scale divergence. In this example, with initial conditions for local quartic and quadratic couplings close to the critical region, the first non-zero value for  $q'$  is  $q' \approx 0.30$ . Note that this computation was done in real-time. In imaginary time, the sign of the coupling is negative with our conventions – see also [64].

This order of magnitude also seems essentially independent of the initial values of the local couplings. This behavior is reminiscent of a first-order phase transition, the final step where the vacuum  $q' = 0$  becomes unstable being blinded by the singularity of the flow<sup>6</sup>. What is important is that we assume that these instabilities are at the origin of the growth of the interactions of the potential  $V_k$ , in the same way, that we assume that the instabilities of the vacuum  $p = 0$  will be linked to the growth of the nonlocal interactions generating  $W_k$ . Because the initial action contains only one non-local sextic interaction and one local propagator, we thus expect that only some interactions dominate the flow when  $q$  and  $q'$  remain small enough, which will be assumed throughout this section. Note that this approximation would be quite good if the transition were of the second order or continuous. But because the transition is first order (discontinuous), with a large enough discontinuity for  $q'$ , and the perturbation assumption constitutes a strong limitation of our study; and a more complete, but also more laborious calculation would be necessary, taking into account the interactions that we have neglected. However, the predictions made from perturbative theory space cannot be taken too seriously either, since they lead to divergences. Our hypothesis, whose relevance can only be assessed by numerical experiments, will be that taking into account these non-perturbative (but small enough) interactions early enough in the flow will prevent or delay the appearance of singularities, without dragging the flow of the latter too far.

Classical spin glass physics in particular teaches us that there are several different characterizations of glass transitions, and as we have pointed out above, correlations between replicas and the breaking of time translation invariance are common signatures.

---

<sup>6</sup>Recall that to construct the potential, we expanded the Schwinger-Dyson equation, and compute coefficient for  $q' = 0$ .

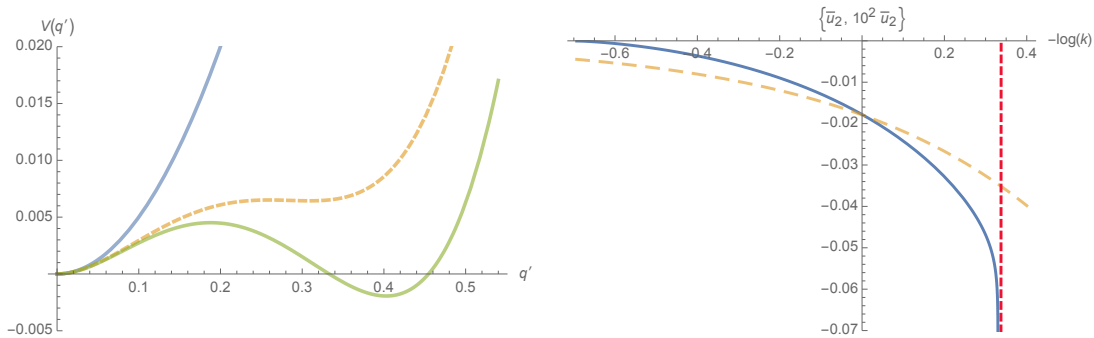


Figure 9: On the left: Evolution of the critical effective potential ( $n = 2$ ) for the quantity  $q'$ , computed from the vertex expansion in the symmetric phase, along some RG trajectory with a finite scale singularity, respectively for  $k = 1.994$  (blue),  $k = 1.81$  (yellow) and  $k = 1.80$  (green). On the right: Behavior of the RG flow near the Gaussian fixed point for vanishing disorder (dashed curve, times 100) and for non-zero disorder above critical value (solid blue edge).

However, in this section we will focus mainly on correlations between replicas, keeping in mind that this approximation restricts the complexity of the exact phase space, which we assume also includes regions where time translation is broken. Note that this choice is also justified by the type of approximation (uniform field in time) that we consider here. Since the flow equations in the Wetterich formalism involve only one effective loop, it is easy to evaluate the importance of the vertices  $v_{2n,p}$  and  $w_{2n,p}$ . We thus find  $v_{4,1} = \mathcal{O}(q')$ ,  $v_{4,2} = \mathcal{O}((q')^3)$ ,  $v_{6,1} = \mathcal{O}((q')^4)$ ,  $v_{6,2} = \mathcal{O}((q')^2)$  and  $v_{6,3} = \mathcal{O}((q')^3)$ . Finally, the approximation we will consider is:

$$\begin{aligned}
\Gamma_k = & \frac{1}{2} \int dt \sum_{\mu=1}^N \sum_{\alpha=1}^n M_{\mu\alpha}(t) \left( -\frac{d^2}{dt^2} + p_\mu^2 \right) M_{\mu\alpha}(t) + \frac{1}{2} \int dt \sum_{\mu=1}^N \sum_{\alpha,\beta} q'(k) M_{\mu\alpha}(t) M_{\mu\beta}(t) \\
& + \int dt \sum_{\alpha} \underbrace{U_k[M_\alpha^2(t)]}_{\text{Local}} + v_{4,1} \text{ (diagram)} + w_{6,1} \text{ (diagram)}. \tag{5.14}
\end{aligned}$$

Now, and as a preliminary for the computation of the flow equations, let us compute the effective 2 point function. Deriving twice with respect to  $M_{\mu\alpha}(t)$  and  $M_{\mu\beta}(t')$ , and projecting along  $M_\alpha^{(0)}$ , we get:

$$\Gamma_k^{(2)}(t, t') + R_k(p_\mu^2) \delta_{\mu\nu} \delta(t - t') = A \delta(t - t') + B \tag{5.15}$$

where:

$$\begin{aligned}
A := & \delta_{\alpha\beta}\delta_{\mu\nu} \left( -\frac{d^2}{dt^2} + p_\mu^2 + \frac{\partial U_k}{\partial \rho_\alpha} + R_k(p_\mu^2) \right) + 2\rho_\alpha \frac{\partial^2 U_k}{\partial \rho_\alpha^2} \delta_{\alpha\beta} \delta_{\mu 0} \delta_{\nu 0} \\
& + \left( q' + 4v_{4,1} \sqrt{\rho_\alpha \rho_\beta} \right) \delta_{\mu\nu} + 4v_{4,1} \left( \sum_{\beta'} \rho_{\beta'} \right) \delta_{\mu 0} \delta_{\nu 0} \delta_{\alpha\beta} + 12\beta w_{6,1} \sqrt{\rho_\alpha} \sum_{\beta'} \rho_{\beta'}^{3/2} \delta_{\mu 0} \delta_{\nu 0} \delta_{\alpha\beta},
\end{aligned} \tag{5.16}$$

and:

$$B := 12w_{6,1} \rho_\alpha \rho_\beta \delta_{\mu\nu}. \tag{5.17}$$

We define Fourier transform of some function  $f(t)$  as:

$$f(t) := \frac{1}{\beta} \sum_{\omega} \tilde{f}(\omega) e^{-i\omega t}, \quad \tilde{f}(\omega) := \int_{-\beta/2}^{\beta/2} dt f(t) e^{i\omega t}, \tag{5.18}$$

where frequencies are assumed to be quantified  $\omega = 2\pi n/\beta$ ,  $n \in \mathbb{N}$ . The function  $G_k(t, t')$  is defined by the condition:

$$AG(t, t') + B \int dt'' G(t'', t') = \delta(t - t'), \tag{5.19}$$

which can be rewritten in the Fourier mode as:

$$\tilde{A}(\omega^2) G(\omega, \omega') + B\beta G(0, \omega') \delta_{\omega, 0} = \beta \delta_{\omega, -\omega'}. \tag{5.20}$$

We expect a solution of the form:

$$G_k(\omega, \omega') = \beta \tilde{A}^{-1}(\omega^2) \delta_{\omega, -\omega'} + D \delta_{\omega, 0} \delta_{\omega', 0}, \tag{5.21}$$

and we get the conditions:

$$\tilde{A}(0)D + \beta^2 B \tilde{A}^{-1}(0) + \beta B D = 0, \tag{5.22}$$

leading to:

$$D = -(\tilde{A}(0) + \beta B)^{-1} B \beta^2 \tilde{A}^{-1}(0), \tag{5.23}$$

and we get:

$$\boxed{G_k(\omega, \omega') = \beta \left( \tilde{A}^{-1}(\omega^2) \delta_{\omega, -\omega'} - (\tilde{A}(0) + \beta B)^{-1} B \beta \tilde{A}^{-1}(0) \delta_{\omega, 0} \delta_{\omega', 0} \right)}. \tag{5.24}$$

Furthermore, the inverse of the matrix  $\tilde{A}$  can be easily computed, projecting  $\rho_\alpha$  along the uniform running vacuum  $\kappa(k)$ :

$$\begin{aligned}
(\tilde{A}^{-1})_{\mu\nu\alpha\beta}(\omega^2) = & \frac{\delta_{\mu\nu}^{(0)}}{\ell_k(p_\mu^2, \omega^2) + R_k(p_\mu^2)} \left[ \delta_{\alpha\beta} - \frac{F}{\ell_k(p_\mu^2, \omega^2) + R_k(p_\mu^2) + nF} \right] \\
& + \frac{\delta_{\mu 0} \delta_{\nu 0}}{\wp_k(\omega^2) + R_k(0)} \left[ \delta_{\alpha\beta} - \frac{F}{\wp_k(\omega^2) + R_k(0) + nF} \right].
\end{aligned} \tag{5.25}$$

where:

$$\ell_k(p_\mu^2, \omega^2) := \omega^2 + p_\mu^2 + \partial_{\rho_\alpha} U_k, \quad (5.26)$$

$$\wp_k(\omega^2) := \omega^2 + \partial_{\rho_\alpha} U_k + 2\rho_\alpha \partial_{\rho_\alpha}^2 U_k + n \left[ 4v_{4,1}\kappa + \beta \left( 12w_{6,1}\kappa^2 \right) \right] \quad (5.27)$$

$$F := q' + 4v_{4,1}\kappa(k), \quad (5.28)$$

and:

$$\delta_{\mu\nu}^{(0)} := \delta_{\mu\nu} - \delta_{\mu 0}\delta_{\nu 0}. \quad (5.29)$$

Note that  $\partial_{\rho_\alpha} U_k = 0$  for  $\rho_\alpha = \kappa$  by construction, we keep the dependency over  $\partial_{\rho_\alpha} U_k$  to keep track of this dependency. Moreover, in the continuum limit, as we replace the discrete sum by an integral over the Wigner distribution, the contribution of the component 0 does not contribute. We then define:

$$(\tilde{A}^{-1})_{\mu\nu\alpha\beta}(\omega^2) =: \delta_{\mu\nu}^{(0)} (\mathfrak{A}_0^{-1})_{\alpha\beta}(p^2, \omega^2) + \delta_{\mu 0}\delta_{\nu 0} (\mathfrak{B}_0^{-1})_{\alpha\beta}(p^2, \omega^2), \quad (5.30)$$

where, projecting along  $\kappa$ :

$$(\mathfrak{A}_0^{-1})_{\alpha\beta}(p^2, \omega^2)|_{\rho_\alpha=\kappa} := \frac{1}{\ell_k(p_\mu^2, \omega^2) + R_k(p_\mu^2)} \left[ \delta_{\alpha\beta} - \frac{F}{\ell_k(p_\mu^2, \omega^2) + R_k(p_\mu^2) + nF} \right]. \quad (5.31)$$

Now, let us return to the flow equation. The exact flow equation is (we make explicit the dependency on the generalized momenta for  $G_k$  until here):

$$\dot{\Gamma}_k = \frac{N}{2} \int \rho(p_\mu^2) dp_\mu^2 \int dt dt' G_k(p_\mu^2, t, t') \dot{R}_k(p_\mu^2, |t - t'|), \quad (5.32)$$

where for our purpose,

$$R_k(p_\mu^2, |t - t'|) = R_k(p_\mu^2) \delta(t - t'). \quad (5.33)$$

Then, projecting it on both sides on the uniform field  $M_\alpha^{(0)}$ , the equation takes the form (the integral over  $p_\mu$  is implied on the left-hand side):

$$\begin{aligned} f[\{\rho_\alpha\}, u_4, u_6, q', v_{4,1}] + \beta g[w_{6,1}, \{\rho_\alpha\}] &= \frac{1}{2\beta} \sum_\omega \int dp^2 \rho(p^2) R_k(p^2) \sum_\alpha (\mathfrak{A}_0^{-1})_{\alpha\alpha}(p^2, \omega^2) \\ &\quad - \frac{1}{2} \int dp^2 \rho(p^2) R_k(p^2) \sum_{\alpha, \beta, \gamma} (\mathfrak{A}_0(p^2, 0) + \beta B)_{\alpha\beta}^{-1} B_{\beta\gamma} (\mathfrak{A}_0^{-1})_{\gamma\alpha}(p^2, 0), \end{aligned} \quad (5.34)$$

where the functional  $f$  and  $g$  will be defined later. For  $\beta$  large enough, the discrete sum can be converted as an integral:

$$\begin{aligned} f[\{\rho_\alpha\}, u_4, u_6, q', v_{4,1}] + \beta g[w_{6,1}, \{\rho_\alpha\}] &= \frac{1}{4\pi} \int d\omega \int dp^2 \rho(p^2) R_k(p^2) \sum_\alpha (\mathfrak{A}_0^{-1})_{\alpha\alpha}(p^2, \omega^2) \\ &\quad - \frac{1}{2} \int dp^2 \rho(p^2) R_k(p^2) \sum_{\alpha, \beta, \gamma} (\mathfrak{A}_0(p^2, 0) + \beta B)_{\alpha\beta}^{-1} B_{\beta\gamma} (\mathfrak{A}_0^{-1})_{\gamma\alpha}(p^2, 0), \end{aligned} \quad (5.35)$$

We can think of identifying the left and right terms according to the power of  $\beta$ . However,  $\beta$  is assumed to be a large parameter. If we take the limit  $\beta \rightarrow \infty$  naively, we conclude that the left-hand side no longer depends on  $B$ , and hence on the non-local coupling. Let us try to go further. A moment of reflection shows that  $\tilde{A}(0) = k^2 \mathcal{O}(1)$ ; moreover  $B$  has a dimension 3 regarding the power counting,  $B = k^3 \bar{B}$ . Then,

$$\tilde{A}(0) + \beta B = \tilde{A}(0) \left( 1 + \frac{\beta k}{\mathcal{O}(1)} \bar{B} \right). \quad (5.36)$$

Then, we have only one interesting regime where the flow of disorder is non-trivial, for

$$\bar{B} \beta k \ll 1. \quad (5.37)$$

From this condition, we can distinguish two different sub-regimes. First, if  $\bar{B} = \mathcal{O}(1)$ , the condition reduces to:

$$\beta k \ll 1. \quad (5.38)$$

In other words, the time scale should be very smaller compared to the generalized momentum scale. Because the eigenvalue spacing is of order  $1/N$  for a Wigner matrix of size  $N$ , we expect that the minimal value for  $k$  is  $\sim N^{-1/2}$ . Then, the larger generalized moment scale is  $\sim \sqrt{N}$ , and we have the larger bound:

$$\beta \ll \sqrt{N}. \quad (5.39)$$

The way we construct the continuous limit in that way is then very non-trivial, and holds only in the deep IR, for  $N$  large enough. Note that for classical spin glass kinetics,  $\beta \sim \sqrt{N}$  is the time lapse in order to recover equilibrium [39]. It is again suitable to read the condition 1 otherwise. Because  $\bar{B} \sim \bar{w}_{6,1} \bar{\kappa}^2$ , we have:

$$\bar{\kappa}^2 \ll \mathcal{O}(1) \frac{k^{-1}}{\beta \bar{w}_{6,1}}, \quad (5.40)$$

or if  $\bar{w}_{6,1} \sim k \mathcal{O}(1)$ ,

$$\boxed{\bar{\kappa}^2 \ll \mathcal{O}(1) \frac{k^{-2}}{\beta}}. \quad (5.41)$$

For  $k$  fixed, taking the limit  $\beta \rightarrow \infty$  imposes  $\bar{\kappa} \rightarrow 0$ . Interestingly, this condition concerns what could be called global magnetization. When  $\lambda \rightarrow 0$  (vanishing tensorial disorder), the system exhibits a second-order phase transition reminiscent of the ferromagnetic transition for which the  $\mu = 0$  component of the  $M_\mu$  field becomes macroscopic ( $M_0 \propto \sqrt{N}$ ), as we showed in our previous work [11] in the limit  $N \rightarrow \infty$ . In other words, we expect that as the magnitude of the vacuum  $M^{(0)}$  becomes large, the flow reaches a regime where the effective matrix-like disorder is very large compared to the rank 3 disorder  $J_{i_1 i_2 i_3}$ . The condition (5.41) means that the theory must be in its critical regime:

$$\kappa^2 \ll \mathcal{O}(1) \frac{k^2}{\beta}, \quad (5.42)$$

and  $\kappa \rightarrow 0$  as  $k \rightarrow 0$ . Expanding  $G_k$  in power of  $\beta$ , we have:

$$\begin{aligned} f[\{\rho_\alpha\}, u_4, u_6, q', v_{4,1}] &= \frac{1}{4\pi} \int d\omega \int dp^2 \rho(p^2) \dot{R}_k(p^2) \sum_\alpha (\mathfrak{A}_0^{-1})_{\alpha\alpha}(p^2, \omega^2) \\ &\quad - \frac{1}{2} \int dp^2 \rho(p^2) \dot{R}_k(p^2) \sum_{\alpha, \beta, \gamma} (\mathfrak{A}_0^{-1})_{\alpha\beta}(p^2, 0) B_{\beta\gamma} (\mathfrak{A}_0^{-1})_{\gamma\alpha}(p^2, 0), \end{aligned} \quad (5.43)$$

and:

$$\begin{aligned} g[w_{6,1}, \{\rho_\alpha\}] &= \frac{1}{2} \int dp^2 \rho(p^2) \dot{R}_k(p^2) \sum_{\alpha, \beta, \gamma, \delta, \eta} (\mathfrak{A}_0^{-1})_{\alpha\beta}(p^2, 0) \\ &\quad \times B_{\beta\eta} (\mathfrak{A}_0^{-1})_{\eta\delta}(p^2, 0) B_{\delta\gamma} (\mathfrak{A}_0^{-1})_{\gamma\alpha}(p^2, 0). \end{aligned} \quad (5.44)$$

We move on to the derivation of the flow equations for the different couplings in the next subsection.

**Remark 5** *before closing this subsection, let us remark on the general case, where non-local couplings are added to the truncation. Consider for instance the case  $q \neq 0$  and  $w_{4,1} \neq 0$ , we have:*

$$\begin{aligned} A &:= \delta_{\alpha\beta} \delta_{\mu\nu} \left( -\frac{d^2}{dt^2} + p_\mu^2 + \frac{\partial U_k}{\partial \rho_\alpha} \right) + 2\rho_\alpha \frac{\partial^2 U_k}{\partial \rho_\alpha^2} \delta_{\alpha\beta} \delta_{\mu 0} \delta_{\nu 0} \\ &\quad + \left( q' + 4v_{4,1} \sqrt{\rho_\alpha \rho_\beta} \right) \delta_{\mu\nu} + 4v_{4,1} \sum_{\beta'} \rho_{\beta'} \delta_{\mu 0} \delta_{\nu 0} \delta_{\alpha\beta} \\ &\quad + \beta \sum_{\beta'} \left( 4w_{4,1} \rho_{\beta'} + 12w_{6,1} \sqrt{\rho_\alpha \rho_{\beta'}}^{3/2} \right) \delta_{\mu 0} \delta_{\nu 0} \delta_{\alpha\beta}, \end{aligned} \quad (5.45)$$

and:

$$B := \left( q + 4w_{4,1} \sqrt{\rho_\alpha \rho_\beta} + 12w_{6,1} \rho_\alpha \rho_\beta \right) \delta_{\mu\nu}. \quad (5.46)$$

The condition  $\beta k \bar{B} \ll 1$  has now a different meaning. In the critical regime, for  $\kappa \rightarrow 0$ , we thus find  $\bar{q} \ll k^{-2}/\beta$ , i.e.  $q \rightarrow 0$  as  $k \rightarrow 0$ . This limit is then incompatible with the existence of a macroscopic value for  $q$  occurring from a phase transition.

## 5.2 Flow equations

In this section we will derive the flow equations for the different couplings explicitly. For simplicity, we moreover assume that  $\epsilon_{\alpha\beta} = 1, \forall \alpha, \beta$ . First, let us consider the coupling  $w_{6,1}$ . The functional  $g$  can be easily computed:

$$g[w_{6,1}, \{\rho_\alpha\}] \Big|_{\rho_\alpha = \kappa} = \frac{1}{2} n^2 \dot{w}_{6,1} \kappa^3. \quad (5.47)$$

Then, projecting the flow equation (5.44) along  $\kappa$ , and using the definition (5.31), we get, assuming  $\kappa \neq 0$ :

$$n^2 \dot{w}_{6,1} = 144 w_{6,1}^2 \kappa \times \int dp^2 \rho(p^2) \dot{R}_k(p^2) \sum_{\alpha, \beta, \gamma, \delta, \eta} (\mathfrak{A}_0^{-1})_{\alpha\beta}(p^2, 0) (\mathfrak{A}_0^{-1})_{\eta\delta}(p^2, 0) (\mathfrak{A}_0^{-1})_{\gamma\alpha}(p^2, 0). \quad (5.48)$$

Because we work with the Litim regulator, the integral over  $p^2$  factorizes, and we get for  $k$  small enough:

$$\int dp^2 \rho(p^2) \dot{R}_k(p^2) \approx \frac{4k^5}{3\pi\sigma^{3/2}}. \quad (5.49)$$

For  $p^2 < k^2$ , we thus have:

$$(\mathfrak{A}_0^{-1})_{\alpha\beta}(p^2, \omega^2)|_{\rho_\alpha = \kappa, p^2 < k^2} := \frac{1}{\omega^2 + k^2} \left[ \delta_{\alpha\beta} - \frac{F}{\omega^2 + k^2 + nF} \right]. \quad (5.50)$$

Then:

$$\dot{w}_{6,1} = \bar{w}_{6,1} + \frac{192}{\pi\sigma^{3/2}} \bar{w}_{6,1}^2 \bar{\kappa} \left( 1 - 3n \frac{\bar{F}}{1 + n\bar{F}} + 3n^2 \frac{\bar{F}^2}{(1 + n\bar{F})^2} - n^3 \frac{\bar{F}^3}{(1 + n\bar{F})^3} \right), \quad (5.51)$$

where:

$$\bar{F} := \bar{q}' + 4\bar{v}_{4,1} \bar{\kappa}(k). \quad (5.52)$$

and  $\bar{\kappa} := k^{-2} \kappa$ ,  $\bar{w}_{6,1} := k w_{6,1}$ . Interestingly, and in contrast with vertex expansion, the disorder renormalizes (we recover the vertex expansion result setting  $\kappa = 0$ ). This is particularly opens the possibility of finding a global fixed point in the deep IR.

Now, let us move on to the local counterpart. We have:

$$\begin{aligned} f[\{\rho_\alpha\}, u_4, u_6, q', v_{4,1}] &= \dot{q}'(k) \sum_{\alpha\beta} \sqrt{\rho_\alpha \rho_\beta} \\ &+ \sum_{\alpha} \left( \frac{\dot{u}_4(k)}{2} (\rho_\alpha - \kappa(k))^2 + \frac{\dot{u}_6(k)}{3} (\rho_\alpha - \kappa(k))^3 + \dots \right) \\ &- \sum_{\alpha} \dot{\kappa}(k) \left( u_4(k) (\rho_\alpha - \kappa(k)) + u_6(k) (\rho_\alpha - \kappa(k))^2 + \dots \right) \\ &+ \frac{1}{2} \sum_{\alpha, \beta} \left( \dot{v}_{4,1}(k) \rho_\alpha \rho_\beta + \dots \right), \end{aligned} \quad (5.53)$$

First, setting  $\rho_\alpha = \kappa$ , the local contributions vanish, and we get:

$$f[\{\rho_\alpha\}, u_4, u_6, q', v_{4,1}]|_{\rho_\alpha = \kappa} = n^2 \dot{q}' \kappa + \frac{1}{2} n^2 \dot{v}_{4,1} \kappa^2, \quad (5.55)$$

and the flow equation (5.43) leads to:

$$\begin{aligned} n^2 \dot{q}' \kappa + \frac{1}{2} n^2 \dot{v}_{4,1} \kappa^2 &= \frac{nk^5}{3\pi^2 \sigma^{3/2}} \int \frac{d\omega}{\omega^2 + k^2} \left[ 1 - \frac{F}{\omega^2 + k^2 + nF} \right] \\ &- \frac{8nk w_{6,1} \kappa^2}{\pi\sigma^{3/2}} \left( 1 - 2n \frac{\bar{F}}{1 + n\bar{F}} + n^2 \frac{\bar{F}^2}{(1 + n\bar{F})^2} \right). \end{aligned} \quad (5.56)$$

Computing the integral, we get finally:

$$n^2(\dot{q}' + 2\bar{q}')\bar{\kappa} + \frac{1}{2}n^2\dot{v}_{4,1}\bar{\kappa}^2 = \frac{1}{3\pi\sigma^{3/2}} \left( \frac{1}{\sqrt{1+n\bar{F}}} + (n-1) \right) - \frac{8n\bar{w}_{6,1}\bar{\kappa}^2}{\pi\sigma^{3/2}} \left( 1 - 2n\frac{\bar{F}}{1+n\bar{F}} + n^2\frac{\bar{F}^2}{(1+n\bar{F})^2} \right). \quad (5.57)$$

Note that our approximation assumes we are far enough from the critical regime, and both  $q' \neq 0$ ,  $v_{4,1} \neq 0$ . At this point, there are several strategies for deriving the remaining flow equations. One way to obtain the other flow equations, we make use of the so-called *Sherman-Morrison* formula, which allows computing the inverse of a matrix  $\mathbf{A}$  perturbed by a rank-1 matrix:

$$(\mathbf{A} + \mathbf{u}\mathbf{v}^T)^{-1} = \mathbf{A}^{-1} - \frac{\mathbf{A}^{-1}\mathbf{u}\mathbf{v}^T\mathbf{A}^{-1}}{1 + \mathbf{v}^T\mathbf{A}^{-1}\mathbf{u}}, \quad (5.58)$$

to compute the inverse of a matrix with entries:

$$X_{\alpha\beta} := a\delta_{\alpha\beta} + b + c\sqrt{\rho_\alpha}\sqrt{\rho_\beta}, \quad (5.59)$$

where, for  $p^2 < k^2$ ,

$$a = \omega^2 + k^2 + U'_k, \quad (5.60)$$

$$b = q', \quad (5.61)$$

$$c = 4v_{4,1}. \quad (5.62)$$

The flow equation for the local sector is then:

$$\begin{aligned} & \dot{q}' \sum_{\alpha\beta} \sqrt{\rho_\alpha\rho_\beta} + \frac{1}{2} \sum_{\alpha,\beta} \left( \dot{v}_{4,1}\rho_\alpha\rho_\beta + \dots \right) \\ & + \sum_{\alpha} \left( \frac{\dot{u}_4(k)}{2} (\rho_\alpha - \kappa(k))^2 + \frac{\dot{u}_6(k)}{3} (\rho_\alpha - \kappa(k))^3 + \dots \right) \\ & - \sum_{\alpha} \dot{\kappa}(k) \left( u_4(k) (\rho_\alpha - \kappa(k)) + u_6(k) (\rho_\alpha - \kappa(k))^2 + \dots \right) \\ & = \frac{k^4}{3\pi^2\sigma^{3/2}} \int_{-\infty}^{+\infty} du \sum_{\alpha} \bar{X}_{\alpha\alpha}^{-1}(u^2) - \frac{8\bar{w}_{6,1}k^4}{\pi\sigma^{3/2}} \sum_{\alpha,\beta,\gamma} \bar{X}_{\alpha\beta}^{-1}(0)\bar{\rho}_\beta\bar{\rho}_\gamma\bar{X}_{\gamma\alpha}^{-1}(0), \end{aligned} \quad (5.63)$$

where we defined the dimensionless quantities  $\bar{a} := k^{-2}a$ ,  $\bar{b} := k^{-2}b$ ,  $c = \bar{c}$ ,  $\bar{X}_{\alpha\beta} = k^{-2}X_{\alpha\beta}$ , and  $u := \omega/k$  is the *dimensionless frequency*. We can thus in principle deduce all the flow equations by differentiating a certain number of times the left and right members with respect to  $\sqrt{\rho_\alpha}$ . The resulting equations are unfortunately very complicated, and it is suitable to assume that ergodicity is maximally broken (i.e. the replica symmetry holds),



and to project the flow equation on both sides along a uniform field  $\rho_\alpha = \rho$ . In that case:

$$\begin{aligned}
& \dot{q}' \rho n^2 + \frac{1}{2} \left( \dot{v}_{4,1} \rho^2 n^2 + \dots \right) \\
& + n \left( \frac{\dot{u}_4(k)}{2} (\rho - \kappa(k))^2 + \frac{\dot{u}_6(k)}{3} (\rho - \kappa(k))^3 + \dots \right) \\
& - n \dot{\kappa}(k) \left( u_4(k) (\rho - \kappa(k)) + u_6(k) (\rho - \kappa(k))^2 + \dots \right) \\
& = \frac{k^4}{3\pi\sigma^{3/2}} \left( \frac{1}{\sqrt{1+n\bar{G}+\bar{U}'_k}} + \frac{n-1}{\sqrt{1+\bar{U}'_k}} \right) \\
& \quad - \frac{8nk^4\bar{w}_{6,1}\bar{\rho}^2}{(1+\bar{U}'_k)\pi\sigma^{3/2}} \left( 1 - 2n \frac{\bar{G}}{1+n\bar{G}+\bar{U}'_k} + n^2 \frac{\bar{G}^2}{(1+n\bar{G}+\bar{U}'_k)^2} \right), \tag{5.64}
\end{aligned}$$

where:

$$\bar{G} := \bar{q}' + 4\bar{v}_{4,1}\bar{\rho}, \tag{5.65}$$

such that  $\bar{\rho} := k^{-2}\rho$ . Note that this approximation makes sense only because we assume to expand all the replicas around the same vacuum  $\kappa$ . We have six independent couplings (we will assume that all couplings not explicitly listed are zero), and already two relations, given by the equations (5.51) and (5.57). We therefore need another 4, and three of them can be obtained by taking the first, second and third derivative of the previous equation with respect to  $\rho$ . We find:

$$\begin{aligned}
& n\bar{\kappa}\dot{\bar{v}}_{4,1} + n(\dot{\bar{q}}' + 2\dot{\bar{q}}') - (\dot{\bar{\kappa}} + 2\dot{\bar{\kappa}})\bar{u}_4 \\
& = -\frac{1}{6n\pi} \left[ \frac{4n(\bar{v}_{4,1}(4n\bar{\kappa}\bar{v}_{4,1} + n\bar{q}' + 1)^{3/2} + 24n\bar{\kappa}\bar{w}_{6,1}\bar{q}' + 24\bar{\kappa}\bar{w}_{6,1})}{(4n\bar{\kappa}\bar{v}_{4,1} + n\bar{q}' + 1)^3} \right. \\
& \left. + \bar{u}_4 \left( \frac{1}{(4n\bar{\kappa}\bar{v}_{4,1} + n\bar{q}' + 1)^{3/2}} + \frac{48n\bar{\kappa}^2\bar{w}_{6,1}(4n\bar{\kappa}\bar{v}_{4,1} + n\bar{q}' - 1)}{(4n\bar{\kappa}\bar{v}_{4,1} + n\bar{q}' + 1)^3} + n - 1 \right) \right], \tag{5.66}
\end{aligned}$$

$$\begin{aligned}
& n\dot{\bar{v}}_{4,1} - 2(\dot{\bar{\kappa}} + 2\dot{\bar{\kappa}})\bar{u}_6 + \dot{\bar{u}}_4 = -\frac{1}{3n\pi} \left[ (n-1)\bar{u}_6 - \frac{3}{4}(n-1)\bar{u}_4^2 - \frac{3(4n\bar{v}_{4,1} + \bar{u}_4)^2}{4(4n\bar{\kappa}\bar{v}_{4,1} + n\bar{q}' + 1)^{5/2}} \right. \\
& + \frac{48n\bar{w}_{6,1}}{(4n\bar{\kappa}\bar{v}_{4,1} + n\bar{q}' + 1)^2} - \frac{96n\bar{\kappa}\bar{u}_4\bar{w}_{6,1}}{(4n\bar{\kappa}\bar{v}_{4,1} + n\bar{q}' + 1)^2} + \frac{48n\bar{\kappa}^2\bar{u}_4^2\bar{w}_{6,1}}{(4n\bar{\kappa}\bar{v}_{4,1} + n\bar{q}' + 1)^2} \\
& - \frac{48n\bar{\kappa}^2\bar{u}_6\bar{w}_{6,1}}{(4n\bar{\kappa}\bar{v}_{4,1} + n\bar{q}' + 1)^2} + \frac{\bar{u}_6}{(4n\bar{\kappa}\bar{v}_{4,1} + n\bar{q}' + 1)^{3/2}} \\
& + \frac{192n^2\bar{\kappa}\bar{w}_{6,1}(4\bar{v}_{4,1}(\bar{\kappa}\bar{u}_4 - 1) + \bar{u}_4\bar{q}')}{(4n\bar{\kappa}\bar{v}_{4,1} + n\bar{q}' + 1)^3} - \frac{96n^2\bar{\kappa}^2\bar{u}_4\bar{w}_{6,1}(4\bar{v}_{4,1}(\bar{\kappa}\bar{u}_4 - 1) + \bar{u}_4\bar{q}')}{(4n\bar{\kappa}\bar{v}_{4,1} + n\bar{q}' + 1)^3} \\
& + \frac{48n^2\bar{\kappa}^2\bar{w}_{6,1}}{(4n\bar{\kappa}\bar{v}_{4,1} + n\bar{q}' + 1)^4} \left( 16n\bar{v}_{4,1}^2(\bar{\kappa}^2(\bar{u}_4^2 + 2\bar{u}_6) - 4\bar{\kappa}\bar{u}_4 + 3) \right. \\
& + \bar{q}'(\bar{u}_4^2(n\bar{q}' - 2) + 2\bar{u}_6(n\bar{q}' + 1)) + 8\bar{v}_{4,1}(\bar{\kappa}\bar{u}_6(2n\bar{q}' + 1) \\
& \left. + \bar{u}_4(\bar{\kappa}\bar{u}_4(n\bar{q}' - 1) - 2n\bar{q}' + 1)) \right) \left. \right], \tag{5.67}
\end{aligned}$$

$$\begin{aligned}
\dot{u}_6 = & 2\bar{u}_6 + \frac{1}{16n\pi} \left[ 12(n-1)\bar{u}_4\bar{u}_6 - 5(n-1)\bar{u}_4^3 - \frac{5(4n\bar{v}_{4,1} + \bar{u}_4)^3}{(4n\bar{\kappa}\bar{v}_{4,1} + n\bar{q}' + 1)^{7/2}} + \frac{12\bar{u}_6(4n\bar{v}_{4,1} + \bar{u}_4)}{(4n\bar{\kappa}\bar{v}_{4,1} + n\bar{q}' + 1)^{5/2}} \right. \\
& + \frac{384n\bar{u}_4\bar{w}_{6,1}}{(4n\bar{\kappa}\bar{v}_{4,1} + n\bar{q}' + 1)^2} - \frac{768n\bar{\kappa}\bar{u}_4^2\bar{w}_{6,1}}{(4n\bar{\kappa}\bar{v}_{4,1} + n\bar{q}' + 1)^2} + \frac{384n\bar{\kappa}^2\bar{u}_4^3\bar{w}_{6,1}}{(4n\bar{\kappa}\bar{v}_{4,1} + n\bar{q}' + 1)^2} \\
& + \frac{768n\bar{\kappa}\bar{u}_6\bar{w}_{6,1}}{(4n\bar{\kappa}\bar{v}_{4,1} + n\bar{q}' + 1)^2} - \frac{768n\bar{\kappa}^2\bar{u}_4\bar{u}_6\bar{w}_{6,1}}{(4n\bar{\kappa}\bar{v}_{4,1} + n\bar{q}' + 1)^2} - \frac{768n^2\bar{w}_{6,1}(4\bar{v}_{4,1}(\bar{\kappa}\bar{u}_4 - 1) + \bar{u}_4\bar{q}')}{(4n\bar{\kappa}\bar{v}_{4,1} + n\bar{q}' + 1)^3} \\
& + \frac{1536n^2\bar{\kappa}\bar{u}_4\bar{w}_{6,1}(4\bar{v}_{4,1}(\bar{\kappa}\bar{u}_4 - 1) + \bar{u}_4\bar{q}')}{(4n\bar{\kappa}\bar{v}_{4,1} + n\bar{q}' + 1)^3} - \frac{768n^2\bar{\kappa}^2\bar{u}_4^2\bar{w}_{6,1}(4\bar{v}_{4,1}(\bar{\kappa}\bar{u}_4 - 1) + \bar{u}_4\bar{q}')}{(4n\bar{\kappa}\bar{v}_{4,1} + n\bar{q}' + 1)^3} \\
& + \frac{768n^2\bar{\kappa}^2\bar{u}_6\bar{w}_{6,1}(4\bar{v}_{4,1}(\bar{\kappa}\bar{u}_4 - 1) + \bar{u}_4\bar{q}')}{(4n\bar{\kappa}\bar{v}_{4,1} + n\bar{q}' + 1)^3} - \frac{1}{(4n\bar{\kappa}\bar{v}_{4,1} + n\bar{q}' + 1)^4} \\
& \times \left( 768n^2\bar{\kappa}\bar{w}_{6,1}(8\bar{v}_{4,1}(\bar{\kappa}\bar{u}_6(2n\bar{q}' + 1) + \bar{u}_4(\bar{\kappa}\bar{u}_4(n\bar{q}' - 1) - 2n\bar{q}' + 1)) \right. \\
& \left. + 16n\bar{v}_{4,1}^2(\bar{\kappa}^2(\bar{u}_4^2 + 2\bar{u}_6) - 4\bar{\kappa}\bar{u}_4 + 3) + \bar{q}'(\bar{u}_4^2(n\bar{q}' - 2) + 2\bar{u}_6(n\bar{q}' + 1)) \right) \\
& + \frac{384n^2\bar{\kappa}^2\bar{u}_4\bar{w}_{6,1}}{(4n\bar{\kappa}\bar{v}_{4,1} + n\bar{q}' + 1)^4} \left( 8\bar{v}_{4,1}(\bar{\kappa}\bar{u}_6(2n\bar{q}' + 1) + \bar{u}_4(\bar{\kappa}\bar{u}_4(n\bar{q}' - 1) - 2n\bar{q}' + 1)) \right. \\
& \left. + 16n\bar{v}_{4,1}^2(\bar{\kappa}^2(\bar{u}_4^2 + 2\bar{u}_6) - 4\bar{\kappa}\bar{u}_4 + 3) + \bar{q}'(\bar{u}_4^2(n\bar{q}' - 2) + 2\bar{u}_6(n\bar{q}' + 1)) \right) \\
& - \frac{768n^2\bar{\kappa}^2\bar{w}_{6,1}}{(4n\bar{\kappa}\bar{v}_{4,1} + n\bar{q}' + 1)^5} \left( 64n^2\bar{v}_{4,1}^3(\bar{\kappa}\bar{u}_4 - 2)(\bar{\kappa}^2\bar{u}_6 - \bar{\kappa}\bar{u}_4 + 1) \right. \\
& + \bar{u}_4\bar{q}'(\bar{u}_4^2(1 - n\bar{q}') + \bar{u}_6(n\bar{q}' - 2)(n\bar{q}' + 1)) \\
& - 16n\bar{v}_{4,1}^2(\bar{u}_4(2\bar{\kappa}\bar{u}_4(n\bar{q}' - 2) - 3n\bar{q}' + \bar{\kappa}^2\bar{u}_4^2 + 3) + \bar{\kappa}\bar{u}_6(\bar{\kappa}\bar{u}_4(1 - 3n\bar{q}') + 4n\bar{q}' + 1)) \\
& - 4\bar{v}_{4,1}(\bar{u}_6(2n^2(\bar{q}')^2 + \bar{\kappa}\bar{u}_4(n\bar{q}'(2 - 3n\bar{q}') + 2) + n\bar{q}' - 1) \\
& \left. \left. + \bar{u}_4^2(n\bar{q}'(n\bar{q}' + 2\bar{\kappa}\bar{u}_4 - 4) - \bar{\kappa}\bar{u}_4 + 1) \right) \right) \left. \right]. \tag{5.68}
\end{aligned}$$

Finally, the last relation requiring to solve the system can be obtained from the full relation (5.63), taking derivation with respect to  $\sqrt{\rho_1}$  and  $\sqrt{\rho_2}$ . A straightforward calculation leads

to:

$$\begin{aligned}
(\dot{q}' + 2\dot{q}') + 2\dot{\bar{v}}_{4,1}\bar{\kappa} &= \frac{8\bar{v}_{4,1}}{3\pi} \frac{\left(n\bar{F}\sqrt{n\bar{F}+1} + \sqrt{n\bar{F}+1} - 1\right)}{2n(n\bar{F}+1)^{3/2}} \\
&+ \frac{8\bar{\kappa}\bar{v}_{4,1}}{3\pi} (\bar{u}_4 + 4v_{4,1}) \left[ \frac{\left(n\bar{F}\left(n\bar{F}(3n\bar{F}+2)\sqrt{n\bar{F}+1} - 5\sqrt{n\bar{F}+1} + 7\right) - 4\sqrt{n\bar{F}+1} + 4\right)}{8n^3\bar{F}(n\bar{F}+1)^{5/2}} \right. \\
&+ \left. 2\bar{v}_{4,1} \frac{\left(-2\sqrt{n\bar{F}+1} + n\bar{F}\left(-2n\bar{F}\sqrt{n\bar{F}+1} - 4\sqrt{n\bar{F}+1} + 5\right) + 2\right)}{4n^2\bar{F}(n\bar{F}+1)^{5/2}} \right] \\
&+ \frac{64\bar{w}_{6,1}\bar{\kappa}}{\pi(1+n\bar{F})^7} \left[ 4n(\bar{F}-3)\bar{\kappa}^2\bar{v}_{4,1}^2(n\bar{F}+1)^3 \right. \\
&+ 2\bar{\kappa}\bar{v}_{4,1} \left( 2\bar{\kappa}\bar{u}_4(n\bar{F}(n\bar{F}+3)-2)(n\bar{F}+1)^3 + 8\bar{F}\bar{\kappa}^3\bar{u}_4^2(n\bar{F}(n\bar{F}+2)-1) + 3(n\bar{F}+1)^4 \right) \\
&\left. - \bar{F}(n\bar{F}+1)^3 \left( \bar{\kappa}\bar{u}_4(2n\bar{F}+5)(n\bar{F}+1) - \bar{\kappa}^2\bar{u}_4^2(n\bar{F}+2) - (n\bar{F}+1)^2(n\bar{F}+2) \right) \right]. \tag{5.69}
\end{aligned}$$

We study these equations numerically in the following section, including the behavior of trajectories involving these new operators correlating to the replicas. Some analytical results can also be obtained in different limits, and we will consider one of them: the  $n \rightarrow \infty$  limit. Assuming that couplings do not depend on  $n$ , the flow equations reduce to<sup>7</sup>:

$$\dot{\bar{\kappa}} = -2\bar{\kappa} + \frac{4\bar{v}_{4,1}}{9\bar{u}_4} - \frac{64\bar{\kappa}\bar{w}_{6,1}}{3\bar{u}_4} + \frac{2}{9\pi\bar{\kappa}\bar{u}_4} + \frac{1}{6\pi}, \tag{5.70}$$

$$\dot{\bar{q}} = -2\bar{q}', \tag{5.71}$$

$$\dot{\bar{u}}_4 = \frac{8\bar{u}_6\bar{v}_{4,1}}{9\bar{u}_4} - \frac{128\bar{\kappa}\bar{u}_6\bar{w}_{6,1}}{3\bar{u}_4} - \frac{8\bar{v}_{4,1}}{9\bar{\kappa}} + \frac{128\bar{w}_{6,1}}{3} + \frac{2}{9\pi\bar{\kappa}^2} + \frac{4\bar{u}_6}{9\pi\bar{\kappa}\bar{u}_4} + \frac{\bar{u}_4^2}{4\pi}, \tag{5.72}$$

$$\dot{\bar{v}}_{4,1} = \frac{8\pi\bar{\kappa}(\bar{v}_{4,1} - 48\bar{\kappa}\bar{w}_{6,1}) - 2}{9\pi\bar{\kappa}^2n}, \tag{5.73}$$

$$\dot{\bar{u}}_6 = +2\bar{u}_6 - \frac{5\bar{u}_4^3}{16\pi} + \frac{3\bar{u}_6\bar{u}_4}{4\pi}, \tag{5.74}$$

$$\dot{\bar{w}}_{6,1} = +\bar{w}_{6,1}. \tag{5.75}$$

Note that the equation for  $\bar{v}_4$  has to be considered at the order  $1/n$ , to have a non-trivial flow (the next to leading order being of order  $1/n^2$ ). In this limit, the flow of  $q'$  decouples from the other equations, and if this parameter necessarily played a role in the UV, this role is now masked in this regime, where only the parameter  $\bar{v}_{4,1}$  remains.

---

<sup>7</sup>Remark that equations assume  $\kappa \neq 0$ .

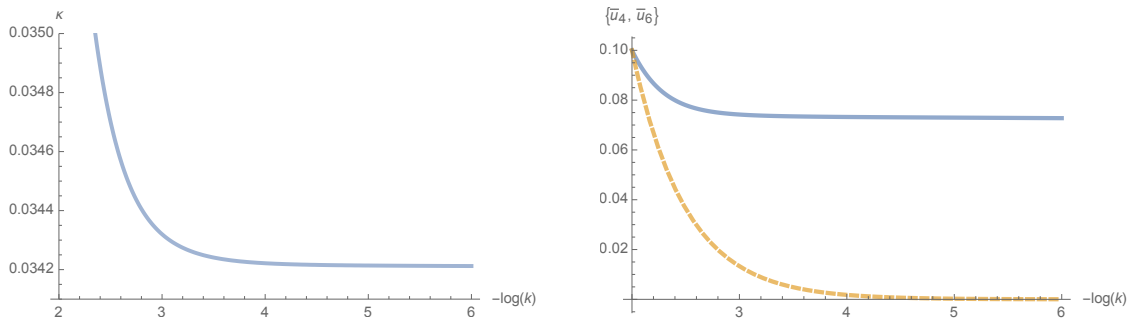


Figure 10: Behavior of the RG flow for  $n = 1$  and initial condition  $S_0$  and  $w_{6,1} = v_{4,1} = q' = 0$ . On the right for  $\kappa(k)$  and on the left for  $\bar{u}_4$  (the solid blue line) and  $\bar{u}_6$  (the dashed yellow line).

### 5.3 Numerical investigations

Let us investigate the flow equations derived above. The full flow equations are difficult to investigate, even numerically, regarding the existence of a global fixed point. However, we can easily verify that our hypotheses concerning the role of local operators coupling the responses are verified, at least on a portion of the phase space close enough to the Gaussian point<sup>8</sup>. Let  $k_0 := e^{-2} \approx 0.13$  some IR scale, and the initial conditions:

$$S_0 := (\bar{\kappa}(k_0) = 2, \bar{u}_4(k_0) = 0.1, \bar{u}_6(k_0) = 0.1). \quad (5.76)$$

Without disorder, and for  $\bar{q}'(k_0) = \bar{v}_{4,1} = 0$ , the result of the numerical integration are showed on Figure 10. The flow reaches some quartic fixed point after a few step RG, and the value for  $\kappa$  converges toward a finite positive value, but no singularity occurs along the flow. In Figure 11, we summarized the same behavior for a strong enough disorder ( $\bar{w}_{6,1}(k_0) \lesssim -0.0005$ ) and we recover the finite scale singularities we observed in the section 4 and in our previous work [11].

Now, we fix the value  $\bar{w}_{6,1}(k_0) = -0.01$ ,  $\bar{v}_{4,1}(k_0) = 1$ , and we varying the value of  $\bar{q}'(k_0)$ . Note that  $v_{4,1}$  is not the sign required to be interpreted as a physical (local in time) disorder<sup>9</sup>, in contrast with  $q'$ . This is imposed by the condition  $1 + n\bar{F}(k_0) > 0$ . This observation is important: *The asymptotic flow is not equivalent to a locally multi-disordered system.* The main results are summarized on Figures 12 and 13, assuming  $n = 2$ . Following our hypotheses, we observed that past a certain critical value  $\bar{q}'(k_0) < \bar{q}'_c(k_0) \approx -2.87$ , the singularities disappear, and the flow can be extended towards the IR (the green and yellow curves are in the vicinity of the critical value and illustrate this point well). The evolution of the coupling  $\bar{q}'$  is shown in Figure 14, for two of the trajectories. Once again, this figure is consistent with our initial intuition: the singularity disappears at the cost of introducing a relevant operator, which will survive in the IR and will quantify the obstruction to the factorization of the effective partition function (recall

<sup>8</sup>Evaluating this notion of proximity however complicated, and we will return to it in a future work where we will precisely establish the phase space of the system, for which it will be necessary to take into account the UV behavior of the flow.

<sup>9</sup>A local disorder takes the form  $\propto \int dt J_{i_1 \dots i_n}(t) x_{i_1}(t) \dots x_{i_n}(t)$ .

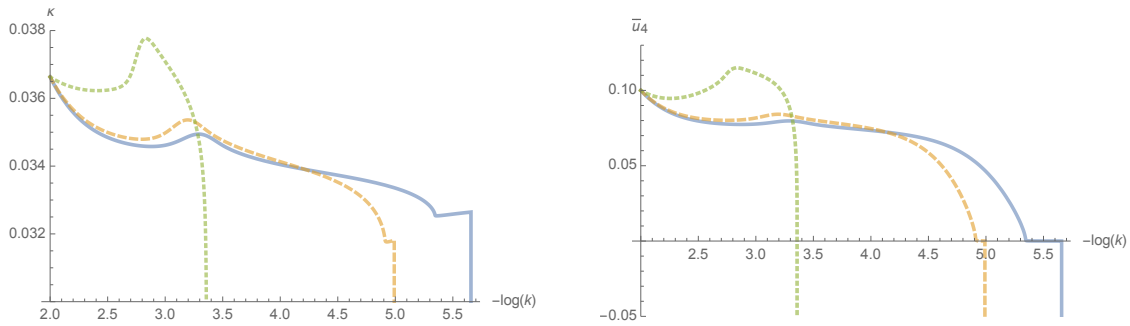


Figure 11: Behavior of the RG flow for initial condition  $S_0$  and  $w_{6,1}(k_0) < -0.0005$ . The solid blue curve is for  $w_{6,1}(k_0) = -0.0006$ , the dashed yellow curve for  $w_{6,1}(k_0) = -0.001$ , and the green dotted curve for  $w_{6,1}(k_0) = -0.005$ .

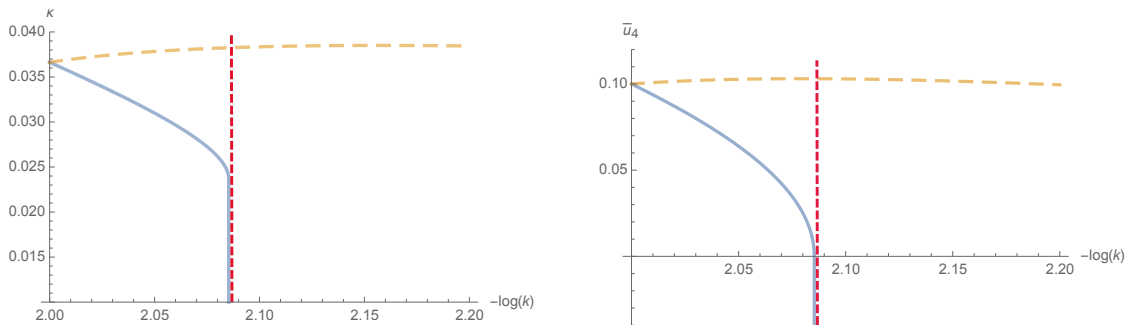


Figure 12: Behavior of the RG flow with disorder  $\bar{w}_{6,1}(k_0) = -0.01$ . The yellow dashed curve is for  $\bar{q}'(k_0) = -5.46$  and the solid blue curve for  $\bar{q}'(k_0) = 0$ . On both cases,  $\bar{v}_{4,1}(k_0) = 1$ .

that the coupling  $w_{6,1}$  is irrelevant). Note that the coupling  $\bar{q}'(k)$  follows an almost perfect scaling law. Looking more closely (in the right figure), we see that the coupling  $q'$  (with dimension) is not exactly constant but reaches a constant value after a transient regime, the value reached being very close to the initial value, and not very far from the estimate of the naive value  $-0.30$  given above. Note at this point that not all divergences are eliminated. Finally, note that despite the numerical analysis we present here for  $n = 2$ , similar results have been obtained for other finite values of  $n$ .

There are still regions of phase space where trajectories diverge, which we put down to our incomplete truncation. For instance, it happens that divergences can be recovered for  $-\bar{q}'(k_0)$  large enough, even if  $1 + n\bar{F} > 0$ . But once again we must not forget that our truncation is very incomplete since it only takes into account strictly local couplings, that the operators only take into account two-replica couplings and that we have limited ourselves to the quartic sector<sup>10</sup>. We can in a way think that these operators extend the domain of analyticity of the flow, but not maximally, and that a complete reconstruction

<sup>10</sup>Numerically, many of these divergences can be removed by a little shift of the initial value for  $\bar{v}_{4,1}(k_0)$ , seeming to outline a complicated phase space. It should still be noted, however, that these observations are made based on a very limited truncation.

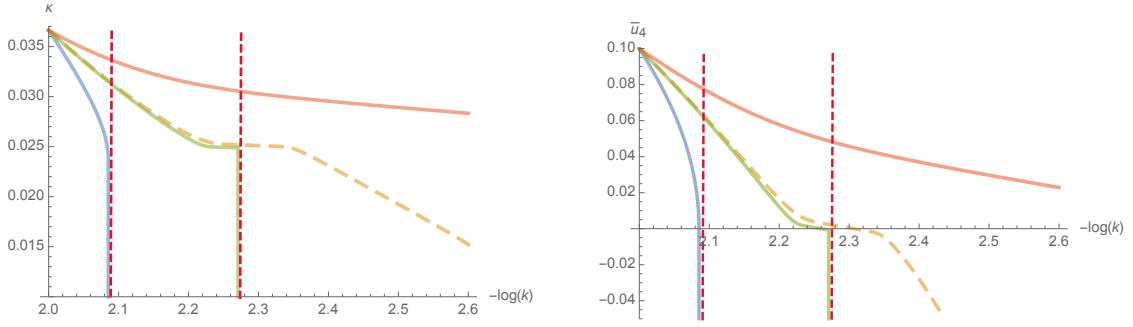


Figure 13: Behavior of the RG flow for  $\bar{w}_{6,1}(k_0) = -0.01$ ,  $\bar{v}_{4,1}(k_0) = 1$  and different values  $\bar{q}'(k_0) = 0$  (blue curve),  $\bar{q}'(k_0) = -2.83$  (green curve),  $\bar{q}'(k_0) = -2.89$  (dashed yellow curve) and  $\bar{q}'(k_0) = -3.82$  (red curve).

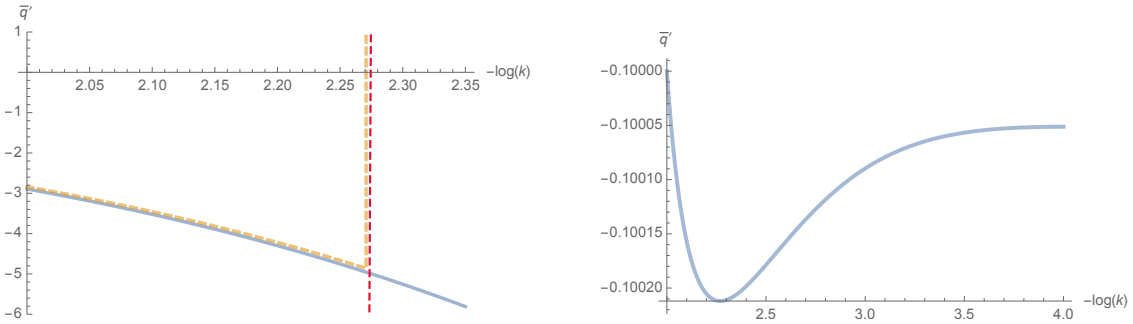


Figure 14: On the left: Behavior of the coupling  $\bar{q}'(k_0)$  for  $\bar{q}'(k_0) = -2.83$  (dashed yellow curve),  $\bar{q}'(k_0) = -2.89$  (solid blue curve); the coupling follows a purely scaling law. On the right, behavior of the RG flow for  $q'(k_0) = -5.46$ .

of the phase space would require more interactions. However, we believe that these results are sufficient to "prove the concept" while waiting for more elaborate methods.

One limitation comes from the sign of  $\bar{F}$ , which in our approximation has only two couplings, and we believe that this limits the physical region of  $\bar{q}'$ , which could be extended by adding more couplings between replicas. Another limitation comes from the assumption (5.41), and in Figure 15 we show that the trajectories we studied here are compatible with a  $\beta$  of the order of 100 – the function  $C(k)$  plotted in the figure is  $C(k) := k^{-1}/(\bar{\kappa}^2 \bar{w}_{6,1})$ , and the values are compatibles with a temperature inverse of order  $\beta \sim 100$ . For this value, the continuous approximation is also perfectly valid. Indeed, defining:

$$S_1[\beta] := \frac{\beta}{2\pi} \int_{-\infty}^{+\infty} \frac{d\omega}{1 + \omega^2} = \frac{\beta}{2}, \quad (5.77)$$

and,

$$S_2[\beta, n_{\max}] := \sum_{n=-n_{\max}}^{+n_{\max}} \frac{1}{\left(\frac{2\pi n}{\beta}\right)^2 + 1} \approx 49.49, \quad (5.78)$$

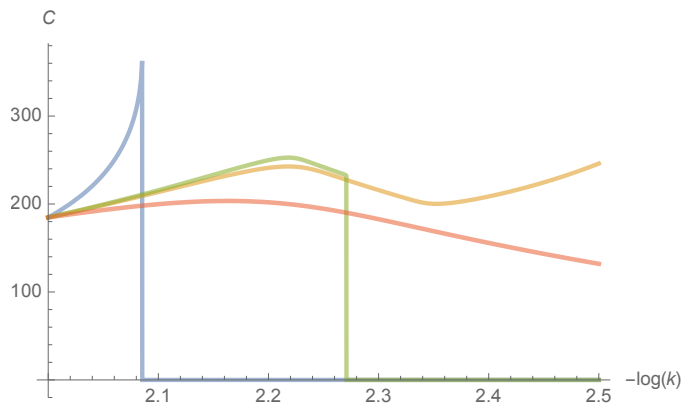


Figure 15: Behavior of  $C(k)$  for the trajectories we investigated.

we get  $S_1[100] = 50$  and  $S_2[100, 1000] \approx 49.49$ , i.e. a difference of just one percent. The rate of convergence is illustrated in Figure 16, for  $n_{\max} = 10^4$ .

Finally, a last limitation may come from the fact that we have limited ourselves to the construction of a symmetric solution in the replicas. The articulation of this argument is probably more subtle<sup>11</sup>, because we do not take the limit  $n \rightarrow 0$ . However, one might think that this kind of solution can only be stable at high temperatures, or in a regime where quantum effects are important. Note that the choice of temperatures is constrained in our continuous model, where we assume  $\beta$  to be sufficiently large. However, one expects that it is above all the relations between the couplings, more than their values, that are important here. Nevertheless, it would be interesting to examine more carefully the high-temperature limit, where the sums will be replaced by integrals. About this point, it should be noticed that the corresponding classical issue can be solved with 1-replica symmetry breaking (1RSB) solution [10, 93]. See also [94] for a discussion about the  $p$ -spin spherical model.

With these many red lights in mind, we can see these preliminary results as evidence for the following statement:

**Claim 1** *There exists in the ferromagnetic phase ( $\kappa > 0$ ) a region of phase space where there is a first-order phase transition to a solution with replica symmetry  $q' \neq 0$  in the vanishing source limit.*

Before concluding this section, let us say a few words about the naive limiting case  $n \rightarrow \infty$  that we considered above. Let us mention that while this study is mathematically motivated, notably by the simplification of the equations that it implies, its physical justification is delicate, and possibly relegated to a later work. It should also be noted that other limits, involving non-trivial scaling could be extended and would lead to different  $n \rightarrow \infty$  limits. Recall that it assumes that couplings (and then fixed point solutions) do

<sup>11</sup>In particular, recall that in our construction, replica symmetry is explicitly broken because replicas are connected with different sources. Moreover, the origin of the replica symmetry breaking is usually due to the construction of the limit  $n \rightarrow \infty$ .

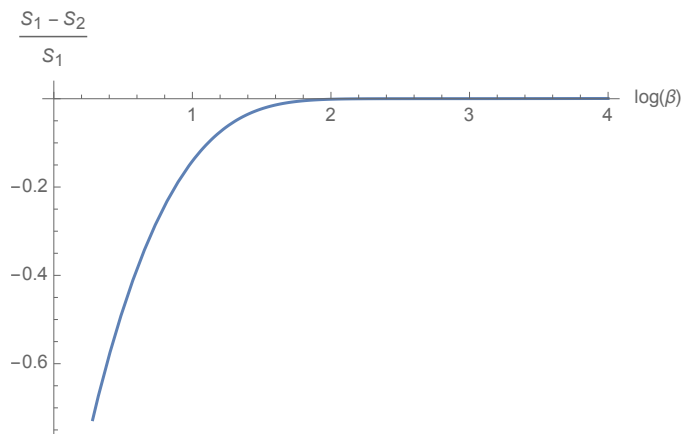


Figure 16: Rate of convergence of the sum toward integral.

not scale as a power on  $n$ . This case is not necessarily the most instructive, because the initial values of the couplings seem on the contrary to be of order  $n$ , and the resulting equations decouple the coupling  $q'$  from the rest of the flow; however, it may have played a role further upstream. We can therefore see this step as an effective regime, including quartic couplings between replicas. We can then essentially make two observations:

1. There are no global fixed points (because the coupling  $w_{6,1}$  does not renormalize). Because  $\bar{w}_{6,1} \rightarrow 0$  asymptotically, it may however exist asymptotic fixed point, and indeed we get:

$$\text{FP1}_\infty = \left( \bar{u}_4 = 4\pi, \bar{v}_{4,1} = -\frac{3}{2}, \bar{u}_6 = 4\pi^2, \bar{\kappa} = -\frac{1}{6\pi} \right), \quad (5.79)$$

with critical exponents:

$$\Theta = \left( \theta_1 \approx 41.75, \theta_2 \approx -41.43, \theta_3 \approx -0.02, \theta_4 = 0 \right). \quad (5.80)$$

The fixed point has one relevant, two irrelevant and one marginal direction spanning a critical surface of dimension 3. Unfortunately, since the sign of  $\kappa$  is negative, our truncation does not seem very appropriate, and the reliability of this result is quite poor. We will come back to this in the next section, using ordinary vertex expansion.

2. Investigating the behavior of RG trajectories, we recover essentially the same conclusions as before in some regions of the phase space, as summarized on the Figure 17, for initial conditions  $(\bar{\kappa}(k_0) = 1, \bar{u}_4(k_0) = 1, \bar{u}_6(k_0) = 1, \bar{w}_{6,1}(k_0) = -5), \bar{v}_{4,1}(k_0) = -10$  for the blue curve and  $\bar{v}_{4,1}(k_0) = -8.1$  for the dashed yellow curve. For this trajectory, the critical value is<sup>12</sup>  $\bar{v}_{4,1,c}(k_0) \approx -8.5$ , and the divergence disappears up to this point. As previously however, divergences are recovered for large

---

<sup>12</sup>The construction of this limit seems to suggest a  $4PI$  formalism, where the four-point function plays the role of the order parameter.



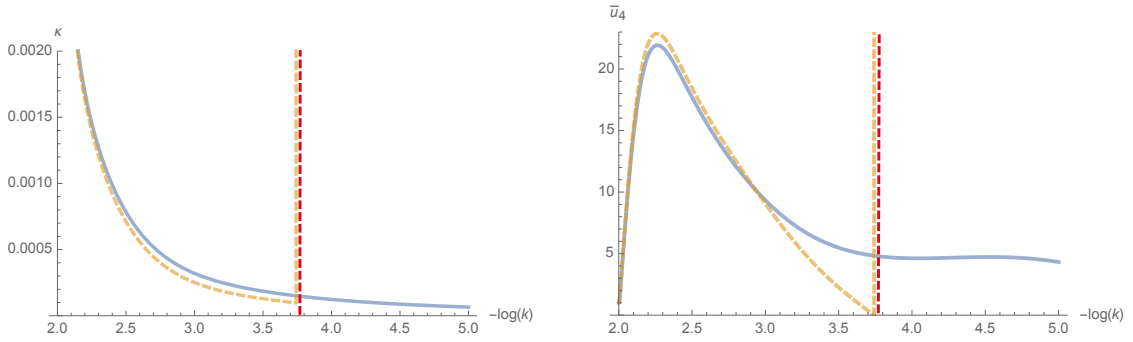


Figure 17: Behavior of the RG flow upper and below the critical value  $\bar{v}_{4,1,c}(k_0)$ .

magnitudes ( $\bar{v}_{4,1}(k_0) < -37$  for the initial conditions we chosen), what we interpret as a spurious effect of our incomplete truncation. Finally, the same remarks we noticed above about the limitation of the method hold.

## 6 Enhanced vertex expansion – a first look

In this section we consider the flow enhanced by non-local and multi-replica interactions in the symmetric phase using vertex expansion. We consider again the case  $p = 3$  (disorder materialized by a rank 3 tensor), and focus on the lowest order sextic truncation. This investigation can be viewed as a complement of the previous one, working on the symmetric phase regarding the mean value of the field,

$$M_{i\alpha} = 0, \quad (6.1)$$

but including interactions which are not generated by the perturbation theory. As we have already said, this approximation is better suited to the non-locality of the interactions, whose flow disappears in the approximation considered previously. Moreover, the vertex expansion allows us to consider more simply the exact regime when the previous approximation only allowed us to study the deep IR and the critical regime without the equations becoming intractable. This section is a kind of invitation to further work, which will evaluate the impact of replica interactions more systematically, as well as the behavior of the flow in the UV.

### 6.1 Truncation including multi-replica

Explicitly, the truncation we consider in this section is the following:

$$\Gamma_{k,\text{int}} = u_4 \text{ (diagram 1) } + u_6 \text{ (diagram 2) } + v_{4,1} \text{ (diagram 3) } + w_{6,1} \text{ (diagram 4) } . \quad (6.2)$$

and for the kinetic part of the effective action:

$$\begin{aligned} \Gamma_{k,\text{kin}} &= \frac{1}{2} \int dt \sum_{\mu=1}^N \sum_{\alpha=1}^n M_{\mu\alpha}(t) \left( -\frac{d^2}{dt^2} + p_\mu^2 + u_2 \right) M_{\mu\alpha}(t) \\ &+ \frac{1}{2} \int dt \sum_{\mu=1}^N \sum_{\alpha,\beta} q'(k) M_{\mu\alpha}(t) M_{\mu\beta}(t). \end{aligned} \quad (6.3)$$

The propagator  $G_k$  reads, in Fourier components:

$$\begin{aligned} G_k(\omega^2, p^2) &:= \frac{\delta_{\alpha\beta}}{\underbrace{\omega^2 + p^2 + u_2 + R_k(p^2)}_{\text{--- --}}} \\ &= \frac{q'}{\underbrace{(\omega^2 + p^2 + u_2 + R_k(p^2))(\omega^2 + p^2 + u_2 + R_k(p^2) + nq')}_{\text{--- -- \times ---}}}. \end{aligned} \quad (6.4)$$

Graphically, the flow equations write:

$$\dot{u}_2 = \text{diagram 1} + \text{diagram 2} + \text{diagram 3} + \text{diagram 4}, \quad (6.5)$$

$$\dot{q}' = \text{diagram 1} + \text{diagram 2}, \quad (6.6)$$

$$\begin{aligned} \dot{u}_4 &= \text{diagram 1} + \text{diagram 2} + \text{diagram 3} + \text{diagram 4} + \text{diagram 5} + \text{diagram 6} \\ &+ \text{diagram 7} + \text{diagram 8} + \text{diagram 9} + \text{diagram 10}, \end{aligned} \quad (6.7)$$

$$\dot{v}_{4,1} = \text{diagram 1} + \text{diagram 2} + \text{diagram 3}, \quad (6.8)$$

$$\dot{w}_{6,1} = 0, \quad (6.9)$$

$$\begin{aligned} \dot{u}_6 = & \text{Diagram 1} + \text{Diagram 2} + \text{Diagram 3} \\ & + \text{Diagram 4} + \text{Diagram 5} + \text{Diagram 6} \\ & + \text{Diagram 7} + \text{Diagram 8} + \text{Diagram 9} \\ & + \text{Diagram 10} + \text{Diagram 11}. \end{aligned} \quad (6.10)$$

## 6.2 Deep IR numerical analysis

As in the rest of this paper, we focus on the IR regime, in which in particular the regulator is well approximated by:

$$R_k(p^2) \approx (k^2 - p^2)\theta(k^2 - p^2). \quad (6.11)$$

Our goal here is to show once again that taking into account the relevant observables correlating the replica “cures” at least part of the divergences observed in the IR – we will return to a detailed study of the UV flow in a later work. In the windows of momenta  $0 \leq p^2 \leq k^2$ , the effective propagator reduces to:

$$G_k(\omega^2, p^2) := \underbrace{\frac{\delta_{\alpha\beta}}{\omega^2 + k^2 + u_2}}_{:=G_k^{(0)}} - \underbrace{\frac{q'}{(\omega^2 + k^2 + u_2)(\omega^2 + k^2 + u_2 + nq')}}_{:=G_k^{(1)}}$$

and the integral becomes singular for the value  $\bar{u}_2 = -1$ , recalling that  $\bar{u}_2 := u_2 k^{-2}$ . Because of the Litim regulator, the global integration along the effective loop (in the large  $N$  limit) factorizes in front of each term:

$$\Omega(k) := \int d^2 p \rho(p^2) \dot{R}_k(p^2) \approx \frac{4k^5}{3\pi\sigma^{3/2}}, \quad (6.12)$$

assuming  $k^2 \ll 4\sigma$ . Many of the flow equations involve a trace  $\text{Tr}G_k^n$ . Moreover, it is easy to check that the  $n \times n$  matrix  $G_k$  has the eigenvalues,  $G_k^{(0)} + nG_k^{(1)}$  with multiplicity 1

and  $G_k^{(0)}$  with multiplicity  $n - 1$ . Then:

$$\text{Tr} (G_k)^n = n(G_k^{(0)})^n + \sum_{p=0}^{n-1} (-1)^{n-p} C_n^p (G_k^{(0)})^p n^{n-p} (G_k^{(1)})^{n-p}, \quad (6.13)$$

and we need the integral:

$$I_{n,p} := (-1)^{n-p} \int \frac{d\omega}{2\pi} (G_k^{(0)})^p (G_k^{(1)})^{n-p}, \quad (6.14)$$

which can be computed exactly in terms of regularized hypergeometric functions. Denoting as  $a := k^2 + u_2$  and  $b := k^2 + u_2 + nq'$ , we have, assuming  $a$  and  $b$  are both positives:

$$I_{n,p}(a, b) := -\pi a^{-2n} b^{n-p} \left( \frac{\sqrt{\pi} a^n (a + bn)^{-n+p+\frac{1}{2}} {}_2\tilde{F}_1\left(\frac{1}{2}, n; -n + p + \frac{3}{2}; \frac{bn}{a} + 1\right)}{\Gamma(n-p)} - \frac{a^{p+\frac{1}{2}} \Gamma\left(2n - p - \frac{1}{2}\right) {}_2\tilde{F}_1\left(n - p, 2n - p - \frac{1}{2}; n - p + \frac{1}{2}; \frac{bn}{a} + 1\right)}{\Gamma(n)} \right). \quad (6.15)$$

We recall that regularized hypergeometric functions  ${}_p\tilde{F}_q$ ,

$${}_p\tilde{F}_q(a_1, \dots, a_p; b_1, \dots, b_q; z) := \sum_{n=0}^{\infty} \frac{\prod_{j=1}^p (a_j)_n z^n}{n! \prod_{j=1}^q \Gamma(n + b_j)}, \quad (6.16)$$

where  $(a_j)_k$  are the standard Pochhammer symbols:

$$(a_j)_0 := 1, \quad (a_j)_n = a_j(a_j + 1) \cdots (a_j + n - 1), \quad n > 0. \quad (6.17)$$

Because we assume that  $q'$  prime and  $u_2$  have the same dimensions i.e.  $\bar{u}_2 := k^{-2}u_2$  and  $\bar{q}' := k^{-2}q'$ , we can define the dimensionless function  $\bar{I}_{n,p}(\bar{a}, \bar{b})$ , expressed in terms of the dimensionless  $\bar{a} := 1 + \bar{u}_2$  and  $\bar{b} := 1 + \bar{u}_2 + n\bar{q}'$ , such that

$$\bar{I}_{n,p}(\bar{a}, \bar{b}) := k^{2n-1} I_{n,p}(a, b). \quad (6.18)$$

Computing each diagrams, using the definition (4.9) for couplings, we get (see also [11]): As in the rest of this paper, we focus on the IR regime, in which in particular the regulator is well approximated by:

$$R_k(p^2) \approx (k^2 - p^2)\theta(k^2 - p^2). \quad (6.19)$$

Our goal here is to show once again that taking into account the relevant observables correlating the replica ‘‘cures’’ at least part of the divergences observed in the IR – we will return to a detailed study of the UV flow in a later work. In the windows of momenta  $0 \leq p^2 \leq k^2$ , the effective propagator reduces to:

$$G_k(\omega^2, p^2) := \underbrace{\frac{\delta_{\alpha\beta}}{\omega^2 + k^2 + u_2}}_{:=G_k^{(0)}} - \underbrace{\frac{q'}{(\omega^2 + k^2 + u_2)(\omega^2 + k^2 + u_2 + nq')}}_{:=G_k^{(1)}}$$

and the integral becomes singular for the value  $\bar{u}_2 = -1$ , recalling that  $\bar{u}_2 := u_2 k^{-2}$ . Because of the Litim regulator, the global integration along the effective loop (in the large  $N$  limit) factorizes in front of each term:

$$\Omega(k) := \int dp^2 \rho(p^2) \dot{R}_k(p^2) \approx \frac{4k^5}{3\pi\sigma^{3/2}}, \quad (6.20)$$

assuming  $k^2 \ll 4\sigma$ . Many of the flow equations involves a trace  $\text{Tr} G_k^n$ . Moreover, it is easy to check that the  $n \times n$  matrix  $G_k$  has to eigenvalues,  $G_k^{(0)} + nG_k^{(1)}$  with multiplicity 1 and  $G_k^{(0)}$  with multiplicity  $n - 1$ . Then:

$$\text{Tr} (G_k)^n = n(G_k^{(0)})^n + \sum_{p=0}^{n-1} (-1)^{n-p} C_n^p (G_k^{(0)})^p n^{n-p} (G_k^{(1)})^{n-p}, \quad (6.21)$$

and we need to the integral:

$$I_{n,p} := (-1)^{n-p} \int \frac{d\omega}{2\pi} (G_k^{(0)})^p (G_k^{(1)})^{n-p}, \quad (6.22)$$

which can be computed exactly in terms of regularized hypergeometric functions. Denoting as  $a := k^2 + u_2$  and  $b := q'$ , we have, assuming  $a$  and  $b$  are both positives:

$$I_{n,p}(a, b) := -\pi a^{-2n} b^{n-p} \left( \frac{\sqrt{\pi} a^n (a + bn)^{-n+p+\frac{1}{2}} {}_2\tilde{F}_1\left(\frac{1}{2}, n; -n + p + \frac{3}{2}; \frac{bn}{a} + 1\right)}{\Gamma(n-p)} - \frac{a^{p+\frac{1}{2}} \Gamma\left(2n - p - \frac{1}{2}\right) {}_2\tilde{F}_1\left(n - p, 2n - p - \frac{1}{2}; n - p + \frac{1}{2}; \frac{bn}{a} + 1\right)}{\Gamma(n)} \right). \quad (6.23)$$

We recall that regularized hypergeometric functions  ${}_p\tilde{F}_q$ ,

$${}_p\tilde{F}_q(a_1, \dots, a_p; b_1, \dots, b_q; z) := \sum_{n=0}^{\infty} \frac{\prod_{j=1}^p (a_j)_n z^n}{n! \prod_{j=1}^q \Gamma(n + b_j)}, \quad (6.24)$$

where  $(a_j)_k$  are the standard Pochhammer symbols:

$$(a_j)_0 := 1, \quad (a_j)_n = a_j(a_j + 1) \cdots (a_j + n - 1), \quad n > 0. \quad (6.25)$$

Because we assume that  $q^{\text{prime}}$  and  $u_2$  have the same dimensions i.e.  $\bar{u}_2 := k^{-2}u_2$  and  $\bar{q}' := k^{-2}q'$ , we can define the dimensionless function  $\bar{I}_{n,p}(\bar{a}, \bar{b})$ , expressed in terms of the dimensionless  $\bar{a} := 1 + \bar{u}_2$  and  $\bar{b} := \bar{q}'$ , such that

$$\bar{I}_{n,p}(\bar{a}, \bar{b}) := k^{2n-1} I_{n,p}(a, b). \quad (6.26)$$

Computing each diagrams, using the definition (4.9) for couplings, we get (see also [11]):

$$\dot{\bar{u}}_2 = -2\bar{u}_2 - \frac{\bar{u}_4}{18\pi} (\bar{I}_{2,2} + 2\bar{I}_{2,1} + n\bar{I}_{2,0}) - \frac{\bar{v}_{4,1}}{36\pi} \frac{1}{(1 + \bar{u}_2)^{\frac{3}{2}}}, \quad (6.27)$$

$$\dot{q}' = -2\bar{q}' - \frac{\bar{v}_{4,1}}{18\pi}(2\bar{I}_{2,1} + n\bar{I}_{2,0}) \quad (6.28)$$

$$\begin{aligned} \dot{u}_4 = & -\frac{\bar{u}_6}{30\pi^2} \frac{1}{(1 + \bar{u}_2)^2} - \frac{\bar{u}_6}{30\pi} (\bar{I}_{2,2} + 2\bar{I}_{2,1} + n\bar{I}_{2,0}) + \frac{\bar{v}_{4,1}\bar{u}_4}{6\pi} \frac{1}{(1 + \bar{u}_2)^{\frac{5}{2}}} \\ & + \frac{2\bar{u}_4^2}{9\pi} (\bar{I}_{3,3} + 3\bar{I}_{3,2} + n\bar{I}_{3,1}). \end{aligned} \quad (6.29)$$

$$\dot{v}_{4,1} = \frac{\bar{u}_6}{30\pi^2(1 + \bar{u}_2)^2} \left[ \frac{2\bar{q}'}{(1 + \bar{u}_2 + n\bar{q}')^2} - \frac{n(\bar{q}')^2}{(1 + \bar{u}_2 + n\bar{q}')^2} \right] + \frac{\bar{v}_{4,1}^2}{12\pi} \frac{1}{(1 + \bar{u}_2)^{\frac{5}{2}}} \quad (6.30)$$

$$\begin{aligned} \dot{u}_6 = & 2\bar{u}_6 + \frac{192\bar{u}_4\bar{u}_6}{5\pi} (\bar{I}_{3,3} + 3\bar{I}_{3,2} + n\bar{I}_{3,1}) + \frac{4}{5\pi^2} \frac{\bar{u}_4\bar{u}_6}{(1 + \bar{u}_2)^3} + \frac{72}{5\pi} \frac{\bar{v}_{4,1}\bar{u}_6}{(1 + \bar{u}_2)^{\frac{5}{2}}} \\ & - \frac{8\bar{u}_4^3}{9\pi} (\bar{I}_{4,4} + 4\bar{I}_{3,2}) - \frac{15}{18\pi} \frac{\bar{u}_4^2\bar{v}_{4,1}}{(1 + \bar{u}_2)^{\frac{7}{2}}}, \end{aligned} \quad (6.31)$$

and:

$$\dot{\bar{u}}_6 = \bar{u}_6. \quad (6.32)$$

Note that, as in section 4, we denote as  $\tilde{u}_6$  the magnitude of the original sextic disorder interaction. Let's start by checking that we once again find the results that we conjectured. We will choose the trajectory with initial conditions,

$$S_1(k_0) := (\bar{u}_2(k_0) := 0.1, \bar{u}_4(k_0) = 1, \bar{u}_6(k_0) = 1), \quad (6.33)$$

which is in the symmetric phase, and for  $k_0 = 0.05$  exhibits a singularity for  $k_c \approx 0.005$  as soon as the disorder becomes larger than the critical value  $\tilde{u}_6(k_0) \approx 3.68$ . The results are summarized in Figure 18, and we recover essentially the same results as before: as we fixed  $\bar{v}_{4,1}(k_0)$ , for  $-\bar{q}'(k_0)$  large enough, the singularity is removed – for the initial conditions we have chosen for the Figure, we get  $-\bar{q}'(k_0) > 10^{-5}$  – and  $q'(k_0)$  undergoes an almost constant but very small value. Remarkably, the values of  $\bar{q}'$  and  $\bar{v}_{4,1}$  are much smaller than those we observed in the symmetric phase, which we attribute to the competition between the “magnetization” and the correlations between replicas. More precisely, we assume that the inertia of the correlations linked to the vacuum of the local potential opposes the establishment of the correlations.

## 7 Conclusion and open issues

In this paper, we have investigated the behavior of the RG flow for a “2 +  $p$ ” quantum spin glass constructed by integrating out degrees of freedom labeled by the eigenvalues of the matrix-like disorder spectrum. In our approach, the effective coupling constants are defined with a special normalization that ensures the effective number of “sites” on the underlying network (representing the system’s volume) remains constant. More precisely, we take the infinite volume limit before performing the coarse-graining.

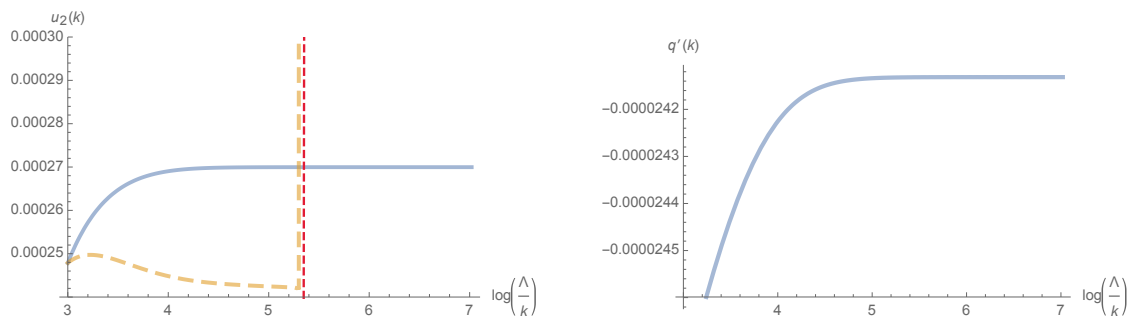


Figure 18: On the left: The RG trajectory for the (dimensioned) mass  $u_2(k)$ , for initial conditions  $S_1(k_0)$ ,  $k_0 = 0.05$ . The dashed yellow curve is for  $q'(k_0) = v_{4,1}(k_0) = 0$ ,  $\bar{u}_6(k_0) = 3.68$ , it exhibits a singularity for  $k_c = 0.005$ . The blue curve is for  $\bar{q}'(k_0) = -0.01$  and  $\bar{v}_{4,1}(k_0) = 0.01$ . On the right: The RG trajectory of  $q'(k)$  along the blue trajectory on the left figure. Computations were done for  $n = 2$ .

This paper has three main results. The first pertains to a non-trivial Ward identity arising from the gauge fixing required in constructing the RG flow, which breaks the model’s underlying  $O(N)$  invariance. Due to these Ward identities, the flow of the field strength renormalization  $Z(k)$  in the symmetric phase is entirely determined by the order  $\mathcal{O}(N^0)$  RG flow of the quartic coupling.

The second result concerns the EVE method, which allows us to close the hierarchy around sextic interactions in the symmetric phase, working at the leading order of the derivative expansion. This method, initially introduced for tensorial field theories [17], is closely related to our topic, especially regarding the theory’s specific non-locality. Our conclusions are similar to those in our previous work [11], where we show finite-scale singularities due to disorder, interpreted as a signal that something is missing from the perturbative theory. The main steps of this approximation’s construction are detailed in the companion paper [64].

The third and primary contribution of this paper is a formalism aimed at going beyond the vertex expansion. This approach resembles a formal expansion around the vacuum of the local potential approximation, where the local potential flow is “dressed” by the flow of non-local interactions. We derive the flow equation for the various couplings, focusing on the next-to-leading order beyond the just-renormalizable sector and examining asymptotic fixed-point solutions. Our numerical investigations indicate that divergences in the symmetric phase cancel out, and where these divergences occur, the flow of non-local couplings becomes relevant—contrary to what is typically expected from perturbation theory. These results provide strong evidence of a phase transition between a regime where replicas are uncorrelated and one where their correlations are non-zero.

The main open challenge is reconstructing the complete theory space from the RG perspective to achieve our overarching goal: understanding the glassy transition via RG. Many intermediate results are essential on this path, particularly regarding the physical properties of the transition. Our upcoming work will focus on the 2PI formalism, which is particularly suited when the 2-point function serves as the order parameter.

Lastly, here are some open issues we plan to address in future work:

1. Evaluating the reliability of the vertex expansion, extending beyond the leading order of the derivative expansion.
2. Considering coarse-graining in both eigenvalue and time dimensions.
3. Developing approximations valid beyond the deep IR, going beyond the derivative expansion.
4. Assessing the accuracy of the derivative expansion by computing anomalous dimensions. More systematically incorporating non-local interactions in truncations.
5. Investigating the breaking of time translation invariance symmetry.

Additionally, we might consider the UV regime, where the non-trivial scaling due to coarse-graining over the Wigner spectrum could play a significant role. Specifically, outside the critical regime investigated in previous work [11], the canonical dimension depends on the relevant couplings  $u_2$  and  $q'$ , presenting a novel challenge in constructing the effective phase space.

## Acknowledgment:

Vincent Lahoche and the authors warmly thank Mrs. Dalila Derdar for these very stimulating and inspiring exchanges from the first stages of the realization of this work. Without these highly stimulating exchanges, this work would not have been the same.



## A Classical solution for $p = 0$

In this section, we examine the solution of the classical move equation for  $p = 0$  – the corresponding quantum problem has been solved in the large  $N$  limit in our previous work [11]. The method we propose to use here is based on [95], which has been also considered for classical spin glasses dynamics in [39, 96]. The move equation for the classical particle reads for a quartic potential:

$$m_0 \frac{d^2 x_i}{dt^2} = - \sum_{j=1}^N K_{ij} x_j - h_1 x_i - \frac{h_2 \mathbf{x}^2}{6} \frac{x_i}{N}. \quad (\text{A.1})$$

It is suitable to work in the basis  $\{u^{(\mu)}\}$ , where the matrix  $K$  is diagonal, and the move equation becomes:

$$m_0 \frac{d^2 x_\mu}{dt^2} = - \left( \xi_\mu + h_1 + \frac{h_2 \mathbf{x}^2}{6} \frac{1}{N} \right) x_\mu, \quad (\text{A.2})$$

where  $x_\mu := \sum_{i=1}^N x_i u_i^{(\mu)}$ , and  $\{\xi_\mu\}$  denote the eigenvalues of  $K$  – see equation (2.14). The equation of move (A.2) is non-linear and difficult to solve exactly. However, in the large  $N$  regime, it is suitable to assume that  $a(t) := \mathbf{x}^2(t)/N$  self averages (what we call the *quenched regime*) and decouples from the explicit  $x$  dependency in the equation of move:

$$\ddot{x}_\mu = -\omega_\mu^2(t) x_\mu, \quad (\text{A.3})$$

where:

$$\omega_\mu^2 := \frac{p_\mu^2 + m^2 + \frac{h_2}{6} a(t)}{m_0}, \quad (\text{A.4})$$

where we used definitions (2.21) and (2.22) for  $p_\mu^2$  and  $m^2$ . Each component  $x_\mu$  behaves accordingly with the move equation for a time-dependent harmonic oscillator, a problem which is encountered in many areas of physics, in cosmology, plasma physics, optics, geophysics and so on – see [97] and reference therein. We will focus on the simpler regime where  $a(t)$  is almost constant, and make use of perturbation theory:

$$a(t) = a_0 + \epsilon(t), \quad (\text{A.5})$$

assuming  $|\epsilon(t)| \ll 1$ . Let us decomposes the solution  $x_\mu(t)$  in series:

$$x_\mu(t) = x_\mu^{(0)}(t) + x_\mu^{(1)}(t) + x_\mu^{(2)}(t) + \dots, \quad (\text{A.6})$$

where  $x_\mu^{(n)}(t)$  is assumed to be of order  $\epsilon^n(t)$ . The solution  $x_\mu^{(0)}(t)$  is:

$$x_\mu^{(0)}(t) = A \cos(\omega_\mu^{(0)} t + \phi_0), \quad (\text{A.7})$$

where we used  $\omega_\mu^{(0)}$  defined as:

$$\omega_\mu^{(0)} := \frac{p_\mu^2 + m^2 + \frac{h_2}{6} a_0}{m_0}. \quad (\text{A.8})$$

In the large  $N$  limit, we must have:

$$\frac{1}{N} \sum_{\mu} (x_{\mu}^{(0)}(t))^2 \rightarrow \int \rho(p^2) (x^{(0)}(p^2, t))^2 =: 2\pi A^2 I(t), \quad (\text{A.9})$$

where the function  $x^{(0)}(p^2, t)$  is the continuum limit of the series  $x_{\mu}^{(0)}(t)$ . The computation of the integral involves the regularized confluent hypergeometric function:

$$I(t) = \pi \left[ {}_0\tilde{F}_1 \left( ; 2; -\frac{4t^2}{m_0^2} \right) \cos \left( 2 \left( \frac{t \left( \frac{a_0 h_2}{6} + m^2 + 2 \right)}{m_0} + \phi_0 \right) \right) + 1 \right], \quad (\text{A.10})$$

and it shows on Figure 19 for the equilibrium condition (low classical energy configuration):

$$a_0 = -\frac{6m^2}{h_2}. \quad (\text{A.11})$$

We furthermore define the time averaging:

$$\text{Int}(t) = \frac{1}{t} \int_0^t I(t') dt', \quad (\text{A.12})$$

also plotted on Figure 19, and we have:

$$\lim_{t \rightarrow \infty} \text{Int}(t) = \pi, \quad (\text{A.13})$$

then, if we assume that the trajectory oscillates weakly around  $a_0$ , we get:

$$A = \sqrt{2a_0} = \sqrt{-\frac{12m^2}{h_2}}, \quad (\text{A.14})$$

and we have for the zero-order solution:

$$x_{\mu}^{(0)}(t) = \sqrt{-\frac{12m^2}{h_2}} \cos(\omega_{\mu}^{(0)} t + \phi_0). \quad (\text{A.15})$$

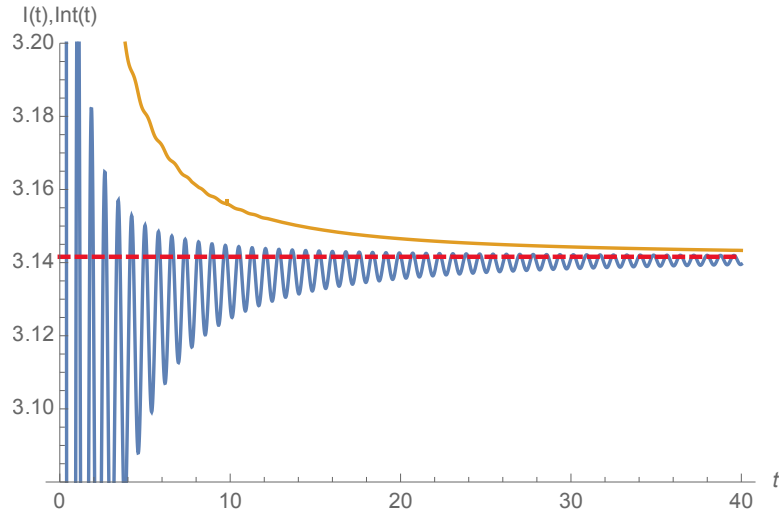


Figure 19: Behavior of the function  $I(t)$  (blue curve) and the average  $\text{Int}(t)$  (yellow). The red curve is for the value  $\pi$ .

## Bibliography

- [1] Baldwin, CL and Laumann, CR and Pal, A and Scardicchio, A, ‘Clustering of nonergodic eigenstates in quantum spin glasses,’ *Physical review letters*, vol. 118, no. 12, p. 127 201, 2017. DOI: [10.1103/PhysRevLett.118.127201](https://doi.org/10.1103/PhysRevLett.118.127201).
- [2] Cugliandolo, LF and Grepel, DR and Lozano, G and Lozza, H, ‘Effects of dissipation on disordered quantum spin models,’ *Physical Review B-Condensed Matter and Materials Physics*, vol. 70, no. 2, p. 024 422, 2004. DOI: [10.1103/PhysRevB.70.024422](https://doi.org/10.1103/PhysRevB.70.024422).
- [3] Blake, Mike and Liu, Hong, ‘On systems of maximal quantum chaos,’ *Journal of High Energy Physics*, vol. 2021, no. 5, 1–20, 2021. DOI: [10.1007/JHEP05\(2021\)229](https://doi.org/10.1007/JHEP05(2021)229).
- [4] D. Chowdhury, A. Georges, O. Parcollet and S. Sachdev, ‘Sachdev-Ye-Kitaev models and beyond: Window into non-Fermi liquids,’ *Rev. Mod. Phys.*, vol. 94, no. 3, p. 035 004, 2022. DOI: [10.1103/RevModPhys.94.035004](https://doi.org/10.1103/RevModPhys.94.035004). arXiv: [2109.05037](https://arxiv.org/abs/2109.05037) [[cond-mat.str-el](#)].
- [5] Rosenhaus, Vladimir, ‘An introduction to the SYK model,’ *Journal of Physics A: Mathematical and Theoretical*, vol. 52, no. 32, p. 323 001, 2019. DOI: [10.1088/1751-8121/ab2ce1](https://doi.org/10.1088/1751-8121/ab2ce1).
- [6] R. Gurau, ‘The  $\epsilon$  prescription in the SYK model,’ *J. Phys. Comm.*, vol. 2, no. 1, p. 015 003, 2018. DOI: [10.1088/2399-6528/aa9b6f](https://doi.org/10.1088/2399-6528/aa9b6f). arXiv: [1705.08581](https://arxiv.org/abs/1705.08581) [[hep-th](#)].
- [7] Dartois, Stéphane and Erbin, Harold and Mondal, Swapnamay, ‘Conformality of  $1/N$  corrections in Sachdev-Ye-Kitaev-like models,’ *Physical Review D*, vol. 100, no. 12, 125 005, 2019. DOI: [10.1103/PhysRevD.100.125005](https://doi.org/10.1103/PhysRevD.100.125005).
- [8] Biroli, Giulio and Cugliandolo, Leticia F, ‘Quantum Thouless-Anderson-Palmer equations for glassy systems,’ *Physical Review B*, vol. 64, no. 1, p. 014 206, 2001. DOI: [10.1103/PhysRevB.64.014206](https://doi.org/10.1103/PhysRevB.64.014206).
- [9] Rokni, Michal and Chandra, Premala, ‘Dynamical study of the disordered quantum  $p = 2$  spherical model,’ *Physical Review B*, vol. 69, no. 9, p. 094 403, 2004. DOI: [10.1103/PhysRevB.69.094403](https://doi.org/10.1103/PhysRevB.69.094403).

- [10] Crisanti, Andrea and Leuzzi, Luca, ‘Spherical  $2 + p$  spin-glass model: An analytically solvable model with a glass-to-glass transition,’ *Physical Review B-Condensed Matter and Materials Physics*, vol. 73, no. 1, 014 412, 2006. DOI: [10.1103/PhysRevB.73.014412](https://doi.org/10.1103/PhysRevB.73.014412).
- [11] V. Lahoche, D. Ousmane Samary and P. Radpay, ‘Large time effective kinetics  $\beta$ -functions for quantum  $(2 + p)$ -spin glass,’ Aug. 2024. arXiv: [2408.02602](https://arxiv.org/abs/2408.02602) [[cond-mat.dis-nn](#)].
- [12] J. Berges, N. Tetradis and C. Wetterich, ‘Nonperturbative renormalization flow in quantum field theory and statistical physics,’ *Phys. Rept.*, vol. 363, pp. 223–386, 2002. DOI: [10.1016/S0370-1573\(01\)00098-9](https://doi.org/10.1016/S0370-1573(01)00098-9). arXiv: [hep-ph/0005122](https://arxiv.org/abs/hep-ph/0005122).
- [13] Delamotte, Bertrand, ‘An introduction to the nonperturbative renormalization group,’ in *Renormalization group and effective field theory approaches to many-body systems*, Springer, 2012, pp. 49–132.
- [14] Tissier, Matthieu and Tarjus, Gilles, ‘Nonperturbative functional renormalization group for random field models. IV: supersymmetry and its spontaneous breaking,’ *arXiv preprint arXiv:1110.5500*, 2011.
- [15] G. Tarjus and M. Tissier, ‘Random-field Ising and  $O(N)$  models: Theoretical description through the functional renormalization group,’ *Eur. Phys. J. B*, vol. 93, no. 3, p. 50, 2020. DOI: [10.1140/epjb/e2020-100489-1](https://doi.org/10.1140/epjb/e2020-100489-1). arXiv: [1910.03530](https://arxiv.org/abs/1910.03530) [[cond-mat.dis-nn](#)].
- [16] Gredat, Damien and Chaté, Hugues and Delamotte, Bertrand and Dornic, Ivan, ‘Finite-scale singularity in the renormalization group flow of a reaction-diffusion system,’ *Physical Review E*, vol. 89, no. 1, 010 102, 2014. DOI: [10.1103/PhysRevE.89.010102](https://doi.org/10.1103/PhysRevE.89.010102).
- [17] V. Lahoche and D. Ousmane Samary, ‘Nonperturbative renormalization group beyond melonic sector: The Effective Vertex Expansion method for group fields theories,’ *Phys. Rev. D*, vol. 98, no. 12, p. 126 010, 2018. DOI: [10.1103/PhysRevD.98.126010](https://doi.org/10.1103/PhysRevD.98.126010). arXiv: [1809.00247](https://arxiv.org/abs/1809.00247) [[hep-th](#)].
- [18] E. Brezin and J. Zinn-Justin, ‘Renormalization group approach to matrix models,’ *Phys. Lett. B*, vol. 288, pp. 54–58, 1992. DOI: [10.1016/0370-2693\(92\)91953-7](https://doi.org/10.1016/0370-2693(92)91953-7). arXiv: [hep-th/9206035](https://arxiv.org/abs/hep-th/9206035).
- [19] N. Dupuis, L. Canet, A. Eichhorn, W. Metzner, J. M. Pawłowski, M. Tissier and N. Wschebor, ‘The nonperturbative functional renormalization group and its applications,’ *Phys. Rept.*, vol. 910, pp. 1–114, 2021. DOI: [10.1016/j.physrep.2021.01.001](https://doi.org/10.1016/j.physrep.2021.01.001). arXiv: [2006.04853](https://arxiv.org/abs/2006.04853) [[cond-mat.stat-mech](#)].
- [20] A. Eichhorn and T. Kosłowski, ‘Towards phase transitions between discrete and continuum quantum spacetime from the Renormalization Group,’ *Phys. Rev. D*, vol. 90, no. 10, p. 104 039, 2014. DOI: [10.1103/PhysRevD.90.104039](https://doi.org/10.1103/PhysRevD.90.104039). arXiv: [1408.4127](https://arxiv.org/abs/1408.4127) [[gr-qc](#)].
- [21] V. Lahoche and D. Ousmane Samary, ‘Revisited functional renormalization group approach for random matrices in the large- $N$  limit,’ *Phys. Rev. D*, vol. 101, no. 10, p. 106 015, 2020. DOI: [10.1103/PhysRevD.101.106015](https://doi.org/10.1103/PhysRevD.101.106015). arXiv: [1909.03327](https://arxiv.org/abs/1909.03327) [[hep-th](#)].
- [22] P. Di Francesco, P. H. Ginsparg and J. Zinn-Justin, ‘2-D Gravity and random matrices,’ *Phys. Rept.*, vol. 254, pp. 1–133, 1995. DOI: [10.1016/0370-1573\(94\)00084-G](https://doi.org/10.1016/0370-1573(94)00084-G). arXiv: [hep-th/9306153](https://arxiv.org/abs/hep-th/9306153).
- [23] J. Zinn-Justin, ‘Vector models in the large  $N$  limit: A Few applications,’ in *11th Taiwan Spring School on Particles and Fields*, Mar. 1998. DOI: <https://saalburg.aei.mpg.de/wp-content/uploads/sites/25/2017/03/zinn.pdf>. arXiv: [hep-th/9810198](https://arxiv.org/abs/hep-th/9810198).

- [24] Kluber, Grant, ‘Trotterization in Quantum Theory,’ *arXiv preprint arXiv:2310.13296*, 2023.
- [25] Zinn-Justin, Jean, *Path integrals in quantum mechanics*. OUP Oxford, 2010.
- [26] Zinn-Justin, Jean, *Phase transitions and renormalization group*. Oxford University Press, 2007.
- [27] Erbin, Harold and Lahoche, Vincent and Tamaazousti, Mohamed, ‘Constructive expansion for vector field theories I. Quartic models in low dimensions,’ *J. Math. Phys.*, vol. 62, no. 4, p. 043 501, 2021. DOI: [10.1063/5.0038599](https://doi.org/10.1063/5.0038599). arXiv: [1904.05933](https://arxiv.org/abs/1904.05933) [hep-th].
- [28] Zinn-Justin, Jean, *Path integrals in quantum mechanics*. OUP Oxford, 2010.
- [29] Mehta, Madan Lal, *Random matrices*. Elsevier, 2004.
- [30] Potters, Marc and Bouchaud, Jean-Philippe, *A first course in random matrix theory: for physicists, engineers and data scientists*. Cambridge University Press, 2020.
- [31] V. Lahoche, D. Ousmane Samary and M. Tamaazousti, ‘Generalized scale behavior and renormalization group for data analysis,’ *J. Stat. Mech.*, vol. 2203, no. 3, p. 033 101, 2022. DOI: [10.1088/1742-5468/ac52a6](https://doi.org/10.1088/1742-5468/ac52a6). arXiv: [2002.10574](https://arxiv.org/abs/2002.10574) [hep-th].
- [32] S. Carrozza, ‘Flowing in Group Field Theory Space: a Review,’ *SIGMA*, vol. 12, p. 070, 2016. DOI: [10.3842/SIGMA.2016.070](https://doi.org/10.3842/SIGMA.2016.070). arXiv: [1603.01902](https://arxiv.org/abs/1603.01902) [gr-qc].
- [33] ‘When random tensors meet random matrices, author=Seddik, Mohamed El Amine and Guillaud, Maxime and Couillet, Romain,’ *The Annals of Applied Probability*, vol. 34, no. 1A, 203–248, 2024. DOI: [10.1214/23-AAP1962](https://doi.org/10.1214/23-AAP1962).
- [34] Goulart, José Henrique de M and Couillet, Romain and Comon, Pierre, ‘A random matrix perspective on random tensors,’ *Journal of Machine Learning Research*, vol. 23, no. 264, pp. 1–36, 2022. DOI: <https://jmlr.org/papers/volume23/21-1038/21-1038.pdf>.
- [35] Gurau, Razvan, ‘On the generalization of the Wigner semicircle law to real symmetric tensors,’ *arXiv preprint arXiv:2004.02660*, 2020.
- [36] H. Lebeau, F. Chatelain and R. Couillet, *A random matrix approach to low-multilinear-rank tensor approximation*, 2024. arXiv: [2402.03169](https://arxiv.org/abs/2402.03169) [stat.ML].
- [37] Castellani, Tommaso and Cavagna, Andrea, ‘Spin-glass theory for pedestrians,’ *Journal of Statistical Mechanics: Theory and Experiment*, vol. 2005, no. 05, P05012, 2005. DOI: [10.1088/1742-5468/2005/05/P05012](https://doi.org/10.1088/1742-5468/2005/05/P05012).
- [38] Mézard, Marc and Parisi, Giorgio and Virasoro, Miguel Angel, *Spin glass theory and beyond: An Introduction to the Replica Method and Its Applications*. World Scientific Publishing Company, 1987, vol. 9.
- [39] De Dominicis, Cirano and Giardinà, Irene, *Random fields and spin glasses: a field theory approach*. Cambridge University Press, 2006.
- [40] Mézard, Marc and Parisi, Giorgio and Sourlas, Nicolas and Toulouse, Gérard and Virasoro, Miguel, ‘Nature of the spin-glass phase,’ *Physical review letters*, vol. 52, no. 13, 1156, 1984. DOI: [10.1103/PhysRevLett.52.1156](https://doi.org/10.1103/PhysRevLett.52.1156).
- [41] Mezard, Marc and Montanari, Andrea, *Information, physics, and computation*. Oxford University Press, 2009.
- [42] Wilson, Kenneth G, ‘The renormalization group and critical phenomena,’ *Reviews of Modern Physics*, vol. 55, no. 3, 583, 1983. DOI: [10.1103/RevModPhys.55.583](https://doi.org/10.1103/RevModPhys.55.583).

- [43] Kadanoff, Leo P, ‘Scaling laws for Ising models near  $T_c$ ,’ *Physics Physique Fizika*, vol. 2, no. 6, 263, 1966. DOI: [10.1103/PhysicsPhysiqueFizika.2.263](https://doi.org/10.1103/PhysicsPhysiqueFizika.2.263).
- [44] Gordon, Amit and Banerjee, Aditya and Koch-Janusz, Maciej and Ringel, Zohar, ‘Relevance in the renormalization group and in information theory,’ *Physical Review Letters*, vol. 126, no. 24, p. 240601, 2021. DOI: [10.1103/PhysRevLett.126.240601](https://doi.org/10.1103/PhysRevLett.126.240601).
- [45] Apenko, Sergey M, ‘Information theory and renormalization group flows,’ *Physica A: Statistical Mechanics and its Applications*, vol. 391, no. 1-2, pp. 62–77, 2012. DOI: [10.1016/j.physa.2011.08.014](https://doi.org/10.1016/j.physa.2011.08.014).
- [46] Bény, Cédric and Osborne, Tobias J, ‘Information-geometric approach to the renormalization group,’ *Physical Review A*, vol. 92, no. 2, p. 022330, 2015. DOI: [10.1103/PhysRevE.92.052101](https://doi.org/10.1103/PhysRevE.92.052101).
- [47] Pessoa, Pedro and Caticha, Ariel, ‘Exact renormalization groups as a form of entropic dynamics,’ *Entropy*, vol. 20, no. 1, p. 25, 2018. DOI: [10.3390/e20010025](https://doi.org/10.3390/e20010025).
- [48] J. Cotler and S. Rezchikov, ‘Renormalization group flow as optimal transport,’ *Phys. Rev. D*, vol. 108, no. 2, p. 025003, 2023. DOI: [10.1103/PhysRevD.108.025003](https://doi.org/10.1103/PhysRevD.108.025003). arXiv: [2202.11737](https://arxiv.org/abs/2202.11737) [hep-th].
- [49] Bradde, Serena and Bialek, William, ‘PCA Meets RG,’ *Journal of Statistical Physics*, vol. 167, no. 3-4, 462–475, 2017, ISSN: 1572-9613. DOI: [10.1007/s10955-017-1770-6](https://doi.org/10.1007/s10955-017-1770-6).
- [50] Carrozza, Sylvain and others, ‘Flowing in group field theory space: a review,’ *SIGMA. Symmetry, Integrability and Geometry: Methods and Applications*, vol. 12, 070, 2016. DOI: [10.3842/SIGMA.2016.070](https://doi.org/10.3842/SIGMA.2016.070).
- [51] Amari, Shun-ichi and Nagaoka, Hiroshi, *Methods of information geometry*. American Mathematical Soc., 2000, vol. 191.
- [52] Bény, Cédric and Osborne, Tobias J, ‘The renormalization group via statistical inference,’ *New Journal of Physics*, vol. 17, no. 8, p. 083005, 2015. DOI: [10.1088/1367-2630/17/8/083005](https://doi.org/10.1088/1367-2630/17/8/083005).
- [53] Cheng, Aohua and Xu, Yunhui and Sun, Pei and Tian, Yang, ‘Simplex path integral and simplex renormalization group for high-order interactions,’ *arXiv:2305.01895*, 2023.
- [54] Villegas, Pablo and Gili, Tommaso and Caldarelli, Guido and Gabrielli, Andrea, ‘Laplacian renormalization group for heterogeneous networks,’ *Nature Physics*, vol. 19, no. 3, pp. 445–450, 2023. DOI: [10.1038/s41567-022-01866-8](https://doi.org/10.1038/s41567-022-01866-8).
- [55] Lahoche, Vincent and Ousmane Samary, Dine and Tamaazousti, Mohamed, ‘Functional renormalization group for multilinear disordered Langevin dynamics II: Revisiting the  $p = 2$  spin dynamics for Wigner and Wishart ensembles,’ *Journal of Physics Communications*, vol. 7, no. 5, p. 055005, 2023. DOI: [10.1088/2399-6528/acd09d](https://doi.org/10.1088/2399-6528/acd09d).
- [56] V. Lahoche and D. Ousmane Samary, ‘Functional renormalization group for  $p = 2$  like glassy matrices in the planar approximation I. Vertex expansion at equilibrium,’ *Nucl. Phys. B*, vol. 1005, p. 116582, 2024. DOI: [10.1016/j.nuclphysb.2024.116582](https://doi.org/10.1016/j.nuclphysb.2024.116582). arXiv: [2403.07577](https://arxiv.org/abs/2403.07577) [hep-th].
- [57] Erbin, Harold and Lahoche, Vincent and Ousmane Samary, Dine, ‘Non-perturbative renormalization for the neural network-QFT correspondence,’ *Mach. Learn. Sci. Tech.*, vol. 3, no. 1, p. 015027, 2022. DOI: [10.1088/2632-2153/ac4f69](https://doi.org/10.1088/2632-2153/ac4f69). arXiv: [2108.01403](https://arxiv.org/abs/2108.01403) [hep-th].

- [58] V. Lahoche, D. Ousmane Samary and M. Ouerfelli, ‘Functional renormalization group for multilinear disordered Langevin dynamics I Formalism and first numerical investigations at equilibrium,’ *J. Phys. Comm.*, vol. 6, no. 5, p. 055002, 2022. DOI: [10.1088/2399-6528/ac61b3](https://doi.org/10.1088/2399-6528/ac61b3). arXiv: [2106.05690](https://arxiv.org/abs/2106.05690) [[hep-th](#)].
- [59] Duclut, Charlie and Delamotte, Bertrand, ‘Frequency regulators for the nonperturbative renormalization group: A general study and the model A as a benchmark,’ *Physical Review E*, vol. 95, no. 1, p. 012107, 2017. DOI: [10.1103/PhysRevE.95.012107](https://doi.org/10.1103/PhysRevE.95.012107).
- [60] Squizzato, Davide and Canet, Léonie, ‘Kardar-Parisi-Zhang equation with temporally correlated noise: A nonperturbative renormalization group approach,’ *Physical Review E*, vol. 100, no. 6, p. 062143, 2019. DOI: [10.1103/PhysRevE.100.062143](https://doi.org/10.1103/PhysRevE.100.062143).
- [61] Zappala, D, ‘Improving the Renormalization Group approach to the quantum-mechanical double well potential,’ *Physics Letters A*, vol. 290, no. 1-2, pp. 35–40, 2001. DOI: [10.1016/S0375-9601\(01\)00642-9](https://doi.org/10.1016/S0375-9601(01)00642-9).
- [62] F. Synatschke, G. Bergner, H. Gies and A. Wipf, ‘Flow Equation for Supersymmetric Quantum Mechanics,’ *JHEP*, vol. 03, p. 028, 2009. DOI: [10.1088/1126-6708/2009/03/028](https://doi.org/10.1088/1126-6708/2009/03/028). arXiv: [0809.4396](https://arxiv.org/abs/0809.4396) [[hep-th](#)].
- [63] M. Heilmann, T. Hellwig, B. Knorr, M. Ansorg and A. Wipf, ‘Convergence of Derivative Expansion in Supersymmetric Functional RG Flows,’ *JHEP*, vol. 02, p. 109, 2015. DOI: [10.1007/JHEP02\(2015\)109](https://doi.org/10.1007/JHEP02(2015)109). arXiv: [1409.5650](https://arxiv.org/abs/1409.5650) [[hep-th](#)].
- [64] Vincent Lahoche and Ousmane Samary, Dine and Parham Radpay, *Frequency regulator for quantum p-spin renormalization group in the large N limit*, 2024, in preparation.
- [65] Duclut, Charlie and Delamotte, Bertrand, ‘Nonuniversality in the erosion of tilted landscapes,’ *Physical Review E*, vol. 96, no. 1, p. 012149, 2017. DOI: [10.1103/PhysRevE.96.012149](https://doi.org/10.1103/PhysRevE.96.012149).
- [66] M. Guilleux and J. Serreau, ‘Quantum scalar fields in de Sitter space from the nonperturbative renormalization group,’ *Phys. Rev. D*, vol. 92, no. 8, p. 084010, 2015. DOI: [10.1103/PhysRevD.92.084010](https://doi.org/10.1103/PhysRevD.92.084010). arXiv: [1506.06183](https://arxiv.org/abs/1506.06183) [[hep-th](#)].
- [67] Canet, Léonie and Chaté, Hugues and Delamotte, Bertrand and Wschebor, Nicolás, ‘Non-perturbative renormalization group for the Kardar-Parisi-Zhang equation,’ *Physical review letters*, vol. 104, no. 15, 150601, 2010. DOI: [10.1103/PhysRevLett.104.150601](https://doi.org/10.1103/PhysRevLett.104.150601).
- [68] L. Canet, H. Chate, B. Delamotte and N. Wschebor, ‘Non-perturbative renormalisation group for the Kardar-Parisi-Zhang equation: general framework and first applications,’ *Phys. Rev. E*, vol. 84, p. 061128, 2011. DOI: [10.1103/PhysRevE.84.061128](https://doi.org/10.1103/PhysRevE.84.061128). arXiv: [1107.2289](https://arxiv.org/abs/1107.2289) [[cond-mat.stat-mech](#)].
- [69] L. Canet, B. Delamotte and N. Wschebor, ‘Fully developed isotropic turbulence: non-perturbative renormalization group formalism and fixed point solution,’ *Phys. Rev. E*, vol. 93, no. 6, p. 063101, 2016. DOI: [10.1103/PhysRevE.93.063101](https://doi.org/10.1103/PhysRevE.93.063101). arXiv: [1411.7780](https://arxiv.org/abs/1411.7780) [[cond-mat.stat-mech](#)].
- [70] Polchinski, Joseph, ‘Renormalization and Effective Lagrangians,’ *Nucl. Phys. B*, vol. 231, pp. 269–295, 1984. DOI: [10.1016/0550-3213\(84\)90287-6](https://doi.org/10.1016/0550-3213(84)90287-6).
- [71] C. Bagnuls and C. Bervillier, ‘Exact renormalization group equations. An Introductory review,’ *Phys. Rept.*, vol. 348, p. 91, 2001. DOI: [10.1016/S0370-1573\(00\)00137-X](https://doi.org/10.1016/S0370-1573(00)00137-X). arXiv: [hep-th/0002034](https://arxiv.org/abs/hep-th/0002034).

- [72] D. F. Litim, ‘Optimized renormalization group flows,’ *Phys. Rev. D*, vol. 64, p. 105 007, 2001. DOI: [10.1103/PhysRevD.64.105007](https://doi.org/10.1103/PhysRevD.64.105007). arXiv: [hep-th/0103195](https://arxiv.org/abs/hep-th/0103195).
- [73] V. Lahoche and D. Ousmane Samary, ‘Functional renormalization group for  $p = 2$  like glassy matrices in the planar approximation II. Ward identities method in the deep IR,’ *Nucl. Phys. B*, vol. 1006, p. 116 627, 2024. DOI: [10.1016/j.nuclphysb.2024.116627](https://doi.org/10.1016/j.nuclphysb.2024.116627). arXiv: [2403.12217](https://arxiv.org/abs/2403.12217) [[hep-th](#)].
- [74] V. Lahoche and D. Ousmane Samary, ‘Functional renormalization group for  $p = 2$  like glassy matrices in the planar approximation III. Equilibrium dynamics and beyond,’ *Nucl. Phys. B*, vol. 1006, p. 116 656, 2024. DOI: [10.1016/j.nuclphysb.2024.116656](https://doi.org/10.1016/j.nuclphysb.2024.116656). arXiv: [2404.11915](https://arxiv.org/abs/2404.11915) [[hep-th](#)].
- [75] Canet, Léonie and Delamotte, Bertrand and Mouhanna, Dominique and Vidal, Julien, ‘Optimization of the derivative expansion in the nonperturbative renormalization group,’ *Physical Review D*, vol. 67, no. 6, 065 004, 2003. DOI: [10.1103/PhysRevD.67.065004](https://doi.org/10.1103/PhysRevD.67.065004).
- [76] V. Lahoche and D. Ousmane Samary, ‘Stochastic dynamics for group field theories,’ *Phys. Rev. D*, vol. 107, no. 8, p. 086 009, 2023. DOI: [10.1103/PhysRevD.107.086009](https://doi.org/10.1103/PhysRevD.107.086009). arXiv: [2209.02321](https://arxiv.org/abs/2209.02321) [[math-ph](#)].
- [77] V. Lahoche, D. Ousmane Samary and M. Tamaazousti, ‘Functional Renormalization Group Approach for Signal Detection,’ Jan. 2022. arXiv: [2201.04250](https://arxiv.org/abs/2201.04250) [[hep-th](#)].
- [78] J. I. Latorre and T. R. Morris, ‘Exact scheme independence,’ *JHEP*, vol. 11, p. 004, 2000. DOI: [10.1088/1126-6708/2000/11/004](https://doi.org/10.1088/1126-6708/2000/11/004). arXiv: [hep-th/0008123](https://arxiv.org/abs/hep-th/0008123).
- [79] A. Caticha, ‘Changes of Variables and the Renormalization Group,’ May 2016. arXiv: [1605.06366](https://arxiv.org/abs/1605.06366) [[hep-th](#)].
- [80] C. Bervillier, ‘Structure of Exact Renormalization Group Equations for field theory,’ May 2014. arXiv: [1405.0791](https://arxiv.org/abs/1405.0791) [[hep-th](#)].
- [81] Rivasseau, Vincent, ‘Loop vertex expansion for higher-order interactions,’ *Letters in Mathematical Physics*, vol. 108, pp. 1147–1162, 2018. DOI: [10.1007/s11005-017-1037-9](https://doi.org/10.1007/s11005-017-1037-9).
- [82] Rivasseau, Vincent and Wang, Zhituo, ‘Loop vertex expansion for  $\Phi^{2k}$  theory in zero dimension,’ *Journal of mathematical physics*, vol. 51, no. 9, 2010. DOI: [10.1063/1.346032](https://doi.org/10.1063/1.346032).
- [83] Gurau, Razvan and Rivasseau, Vincent, ‘The multiscale loop vertex expansion,’ in *Annales Henri Poincaré*, Springer, vol. 16, 2015, pp. 1869–1897. DOI: [10.1007/s00023-014-0370-0](https://doi.org/10.1007/s00023-014-0370-0).
- [84] V. Lahoche, D. Ousmane Samary and M. Tamaazousti, ‘Generalized scale behavior and renormalization group for data analysis,’ *J. Stat. Mech.*, vol. 2203, no. 3, p. 033 101, 2022. DOI: [10.1088/1742-5468/ac52a6](https://doi.org/10.1088/1742-5468/ac52a6). arXiv: [2002.10574](https://arxiv.org/abs/2002.10574) [[hep-th](#)].
- [85] D. Benedetti, J. Ben Geloun and D. Oriti, ‘Functional Renormalisation Group Approach for Tensorial Group Field Theory: a Rank-3 Model,’ *JHEP*, vol. 03, p. 084, 2015. DOI: [10.1007/JHEP03\(2015\)084](https://doi.org/10.1007/JHEP03(2015)084). arXiv: [1411.3180](https://arxiv.org/abs/1411.3180) [[hep-th](#)].
- [86] H. Grosse and R. Wulkenhaar, ‘Progress in solving a noncommutative quantum field theory in four dimensions,’ Sep. 2009. arXiv: [0909.1389](https://arxiv.org/abs/0909.1389) [[hep-th](#)].
- [87] V. Lahoche and D. Ousmane Samary, ‘Unitary symmetry constraints on tensorial group field theory renormalization group flow,’ *Class. Quant. Grav.*, vol. 35, no. 19, p. 195 006, 2018. DOI: [10.1088/1361-6382/aad83f](https://doi.org/10.1088/1361-6382/aad83f). arXiv: [1803.09902](https://arxiv.org/abs/1803.09902) [[hep-th](#)].



- [88] A. Connes and C. Rovelli, ‘Von Neumann algebra automorphisms and time thermodynamics relation in general covariant quantum theories,’ *Class. Quant. Grav.*, vol. 11, pp. 2899–2918, 1994. DOI: [10.1088/0264-9381/11/12/007](https://doi.org/10.1088/0264-9381/11/12/007). arXiv: [gr-qc/9406019](https://arxiv.org/abs/gr-qc/9406019).
- [89] C. Rovelli, ‘Statistical mechanics of gravity and the thermodynamical origin of time,’ *Class. Quant. Grav.*, vol. 10, pp. 1549–1566, 1993. DOI: [10.1088/0264-9381/10/8/015](https://doi.org/10.1088/0264-9381/10/8/015).
- [90] Zia, Royce KP and Redish, Edward F and McKay, Susan R, ‘Making sense of the Legendre transform,’ *American Journal of Physics*, vol. 77, no. 7, 614–622, 2009. DOI: [10.1119/1.3119512](https://doi.org/10.1119/1.3119512).
- [91] L. Canet, H. Chate and B. Delamotte, ‘General framework of the non-perturbative renormalization group for non-equilibrium steady states,’ *J. Phys. A*, vol. 44, p. 495 001, 2011. DOI: [10.1088/1751-8113/44/49/495001](https://doi.org/10.1088/1751-8113/44/49/495001). arXiv: [1106.4129](https://arxiv.org/abs/1106.4129) [[cond-mat.stat-mech](#)].
- [92] Tarjus, Gilles and Tissier, Matthieu, ‘Nonperturbative functional renormalization group for random field models and related disordered systems. I. Effective average action formalism,’ *Physical Review B-Condensed Matter and Materials Physics*, vol. 78, no. 2, 024 203, 2008. DOI: [10.1103/PhysRevB.78.024204](https://doi.org/10.1103/PhysRevB.78.024204).
- [93] Crisanti, Andrea and Sommers, H-J, ‘The spherical p-spin interaction spin glass model: the statics,’ *Zeitschrift für Physik B Condensed Matter*, vol. 87, no. 3, 341–354, 1992. DOI: [10.1007/BF01309287](https://doi.org/10.1007/BF01309287).
- [94] Cugliandolo, Leticia F and Grepel, DR and da Silva Santos, Constantino A, ‘Imaginary-time replica formalism study of a quantum spherical p-spin-glass model,’ *Physical Review B*, vol. 64, no. 1, 014 403, 2001. DOI: [10.1103/PhysRevB.64.014403](https://doi.org/10.1103/PhysRevB.64.014403).
- [95] Bray, Alan J, ‘Theory of phase-ordering kinetics,’ *Advances in Physics*, vol. 43, no. 3, 357–459, 1994. DOI: [10.1080/00018739400101505](https://doi.org/10.1080/00018739400101505).
- [96] Lahoche, Vincent and Ousmane Samary, Dine, ‘Low-temperature dynamics for confined  $p = 2$  soft spin in the quenched regime,’ *The European Physical Journal Plus*, vol. 138, no. 5, 1–10, 2023. DOI: [10.1140/epjp/s13360-023-04039-5](https://doi.org/10.1140/epjp/s13360-023-04039-5).
- [97] Gomez Vergel, Daniel and Villasenor, Eduardo J. S, ‘The Time-dependent quantum harmonic oscillator revisited: Applications to Quantum Field Theory,’ *Annals Phys.*, vol. 324, pp. 1360–1385, 2009. DOI: [10.1016/j.aop.2009.03.003](https://doi.org/10.1016/j.aop.2009.03.003). arXiv: [0903.0289](https://arxiv.org/abs/0903.0289) [[math-ph](#)].